ISSN 8755-6839

SCIENCE OF TSUNAMI HAZARDS

Journal of Tsunami Society International

Volume 37 Number 3 2018

DEVELOPMENT OF A GROUP OF MOBILE ROBOTS FOR CONDUCTING COMPREHENSIVE RESEARCH OF DANGEROUS WAVE CHARACTERISTICS IN COASTAL ZONES

A. Kurkin[1)], D. Tyugin[1)], V. Kuzin[1)], D. Zeziulin[1)], E. Pelinovsky[1,2)], A. Malashenko[2)], P. Beresnev[1)], V. Belyakov[1)]

1) Laboratory of Modeling of Natural and Anthropogenic Disasters, Nizhny Novgorod State Technical University n.a. R.E. Alekseev, Nizhny Novgorod, **RUSSIA**.
2) Special Research Bureau for Automation of Marine Researches, Yuzhno-Sakhalinsk, **RUSSIA**

EVALUATION OF THE TSUNAMI VULNERABILITY IN THE COASTAL ECUADORIAN TOURIST CENTERS OF THE PENINSULAS OF BAHIA DE CARÁQUEZ AND SALINAS

Andres Sebastian Matheus-Medina[1], Theofilos Toulkeridis[1]*, Oswaldo Padilla-Almeida[1], Mario Cruz-D´Howitt[1] and Kervin Chunga[2]

[1]Universidad de las Fuerzas Armadas ESPE, Sangolquí, **ECUADOR**
[2]Universidad Estatal Península Santa Elena UPSE, Salinas, **ECUADOR**

EVALUATION OF TSUNAMI DANGER FOR THE WESTERN COAST OF THE BLACK SEA BY POSSIBLE CATASTROPHIC UNDERWATER EARTHQUAKES

R.Kh.Mazova[1], Kolchina E.A.[2]

[1]*R.E. Alekseev Nizhny Novgorod State Technical University, Nizhny Novgorod,* **RUSSIA***,*
[2]*LCC SPE Prima, Nizhny Novgorod,* **RUSSIA***,*

VULNERABILITY ANALYSIS BASED ON TSUNAMI HAZARDS IN CRUCITA, CENTRAL COASTAL OF ECUADOR

Julio Cesar Celorio-Saltos[1], Jhonny Marcelo García-Arias[1], Alfredo Bienvenido Guerra-Luque[1] Grey Barragan-Aroca[1] and Theofilos Toulkeridis[2]*

[1]Escuela de Gestión de Riesgo, Facultad de Ciencias de la Salud y del Ser Humano, Universidad Estatal de Bolívar, Guaranda, **ECUADOR**
[2]Universidad de las Fuerzas Armadas ESPE, Sangolquí, **ECUADOR**

TSUNAMI SOCIETY INTERNATIONAL, 1741 Ala Moana Blvd. #70, Honolulu, HI 96815, USA.
SCIENCE OF TSUNAMI HAZARDS is a CERTIFIED OPEN ACCESS Journal included in the prestigious international academic journal database DOAJ, maintained by the University of Lund in Sweden with the support of the European Union. SCIENCE OF TSUNAMI HAZARDS is also preserved, archived and disseminated by the National Library, The Hague, NETHERLANDS, the Library of Congress, Washington D.C., USA, the Electronic Library of Los Alamos, National Laboratory, New Mexico, USA, the EBSCO Publishing databases and ELSEVIER Publishing in Amsterdam. The vast dissemination gives the journal additional global exposure and readership in 90% of the academic institutions worldwide, including nation- wide access to databases in more than 70 countries.

OBJECTIVE: Tsunami Society International publishes this interdisciplinary journal to increase and disseminate knowledge about tsunamis and their hazards.

Submit manuscripts of research papers, notes or letters to the Editor. If a research paper is accepted for publication the author(s) must submit a scan-ready manuscript, a Doc, TeX or a PDF file in the journal format. Issues of the journal are published electronically in PDF format. There is a minimal publication fee for authors who are members of Tsunami Society International for three years and slightly higher for non-members. Tsunami Society International members are notified by e-mail when a new issue is available. Permission to use figures, tables and brief excerpts from this journal in scientific and educational works is granted provided that the source is acknowledged. Recent and all past journal issues are available at: http://www.TsunamiSociety.org CD-ROMs of past volumes may be purchased by contacting Tsunami Society International at postmaster@tsunamisociety.org Issues of the journal from 1982 thru 2005 are also available in PDF format at the U.S. Los Alamos National Laboratory Library http://epubs.lanl.gov/tsunami/
WWW.TSUNAMISOCIETY.ORG

ISSN 8755-6839

SCIENCE OF **TSUNAMI HAZARDS**

Journal of Tsunami Society International

Volume 37 Number 3 2018

DEVELOPMENT OF A GROUP OF MOBILE ROBOTS FOR CONDUCTING COMPREHENSIVE RESEARCH OF DANGEROUS WAVE CHARACTERISTICS IN COASTAL ZONES

A. Kurkin[1)], D. Tyugin[1)], V. Kuzin[1)], D. Zeziulin[1)], E. Pelinovsky[1,2)],
1.1 **A. Malashenko[2)], P. Beresnev[1)], V. Belyakov[1)]**

1) Laboratory of Modeling of Natural and Anthropogenic Disasters, Nizhny Novgorod State Technical University n.a. R.E. Alekseev, Nizhny Novgorod, Russia.
2) Special Research Bureau for Automation of Marine Researches, Yuzhno-Sakhalinsk, Russia

ABSTRACT

New methods and approaches for carrying out comprehensive measurements of hazardous waves (tsunami, storm surges) and background wave climate with telemetrically related group of ground, surface and underwater based robots are discussed. The design and equipment list of the ground robot are considered. It includes three various types of movers, an add-on for the installation of devices on the mobile platform and the hardware part. Ground robot was tested in 2016 on the coast of Sakhalin Island, cape Svobodny. Based on test results there were made conclusions on the possibility of increasing mobility of the ground robot and expanding its use. Specially designed underwater robot collects data using a video inspection system and a hydrostatic wave recorder with a string sensor. It has the ability to adjust the position of the center of gravity to increase stability when driving on steep slopes of the seabed. The surface robot was designed for conducting detailed bathymetry measurements of investigated water areas by means of a multi-beam echo sounder. Underwater and surface-based robots were tested in July 2017 on Sakhalin Island. Both robotic systems were merged into the united local network. The results of their operation were obtained to verify the data from measuring systems of the ground robot. In 2018, it is planned to conduct a series of tests involving the three robots and merging them into a local network to manage and process data in real-time.

Keywords: *coastal monitoring, marine hazards, Okhotsk Sea, Sakhalin Island, autonomous mobile robot*

1. INTRODUCTION

Tsunami waves, storm surges, wind wave, hurricane waves are very danger in the coastal zone of many states of Pacific. Several networks of buoys are developed in Pacific (DART, JMA, JAMSTEC, DONET, etc) to register large-amplitude waves in the open ocean and coastal zone; they are active used for forecasting of marine natural hazards having wave origin. Long-term prediction of hazardous waves should be based on knowledge on background characteristics of the wave climate in the same frequency range and variable bathymetry and topography in near-shore zone. The use of mobile robot systems that can significantly improve the efficiency of measurements. There are several ways of coastal monitoring, which are briefly described in [1].One of them is determination of the current situation in coastal areas by using satellites. However, satellite images have a lower resolution in comparison with the results of aerial photography and cannot be obtained with strong cloud cover. The possibilities of coastal zones characteristics researching by means of aircrafts are limited by the conditions of loading capacity and flight safety. Therefore, vehicles that move along the bottom of coastal areas are also used to research the characteristics of the coastal zone. Modern designs of such research systems are given in the papers [2, 3].

Currently, promising techniques of inspection of coastal zones are methods of remote sensing. Such methods are based on the use of sensors that provide information about the distance to an object based on scanning devices of the radio-waves range [4] or laser wave range [5, 6]. Laser methods allow obtaining high-resolution data, but the range is limited to several tens of meters. Radar stations allow capturing much larger area (several kilometers), so their application seems more perspective.

However, they have some disadvantages. The size of such stations is usually a few meters. They need a high-power source and installation on the mast. In addition, compared to laser devices that give information to an object in meters, the radar stations give only the value of the reflected signal intensity and require on-site calibration. Data in absolute values in any point getting to a scanning zone of radar station are necessary for calibration. Knowing absolute wave amplitude and signal strength in one point, it is possible to recalculate intensity into the wave height for a zone in which measurements are taken with the help of scanning devices.

For calibration of wave characteristics there can be used bottom pressure sensors of cable or autonomous types (Fig. 1). The device is made in stainless steel cases and have cylindrical shape. Quartz resonators are used as primary converters of physical quantities. The piezo-resonator elements have a low temperature dependence and high accuracy. There is pressure measuring range (immersion depth) up to 100 m; pressure accuracy 0.06%, temperature accuracy ± 0.3; ± 0.1 or ± 0.05 °C; operating temperature range from -4 to 40 Celsius degrees (°C). Autonomy of devices is about 6 months. Measurement resolution is 1 sec. This sensor was successfully used during our experiment in 2016 [7]. Nevertheless, the use of such sensors has some of disadvantages. Their installation requires the boat. To fix them to the bottom a holding weight is required. Autonomous sensors cannot be used in real-time mode, because the necessary information is only available after raising the sensors, and cable sensors require cabling to coast using the boat. When changing the place of the experiment, it takes a long time to move the sensor.

Fig. 1. Bottom pressure sensor

For express assessments of wave activity in the region through analytical and numerical mathematical models, in addition to the registration of the wave amplitude, detailed bathymetry of the researched water area is necessary. Such bathymetry can be obtained by scanning the water area with an echo sounder from a boat in the immediate measurement area. These factors reduce mobility of research, limit the number of experiments and require significant human and temporal resources.

Methods based on the use of mobile robots are devoid of many disadvantages and have proved themselves in experimental research in single robot configuration [8 – 10] and multi-robot configuration [11] as well. In this article, we propose a new methods and approaches for carrying out a complex measurement of wave climate based on a telemetrically group of ground, surface and underwater-based robots. A possible scheme of conducting experiments and the scheme of interaction of mobile robots are shown in Fig. 2.

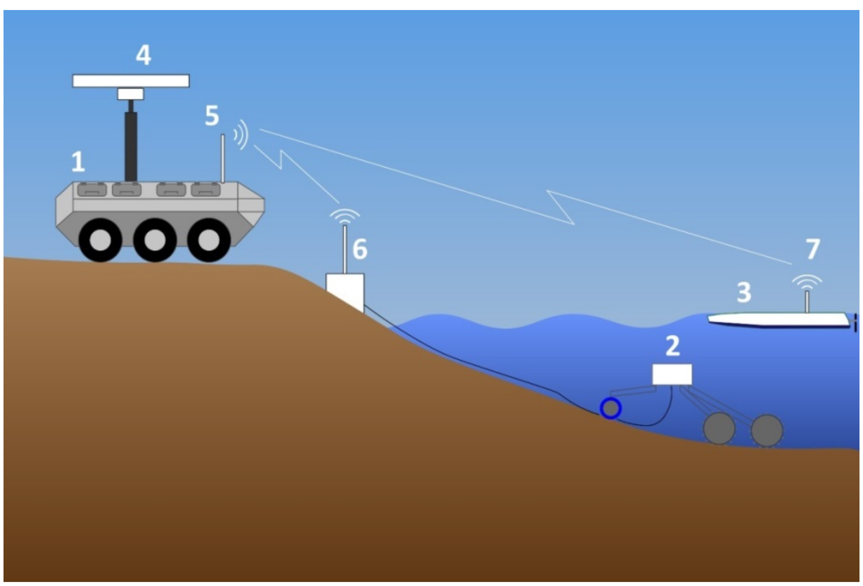

Fig. 2. Scheme of mobile robots interaction

The scheme of the experiment includes the use of three types of robots: ground (1), underwater (2) and surface (3). The robots can be controlled remotely or in autopilot mode. The ground robot has radar (4) for remote wave activity measurement and Wi-Fi transceiver (5). The robot collects information about the height of waves in a certain area by using the radar. The obtained data correspond to the intensity of the reflected signal.The underwater robot (2) is immersed to water and moves along the bottom. It is controlled by the cable connected to the base station (6) that also has Wi-Fi transceiver. The base stations of the underwater and the ground robots are connected to the local network. The task of the underwater robot is to find the wave height at one point in absolute values (meters) using a string sensor. The received data are sent via Wi-Fi to the onboard computer of the ground robot in real-time and after that the calibration of the radar is carried out. It is possible to translate the obtained data from the conventional values of signal intensity into absolute values in meters.

The surface robot (3) is also connected to the local network of the ground robot (1) via the Wi-Fi transceiver (7) and transmits the bathymetry data of the investigated zone. The onboard computer of the ground robot (1) carries out processing and binding data then sends it to the command center or to the operator's laptop. Let us consider details of the implementation of each robot and its description are discussed below.

2. GROUND ROBOT

Ground robots with a variety of equipment are widely used in environment measurement tasks [12-14] due to their ability to perform measurements in autonomous or semi-autonomous mode in hazardous and non-friendly environment. The autonomous mobile robotic system (AMRS) [15, 16] can conduct monitoring in all coastal conditions due to three various types of movers, Fig. 3. Wheeled mover is designed for using on solid ground bases, as well as dry and wet soils. Tracked type of the mover allows increasing the efficiency of the complex operation when driving in difficult areas, such as sandy terrain, wet soils, snow, etc. Rotor-screw mover can be used for work in conditions of wetlands, swamps, flooded areas of the terrain.

Fig. 3. General view of AMRS

The chassis is equipped with a 165 kW internal combustion engine, an automatic gear-box and a mechanical transmission. The general view of AMRS is shown in Fig. 3. The technical characteristics of AMRS are presented in Table 1. Also, the structure of the developed AMRS includes an add-on for the installation of devices on the mobile platform and the hardware part, Fig. 4.

Table 1. Technical characteristics of AMRC

Characteristics	Value
Mass, kg	1500
Engine power, kW	165
Maximum speed, km / h	45 – Wheeled mover 35 – Track mover
Fuel consumption l/100km	18
Dimensions	
Length, mm	3800
Width, mm	2100
Height, mm	1200
Ground clearance, mm	300
Angles of overhang (front and rear), degrees.	45
Model of tires	33x12,5 R15

The hardware consists of the following components: the radar station Mikran River MRS-1000, the weather station Vaisala WXT520, the light detection system LIDAR Sick LMS291Pro, the video camera AXIS Q6045-E, the high-precision mobile GPS/GLONASS receiver (OS-103). For controlling the measuring equipment, collecting, accumulating and processing data on AMRS, the on-board computer Adlink MXE-5400 is installed. Notebook Panasonic Toughbook CF-31WEUAHM9 is used for remote connection to the AMRS on-board computer via Wi-Fi, for viewing data and status of measuring equipment, sending commands to control measuring equipment. To control the movement of the AMRS there is used actuators controlled from the lower level controller based on a single-board computer Raspberry Pi 2.

The robotic system has two control interfaces. There is Tablet TOREX PAD 4G for remote movement control of the complex and the operator's laptop that allows transferring commands to start of the measuring equipment and to display conditions of the system operation. The AMRS passed successfully tests in July 2016 on Sakhalin Island. Test results showed that the approach of using various types of movers allows increasing mobility of the robotic system and expanding the area of its territorial using. Tests of chassis were conducted to check the design of the robot and research its mobility. Tests of functioning hardware, installed on board of the AMRS, were carried out.

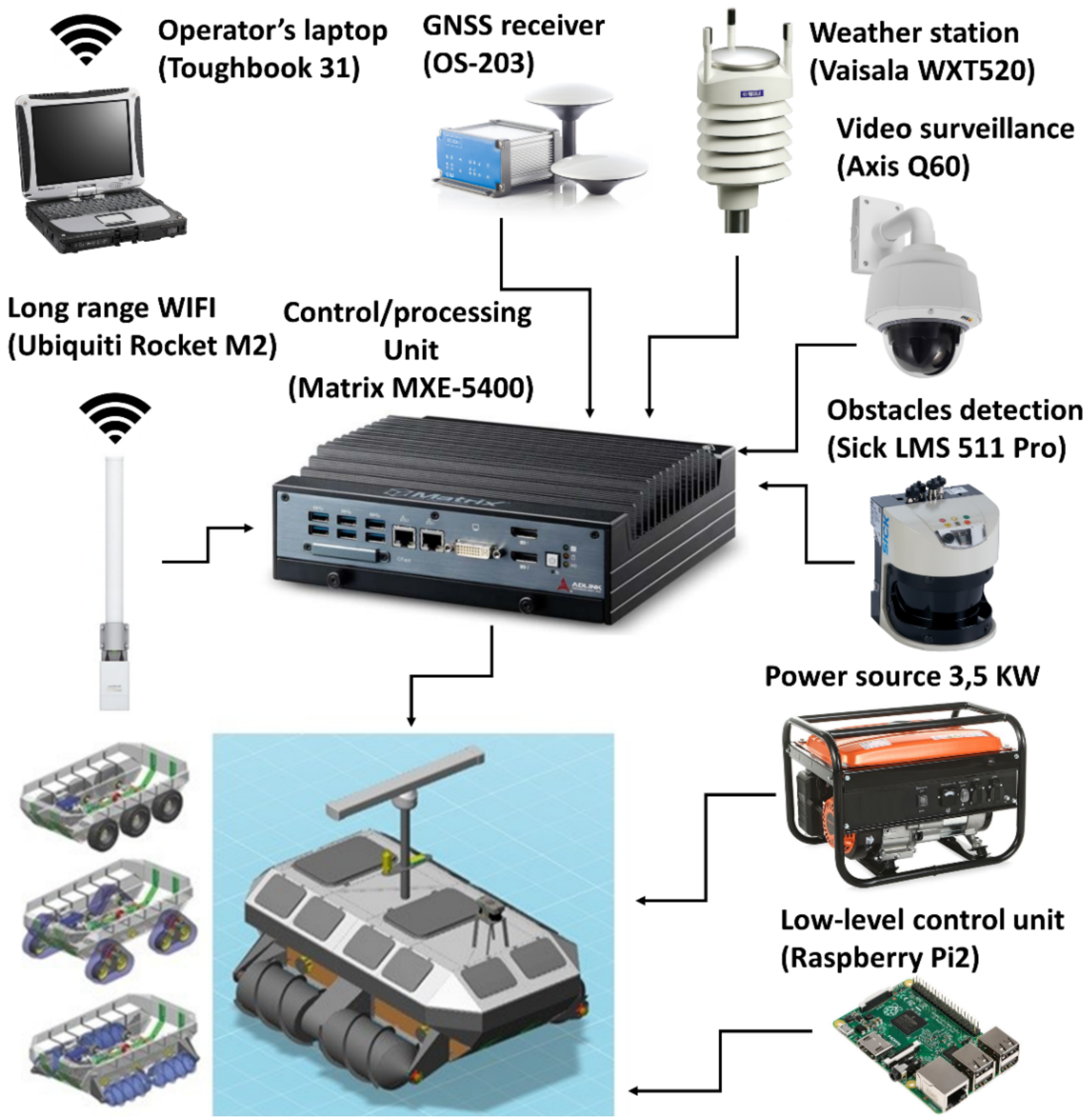

Fig. 4. Equipment of AMRS

Consider an example of processing experimental data obtained from the measuring equipment. Weather station Vaisala WXT520 is used for obtaining meteorological data, such as atmospheric pressure, relative humidity, precipitation, temperature, wind speed and direction. This equipment is resistant to flooding, priming and loss by evaporation during the measurement of precipitation. The meteorological complex is installed on the side part of AMRS with the possibility of fixing at different heights. It connects to the on-board computer via the serial port by the RS-485 interface and is configured for data transfer using the NMEA-0183 protocol.

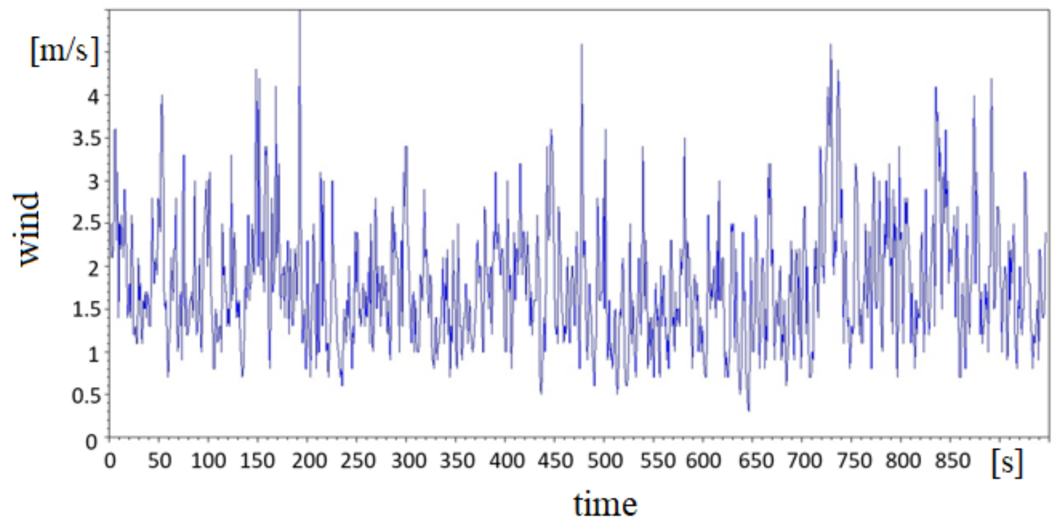

a)

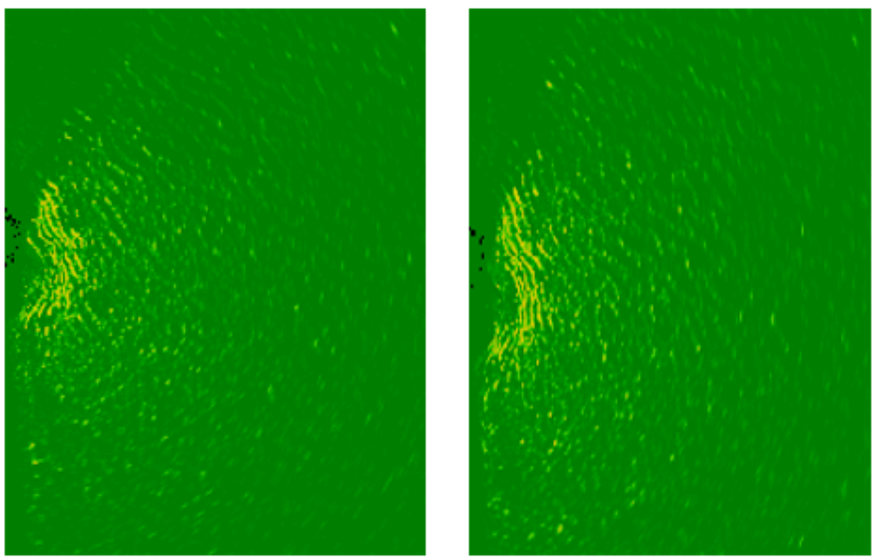

b)

Fig. 5. Graph of changing in the average wind speed during the measurements (*a*) and the screenshots of the radar (*b*)

The determination of wave parameters using the radar station Mikran "River" MRS-1000 is based on the dependence between the intensity of the reflected signal and the wave height. The power of the reflected echo signal from the sea surface is different depending on force and type of sea waves. Screenshots of the software complex's operation for recording the intensity of sea waves and an example of the meteorological data are shown in Fig. 5.

The robotic system is equipped with the AXIS Q6044-E camera and receives a video stream synchronized with the radar. An example of video, recorded during the test, is shown in Fig. 6.

Fig. 6. Video from camera during the tests

3. UNDERWATER ROBOT

Underwater robots are essential equipment for in situ measurements due to difficulty of accessing the environment by researches. However, their configuration may significantly depend on the task. Typical tasks for this class of robots are surveying, inspection, in situ measurements of water samples. Most commonly used configurations are represented by floating in the water robots [17-19]. For our task we propose bottom robot since typical target depth for this robot is 1-3 meters and bottom robot provide better stability in coastal areas with intensive water fluctuations.

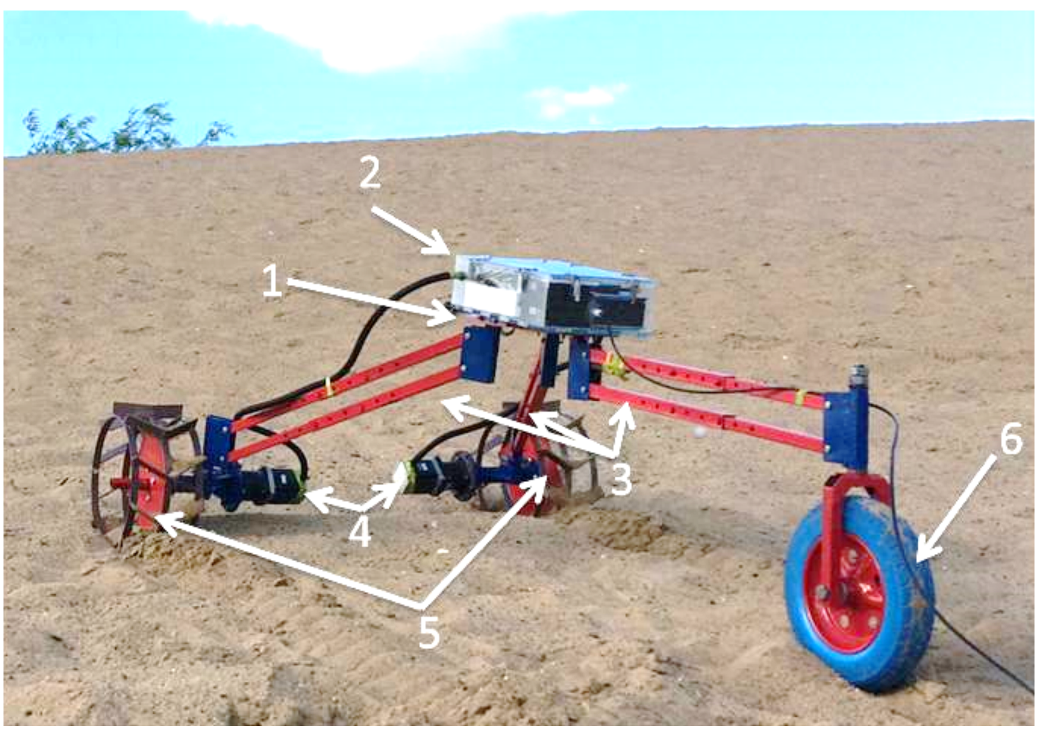

Fig. 7. General view of AMV

Amphibious mobile vehicle (AMV) is consisted of several main components, Fig.7: 1 - supporting platform, 2 - sealed container with measuring equipment, 3 - adjustable levers, 4 - stepper motors, 5 - driving wheels, 6 - support wheel. The AMV collects data using a video inspection system (Fig. 8a) and a hydrostatic wave recorder with a string sensor (Fig. 8b) fixed on the body of the vehicle. The operation of the string sensor is the work of the capacitor plates between the dielectric. Conductors are water and copper wire.

a)

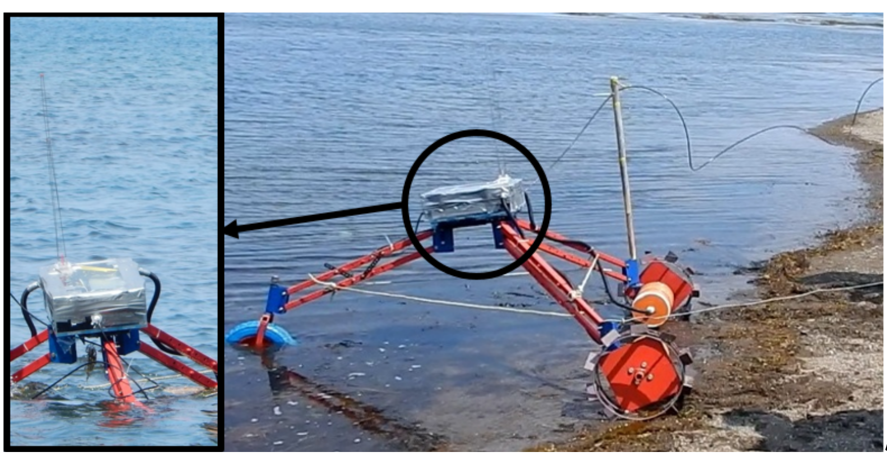

b)

Fig. 8. *a* – fragments of the video inspection system operation at the entrance to water; *b* – string sensor for research conducting

AMV has the ability to adjust the position of the center of gravity to increase stability when driving on steep slopes of the seabed and with significant hydrodynamic effects. Adjustment in the vertical plane is done by reducing or increasing the lengths of each lever, Fig. 9. The maximum length of the arm is 920 mm, the minimum is 770 mm. The adjustment in horizontal plane is done by changing the angle between the levers of drive wheels, Fig. 10. The minimum angle is 39°, the maximum angle is 119°. The axes of motion of the driving wheels are diverged when the positions of the mass center in the two planes are changed. This leads to a mismatch in the direction of the action of traction forces, increasing force of resistance to movement and loss of controllability of the AMV. An adjustment node is used to correct this problem. It allows changing the position of the direction of the motion axes of the driving wheels and turning them in parallel with an accuracy of ± 1 degree.

At this stage, the change in the position of the center of gravity of underwater robot occurs manually. Before the tests, the operator changes the parameters of the robot arms depending on the angle of the bottom of the shore, obtained from the results of bathymetry using a remote-controlled research boat. The use of this type of construction increases the patency of the complex and allows you to do the task set by the operator. In the future, it is planned to use servos for remotely change the geometric parameters of the robot according to the tilt sensor data to keep a position of the container with the measuring equipment close to horizontal and vertical positioning of the string sensor at AMV moving. Electronics of AMV consists of control and power parts. The control part is including a single-board computer Raspberry Pi2. Other sensors are connected to Raspberry Pi 2: a tilt sensor based on a gyroscope MPU-6050, a string sensor for recording the wave height, a Logitech C920 video camera, and a power supply Energizer PB. Controlling is carried out remotely via Ethernet cable from the coastal or through Wi-Fi if the cable is connected to a buoy floating on water surface. The power section consists of two stepped motors with reducers (1:10) and drivers of stepper motors OMD-88. Power supply is lithium battery 48V 10Ah. This power supply is enough for 4 hours of continuous movement that allows conducting the several experiments on immersion. The motors are controlled via the Step/Dir interface, Fig. 11.

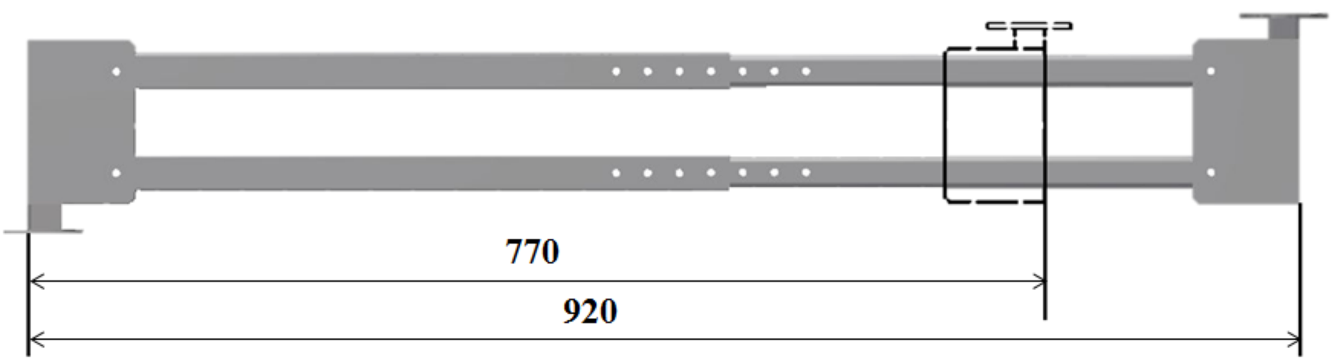

Fig. 9. Adjusting the position of the center of gravity in vertical plane

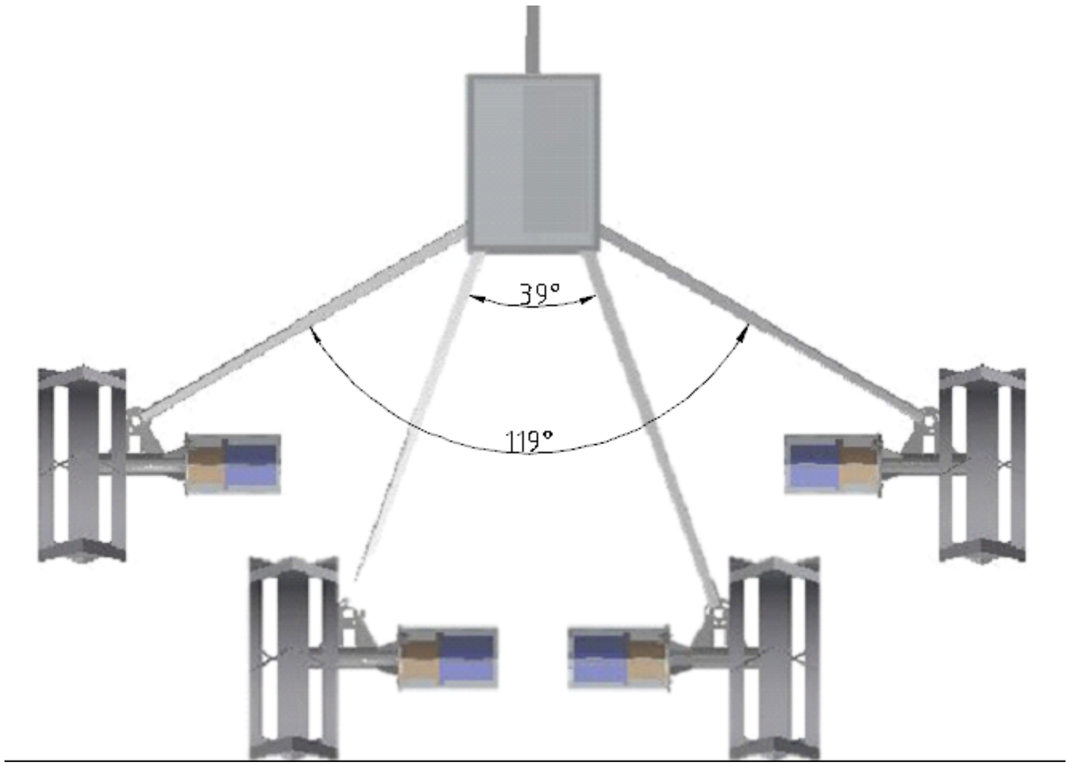

Fig. 10. Adjusting the center of gravity in horizontal plane

As mentioned above, AMV is controlled by a cable connected to the base station, located on the coast and containing a Wi-Fi transceiver that sends control signals from the AMRS and receives data on the value of the wave height (in meters). This data is necessary to recalculate the relative values of signal intensity obtained from radar in absolute values.

During the experiments, it was revealed that winding underwater vegetation takes place on the propeller and AMV design elements. There was an entanglement of the control cable when the chassis landed on the shore. In addition, it was fixed winding the cable on the propeller and its breakage. Therefore, it was decided to use a buoy equipped with a Wi-Fi transmitter instead of laying the underwater cable.

4. SURFACE-BASED ROBOT

Remote-controlled research boat (RCRB) is designed for conducting detailed bathymetry measurements of the investigated water area. This type of robots is very efficient for ocean exploration using on board sensors [20-21] like bathymetry recording [22]. It allows building a depth map quickly with a multi-beam echo sounder. The robot is shown in Fig. 12.

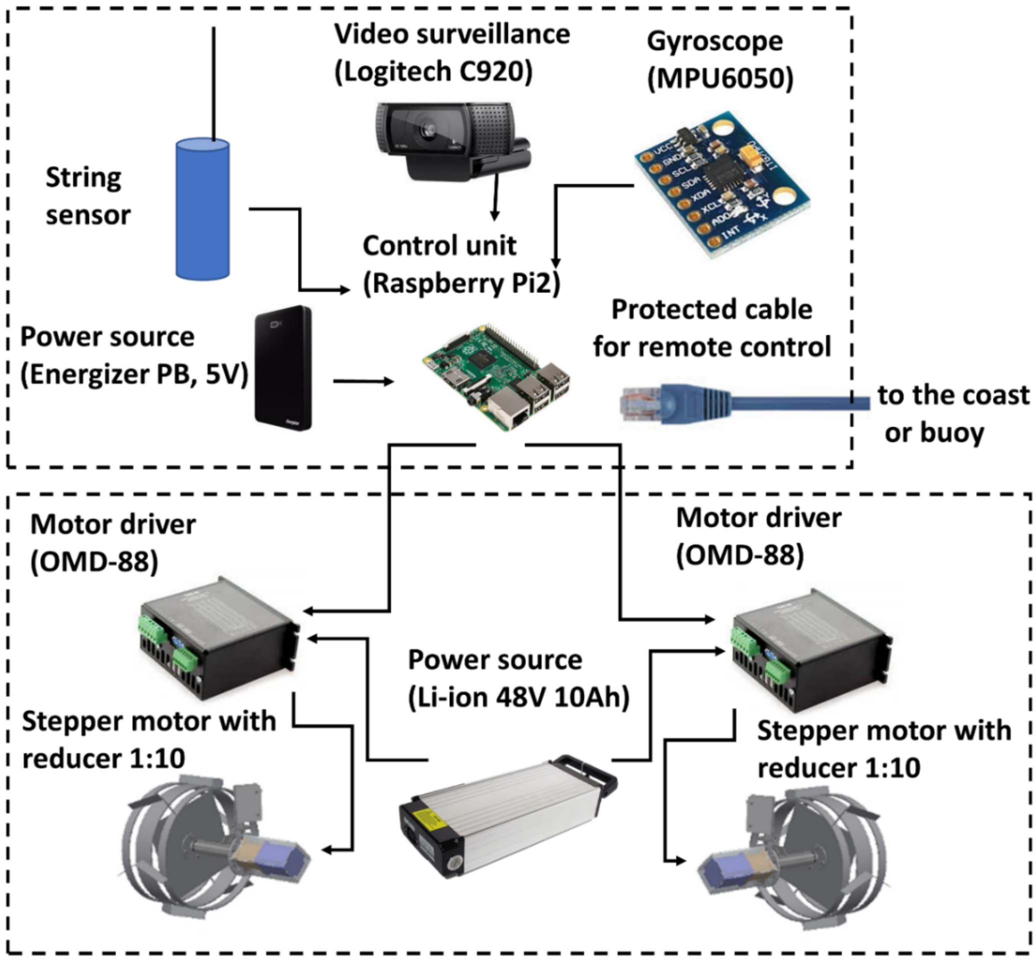

Fig. 11. Equipment of AMV

Fig. 12. Remote-controlled research boat

The development of the remote-controlled research boat was carried out by specialists of the Special Design Bureau for Automation of Marine Research, Far Eastern Branch of the Russian Academy of Sciences. They have extensive experience in creating research systems and conducting scientific research in the field of oceanology, hydro-acoustic research, hydro-physical and hydrodynamic processes, the interaction of atmosphere and ocean, dangerous marine phenomena and safety of seafaring. Equipment installed on board of the robot is shown in Fig. 13. The developed robot conducts amplitude and phase scanning of the bottom. The echo sounder software allows you to build a depth map of the seabed. This card is sent to the ground robot for further analysis.

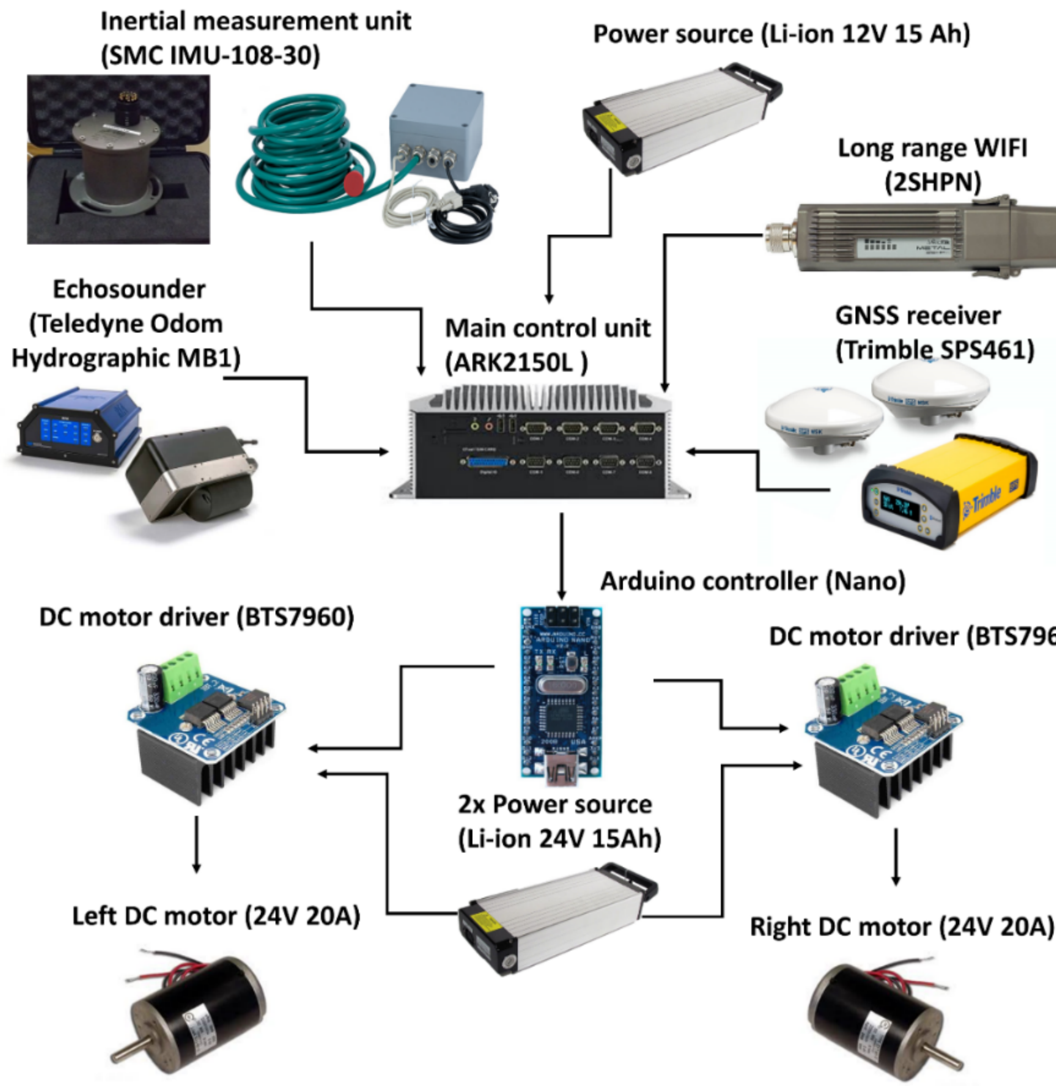

Fig. 13. Equipment of RCRB

The trimble SPS461 GNSS receiver is used for positioning of the robot. The IMC-108-30 SMC is used to find the robot's tilt parameters. The bathymetry data is collected by the Teledyne MB1 multi-beam echo sounder. Data processing and robot control are carried out by the protected computer ARK2105L with a separate power source 12V 15Ah. The power section is based on two direct current motors. The BTS7960 and arduino nano drivers are used as the driver controller. The RCRB control is carried out remotely. Maneuvering is performed by changing the speed of rotation of the right and left motors. Communication with the robot is provided with the help of the Wi-Fi module of the increased range of action on the basis of the access point MikroTik 2SHPN.

5. EXPERIMENT

In July 2017 there were conducted experiments AMV and RCRB functioning. Three expeditions were conducted in coastal zones of the Sea of Okhotsk on Sakhalin Island: at Cape Svobodny, Fig. 14.

Fig. 14. Place of experiments conducting (red point – cape Svobodny)

The terrain is characterized by the small depth of 2-4 meters for several hundred meters away from the coast. The AMV was immersed in water by remote control for a distance of about 50 meters from the coast and a depth of about 2 meters, Fig. 15.

At the same time, bathymetry data was collected using by the surface robot that controlled by a remote operator. An access point Ubiquiti was installed on the coast and the AMV control cable was connected to it, Fig. 15. Thus, both robotic devices were joined into the united local network.

Fig. 15. Immersion of AMV

The wave height data was collected for 60 minutes and displayed in real time on the operator's laptop. Also, the recording of wave height data was duplicated on the on-board computer of the AMV, Fig. 16.

The AMV can be used to verify data received from a radar station installed on a large-scale research chassis for working in a group of mobile ground-based and surface-based robots necessary for comprehensive research of wave dynamics.

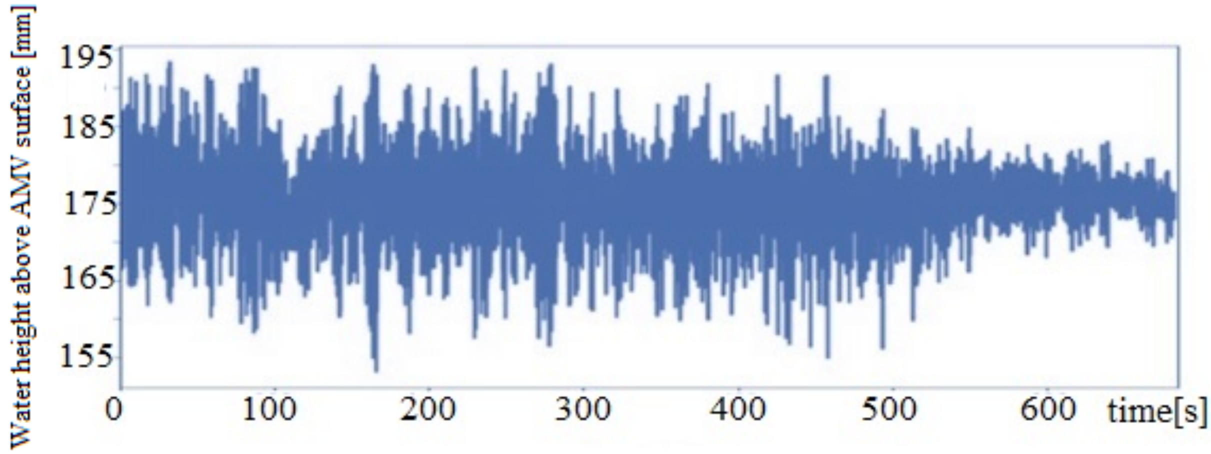

Figure 16. Data obtained by the string sensor of AMV

5. CONCLUSIONS

For registration of the hazardous waves (tsunami, storm surges, wind waves) and background wave climate, several robot system are developed. Also we examine the risk factors for carrying out monitoring of coastal zone. Disadvantages of existing methods have been identified and ways of their solutions have been determined. New perspective methods and approaches have been proposed for effective measurement in coastal zones using a group of mobile ground, underwater and surface-based robots. We present here results of some tests in natural conditions on Sakhalin Island in the Okhotsk Sea.

The registration of waves by different types of sensors simultaneously allows us to overcome these disadvantages of separate measuring instruments. The use of mobile robots, worked in different environments, allows achieving high mobility and efficiency of conducting experimental researches and surveying long coastal areas in a short time that is necessary for instance for post-tsunami surveys.

ACKNOWLEDGEMENTS

This study was initiated in the framework of the state task program in the sphere of scientific activity of the Ministry of Education and Science of the Russian Federation (projects No. 5.4568.2017/6.7 and No. 2.1433.2017/4.6) and financially supported by this program, grant of the President of the Russian Federation No. NSh-2685.2018.5 and grant from Russian Fund for Basic Research (18-05-80019- program “Dangerous phenomena”).

References

1. Kurkin A., Belyakov V., Makarov V., Zeziulin D., Pelinovsky E. Methods of tsunami detection and of post-tsunami surveys. *Science of Tsunami Hazards*. 2016. V. 35. No. 2. P. 68-83.

2. Surfzone Crawler 1. Available at: http://my.fit.edu/~swood/AUV_Crawler1.html (accessed 12 July 2018).

3. The SPROV'er. Available at http://my.fit.edu/~swood/SPROVER/The%20SPROV'er.htm (accessed 12 July 2018).

4. Cheng H., Chien H. Implementation of S-band marine radar for overwater wave measurement under precipitation. *Remote Sensing of Environment*. 2017. V. 188. P. 85-94.

5. Park H.S., Sim J.S., Yoo J., Lee D.Y. Breaking wave measurement using terrestrial LIDAR: validation with field experiment on the Mallipo Beach. *Journal of Coastal Research*. 2011. V. 64. P. 1718-1721.

6. Martin K., Bonneton P., Frappart F., Detandt G., Bonneton N., Blenkinsopp C.E. High frequency field measurements of an undular bore using a 2D LiDAR Scanner. *Remote Sensing*. 2017. V. 9. P. 2-14.

7. Zaytsev A., Belyakov V., Beresnev P., Filatov V., Makarov V., Tyugin D., Zeziulin D., Pelinovsky E., Yalciner A., Yalciner B., Oshmarina O., Kurkin A. Coastal monitoring of the Okhotsk sea using an autonomous mobile robot. *Science of tsunami hazards*. 2017. V. 36. No. 1. P. 1-12.

8. Incoul A., Nuttens T., De Maeyer P., Seube N., Stal C., Touzé T., De Wulf A. Mobile laser scanning of intertidal zones of beaches using an amphibious vehicle. *INGEO 2014: 6th Int. Conference on Engineering Surveying*, Prague, Czech Republic, 2014. P. 87-92.

9. Wood S. Modular amphibious research crawler. *Sea Technology*. 2006. V. 47. No. 2. P. 71-77.

10. Wübbold F., Hentschel M., Vousdoukas M., Wagner B. Application of an autonomous robot for the collection of nearshore topographic and hydrodynamic measurements. *Coastal Engineering Proceedings*. 2012. V. 1. No. 3. P. 2133-2143.

11. Dong-Woo M., Hyeon-Seung K., Hyun-Sik K. Collaborative control method of underwater, surface and aerial robots based on sensor network. *Transactions of the Korean Institute of Electrical Engineers*. 2016. V. 65. No. 1. P. 135-141.

12. Morita M., Nishida T., Arita Y., Shige-eda M., Maria E., Gallone R., Giannoccaro N. Development of robot for 3D measurement of forest environment. *Journal of Robotics and Mechatronics*. 2018. V. 30. No. 1. P. 145-154.

13. Jilek T. Autonomous field measurement in outdoor areas using a mobile robot with RTK GNSS. *IFAC-PapersOnLine*. 2015. V. 48. No. 4. P. 480-485.

14. Qian F., Jerolmack D., Lancaster N., Nikolich G., Reverdy P., Roberts S., Shipley T., Van Pelt S., Zobeck T., Koditschek D. Ground robotic measurement of aeolian processes. *Aeolian Research*. 2017. V. 27. P. 1–11.

15. Kurkin A., Pelinovsky E., Tyugin D., Kurkina O., Belyakov V., Makarov V., Zeziulin D., Unmanned ground vehicles for coastal monitoring. *International Journal of Imaging and Robotics*. 2017. V. 17. No. 1. P. 64-75.

16. Kurkin A., Tyugin D., Kuzin V., Chernov A., Makarov V., Beresnev P., Filatov V., Zeziulin D. Autonomous mobile robotic system for environment monitoring in a coastal zone. *Procedia Computer Science*. 2017. V. 103. P. 459-465.

17. Harvey J., Ryan J., Marin R., Preston C., Alvarado N., Scholin C., Vrijenhoek R. Robotic sampling, in situ monitoring and molecular detection of marine zooplankton. *Journal of Experimental Marine Biology and Ecology*. 2012. V. 413. P. 60-70.

18. Aro E. The uility of an autonomous multi-robot system of underwater floats. *IFAC Proceedings Volumes*. 2012. V. 45. Iss. 28. P. 55-59.

19. Chocron O., Vega E., Benbouzid M. Dynamic reconfiguration of autonomous underwater vehicles propulsion system using genetic optimization. *Ocean Engineering*. 2018. V. 156. No. 15. P. 564-579.

20. Seegers B., Teel E., Kudela R., Carod D., Jones B. Glider and remote sensing observations of the upper ocean response to an extended shallow coastal diversion of wastewater effluent. *Estuarine, Coastal and Shelf Science*. 2017. V. 186. No. 15. P. 198-208.

21. Fumagalli E., Bibuli M., Caccia M., Zereik E., Del Bianco F., Gasperini L., Stanghellini G., Bruzzone G. Combined acoustic and video characterization of coastal environment by means of unmanned surface vehicles. *IFAC Proceedings Volumes*. 2014. V. 47. Iss. 3. P. 4240-4245.

22. Ying J., Zhiguo Y., Zongwei L., Chunmei Y. High-resolution bottom detection algorithm for a multibeam echo-sounder system with a U-shaped array. *Acta Oceanologica Sinica*. 2018. V. 37. No. 7. P. 78-84.

ISSN 8755-6839

SCIENCE OF TSUNAMI HAZARDS

Journal of Tsunami Society International

Volume 37 Number 3 2018

EVALUATION OF THE TSUNAMI VULNERABILITY IN THE COASTAL ECUADORIAN TOURIST CENTERS OF THE PENINSULAS OF BAHIA DE CARÁQUEZ AND SALINAS

Andres Sebastian Matheus-Medina[1], Theofilos Toulkeridis[1]*, Oswaldo Padilla-Almeida[1], Mario Cruz-D´Howitt[1] and Kervin Chunga[2]

[1]Universidad de las Fuerzas Armadas ESPE, Sangolquí, Ecuador
[2]Universidad Estatal Península Santa Elena UPSE, Salinas, Ecuador

*Corresponding author: ttoulkeridis@espe.edu.ec or theousfq@yahoo.com

ABSTRACT

Potential occurrences of tsunamis are the main coastal hazards for the highly touristic peninsulas of Bahía de Caráquez and Salinas in Ecuador. Their hotel infrastructure is of top quality, in addition to having a significant population density at the natonal level. The current study aims to identify the vulnerabilities of the population in order to reduce the tsunami hazard level, and to protect the physical integrity of the present population. Thus, in both cities we have obtained results about the vulnerabilities of basic services, socioeconomic, structural characteristics, community organization and communal services, risk perception as well as communication channels with their respective maps that allow their spatial location. The overall vulnerability results of the conducted analysis demonstrated that there is a medium to high vulnerability for the population of Salinas while Bahía de Caráquez the vulnerability is medium to low. Vulnerability for basic services has a high value of about 80%, while the socioeconomic vulnerability is of about 60%, in both cities. The structural characteristics of the two cities are quite different. Salinas is considered an area of higher surplus value with earthquake-resistant buildings and quality construction materials, a fact almost absent in Bahía de Caráquez, in their respective piers. While within the study areas the predominant structural characteristics are of a modest nature, both from the point of view of movable property and as construction materials. Therefore, the vulnerability for the two cities based on infrastructure is medium to high (60-80%). The community organization and communal services in both cities have a low vulnerability value (40%). The vulnerability of risk perception in Salinas is low (40%) while in Bahía de Caráquez it has a very high vulnerability (100%). Vulnerability by means of communication in the two cities reaches a very low value (20%), due to the fact that the road network is in optimal conditions.

Keywords: Tsunami, Vulnerability, Risk assessment, Evacuation plans, Ecuador

1. INTRODUCTION

Vulnerability studies within the context of natural hazards demonstrate the state or grade of preparedness or response towards an unfortunate situation due to internal or external forces. As a disaster is defined to be the sum of vulnerability plus the hazard(s), then studies or research of vulnerabilities need to be elaborated in the same detailed way as we analyze hazards (Cannon, 2000). The growing awareness of the research of a variety of vulnerabilities of different hydrometeorologic or geologic hazards strengthen the evaluation of the grade preparedness of an exposed public or their infrastructure (Varley, 1994; Cannon, 1994; Cutter, 1996; Morrow, 1999; Cannon, 2000; Paton & Johnston, 2001; Alcantara-Ayala, 2002; Turner et al., 2003: Pelling, 2003; Thomalla et al., 2006; Adger, 2006; Blaikie et al., 2014; Pararas-Carayannis, 2018). Vulnerability studies or assessments about tsunami hazards are scarce but not rare, where such methods have been applied considering the past and potential future tsunami impacts with the worse-case scenario (Papathoma & Dominey-Howes, 2003; Papathoma et al., 2003; Birkmann, & Fernando, 2008; Cochard et al., 2008; Calgaro, Lloyd, 2008; Khasalamwa, 2009; Wood et al., 2010; Omira et al., 2010; Leone et al., 2011; Shimozono, & Sato, 2016; Madani et al., 2017).

Due to the tsunami disasters in recent times in Chile (2010) and Japan (2011), which both attract a high concern of potential impacts and the corresponding vulnerability in the coastal area on Ecuador (Fritz et al., 2011; Vargas et al., 2011; Mori et al., 2011; Muhari et al., 2011; Brizuela et al., 2014). Therefore, as the Ecuadorian government has been recently aware of potential damages from regional and local tsunamis, Ecuador opted to evaluate the associated risks of any tsunami impacts in touristic centers. These particular touristic sites have been easily identified to be represented by the highly-visited peninsulas of Bahia de Caráquez and Salinas in the coastal provinces of Manabí and Santa Elena, respectively. Its hotel infrastructure is of first quality, besides having a significant population density at the cantonal level. The occurrence of a tsunamigenic event in these cities would cause great affection because most of its inhabitants are settled in areas of high risk of flooding by tsunami and the times of evacuation of the population are greater than those of arrival of the first wave (Matheus et al., 2016).

Therefore, the main aim of this study has been to identify the areas of influence for tsunami events and the areas of greater and lesser vulnerability in Bahia de Caráquez and Salinas. The development of this research is aimed at identifying the vulnerabilities of the population in order to revert the level of risk to which they are subjected, and to safeguard the physical integrity of the population immediately, at the first tsunami alert on the coasts of the selected cities. The final result of the study will provide very high-value information that will feed back to the municipalities and the population in potential danger.

2. GEODYNAMIC SETTING

In Ecuador appear the northern Andes, which are part of the 7000 km long classical example of an active continental margin along the South American continent with several volcanic sequences of Mesozoic and Cenozoic ages (De Mets et al., 1989; Trenkamp et al., 2002; Toulkeridis, 2013; Toulkeridis and Zach, 2017). Variations of the volcanic sequences are displayed within the observed geotectonic structures and have evolved due to different subduction geometries along the margin as well as the subduction angle of the subducting plate underneath Southern and Central America (Kellogg and Vega, 1995). In the north, the Cocos plate is subducted underneath the Central American plate, while further to the south the Nazca Pazific plate, is subducted with an angle slightly oblique to the southern American continent producing an overall active tectonic regime with transpression due to its convergence (Fig. 1; Shumway, 1954; Daly, 1989; Gutscher et al., 1999). This Nazca Plate incorporates the aseismic Carnegie Ridge, which was produced by the passage of the ESE moving Nazca Plate over the Galapagos hot spot (Shumway, 1954; Lonsdale, 1978; Freymuller et al., 1993; Jaillard et al., 1995; Toulkeridis, 2011).

The propagation of deformation towards the continent seems to be influenced also by the collision (and mechanical coupling) of the Carnegie Ridge below the South American continent (Gutscher et al., 1999; Dumont et al., 2014). Deformation is partitioned in a NNE-SSW trending strike-slip and reverse faults (Hughes and Pilatasig, 2002). The South American continent itself is composed of two different continental plates, the Caribbean and South American continental plates, of which contact is represented by a transformal or strike-slip fault named Guayaquil-Caracas Mega-Fault or Shear, which extends from the Gulf of Guayaquil in Ecuador until Venezuela (Kellogg and Vega, 1995; Dumont et al., 2005).

As result of both, the collision and subsequent subduction between the Nazca oceanic and the Caribbean with the South American continental plates as well as the movement of the referred Mega-Fault, extreme destruction by a variety of landslides, earthquakes and tsunamis have been manifested in past along the subduction trench and along and aside the fault with high losses of both, life and infrastructure (Barazangi and Isacks 1976; Mendoza and Dewey, 1984; Atakan, 1995; Tibaldi et al., 1995; Pararas-Carayannis, 2012; Chunga, and Toulkeridis, 2014; Parra et al, 2016; Toulkeridis et al., 2018). Therefore, strong earthquakes with catastrophic results for life and infrastructure occur in regular form in the Ecuadorian territory. In a time period of almost five centuries since 1587 until recent times more than 140 earthquakes destructed parts of cities and urban areas, with a total fatality sum of more than 80,000 deaths (Fig. 2; Kahn, 2005; Toulkeridis et al., 2017a).

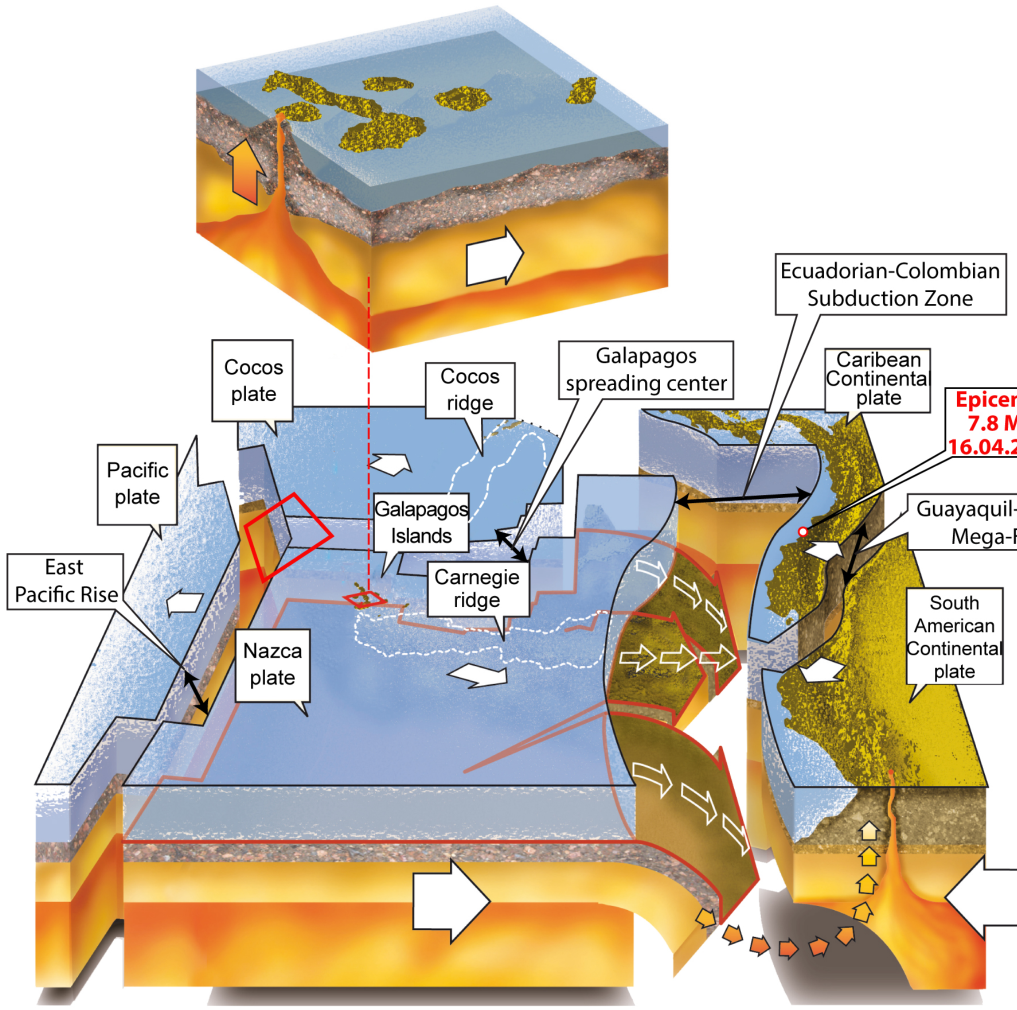

Figure 1: Geodynamic setting and associated continental and oceanic plates as well as plate boundaries of the surrounding of Ecuador, the Galapagos Islands and the Carnegie Ridge. In red has been indicated the most recent epicenter. Adapted from Toulkeridis, 2013 and Rodriguez et al., 2016.

Of these telluric movements, more than 96 (+X) earthquakes had an intensity of VI to VII, another 25 (+X) earthquakes had an intensity of VIII while some 12 (+X) had an intensity equal or higher IX on the international Mercalli Scale. Remarkable of these seismic events have been those at 1797 (XI), 1868 (X) and that of 1949 (X) (Engdahl and Villasenor, 2002; Beauval et al., 2010; USGS/NEIC, 2017). From 1900 until 2017, some 65 seismic events occurred in the area of Ecuador surpassing 6,0 and reaching up to 8,8 in 1906 on the Richter Scale (USGS/NEIC, 2017). The three last earthquakes with a high number of fatalities have been a 6.8 Mw in 1949 with 6,000 deadly victims (Ganse, and Nelson, 1982; Housner, 1984;), a 6.9 Mw in 1987 with more than 1100 deaths (Berz, 1988; Tibaldi et al., 1995; Schuster et al., 1996), and a 7.8 Mw in 2016 with 663 fatalities (Ye et al., 2016; Toulkeridis et al., 2017a; b; Navas et al., 2018).

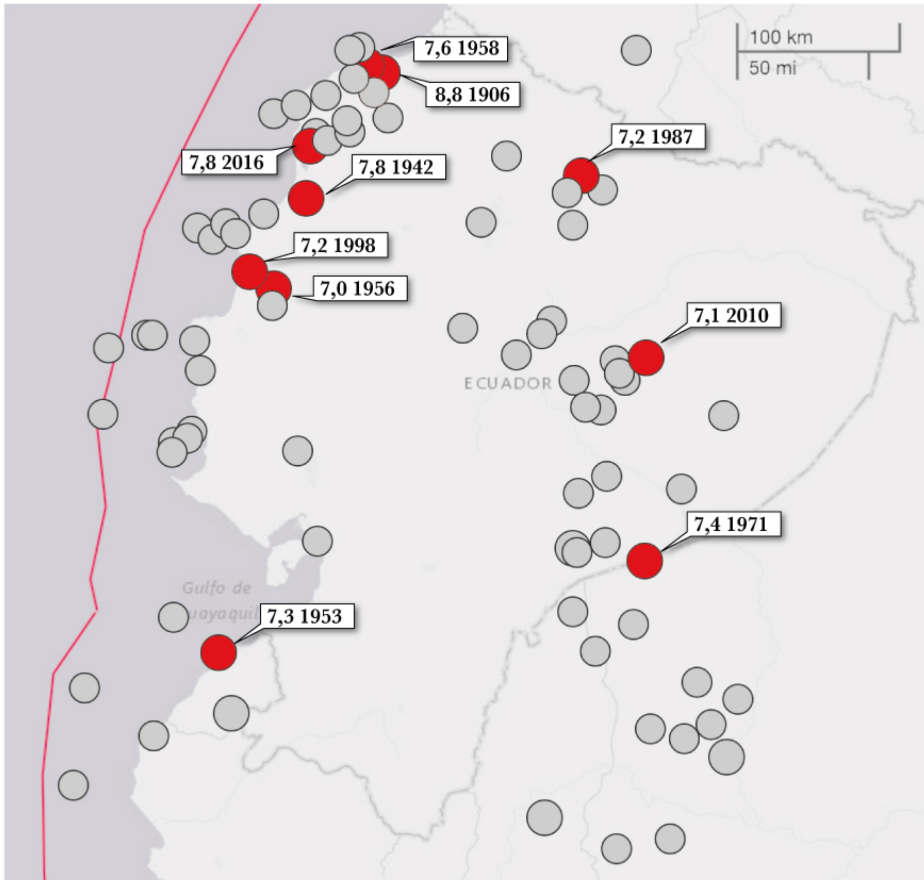

Figure 2: Seismicity of Ecuador from 1900-2017, with epicenters superior 6,0 on the Richter Scale based on the archive and catalogue of the United States Geological Survey (USGS/NEIC, 2017).

3. LOCATION OF THE STUDIED SITES

The coastal territory constitutes a great resource of tourist exploitation since it counts on attractive spas and beaches for the national and international tourists. The most visited coastal sites in Ecuador are Bahía de Caráquez and Salinas, which have a very advanced infrastructure and tourist services. Hereby, the westernmost peninsula of Ecuador constitutes the Santa Elena province, of which canton Salinas is made up of six parishes (Carlos Larrea, Alberto Gallo, Vicente Rocafuerte, Santa Rosa, José Luis Tamayo and Anconcito). This canton has a population of 68,675 inhabitants and a population density of 1007.40 persons per km^2, and is characterized by having a young population as 48.8% of the population comprises people younger than twenty years. For the present study, we used data of urban population of the canton that corresponds to 29,294 inhabitants. (Population Census 2010, GAD Salinas, 2011).

The city of Salinas has two coastal fronts, being South and North. The southern coast (Mar Bravo) does not yet have a high population density and land use is predominantly for the production of salt, (Fig. 3), which constitutes an important economic activity of the canton.

The elevated western coast is occupied by the military bases of the Air Force and Navy, respectively. In the northern coast the main economic activity of the city is carried out, being the tourist sector, since in the area are the main hotel complexes with buildings up to 20 floors. The hotel zone is where the level of the tide reaches the highest level, so the seawall has been protected with walls of cast iron (Fig. 4)

Figure 3: Aerial view of the beach, hotel and commercial area of northern Salinas as well as uninhabited southern area of the peninsula. Courtesy by Marco Villavicencio.

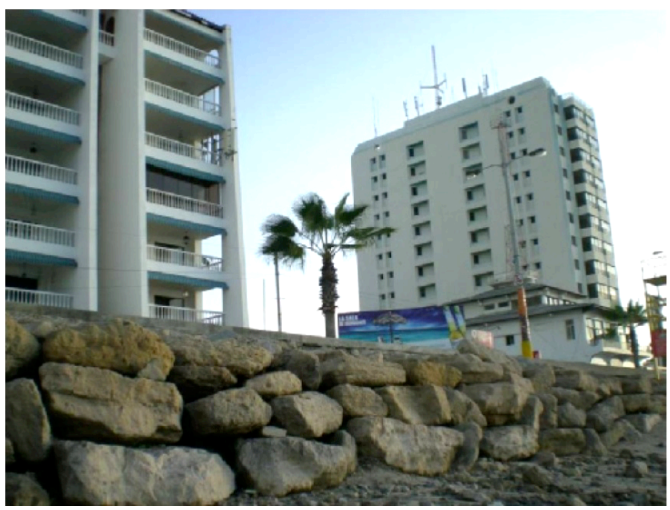

Figure 4: Cast rock-wall around the boardwalk of Salinas

Bahía de Caráquez is located in the northern side of the province of Manabí, forming part of the canton Sucre, that counts on a population of 57,159, a population density of 143,55 persons per km^2, that in the majority is considered young since 46.4% are younger than twenty years of age. For the present study, we have used data of the City of Bahía de Caráquez, which counts on a population of 24,963 inhabitants. At the western edge of Bahía de Caráquez is located the pier Virgilio Ratti in which are several buildings with departments of six to ten floors, while in the center-south zone occur many particular buildings with five floors of average height (Fig. 5).

Figure 5: Aerial panoramic view of the city of Bahía de Caráquez. In the center of the image is the bridge, which connects Bahía with the city of San Vicente. In the lower left part of the picture is situated the pier Virgilio Ratti. Taken from the west. Courtesy by Galahar

Horizontal evacuation is not possible in the pier Virgilio Ratti. In the southeastern zone is the so - called Port Amistad in which tourists sail boats from different areas and the Bahía - San Vicente bridge joins these two localities. In this area, there are private houses with two to three floors on average (Fig. 5). To the southwest is the area called "Mirador La Cruz" where there are modest single or double-storey houses of mixed materials (block, wood, zinc) in usually poor condition. Although this area is an elevated zone, and might be used as safe against flooding, it is still a zone of high risk for landslides and therefore not recommended to be used as zone of security towards incoming tsunamis (Fig. 6).

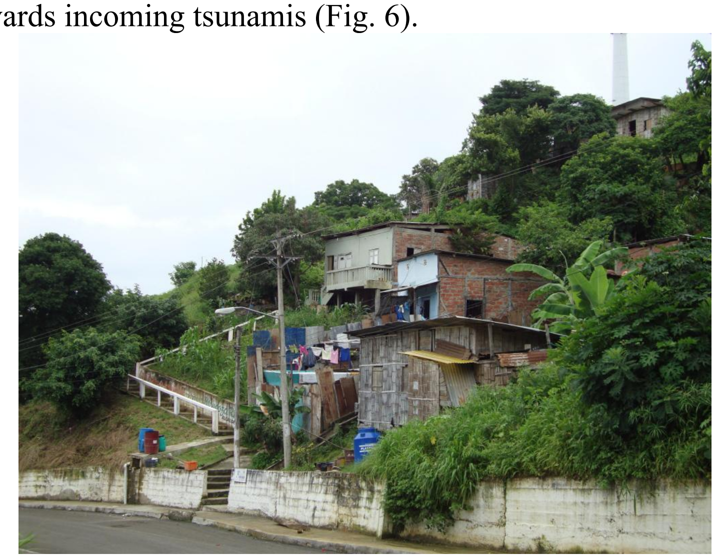

Figure 6: Type of housing in the suburb “La Cruz”.

4. METHODOLOGY

a) Definition

Vulnerability is defined as the weakness or susceptibility of a population, building or infrastructure to suffer damage of such magnitude that it changes its life condition in the case of a population or that it exceeds the capacity of resistance for which it has been designed in case of a building or other structure, due to an adverse event of natural or anthropic origin. There are detailed studies that also address vulnerabilities of natural, physical, economic, social, technical, structural, basic or community services, risk perception and communication pathways (Wilchez-Chaux, 1993). However, the most important vulnerability modifiers are highlighted, such as physical, economic and social (Anderson, 1995; Levine, 2004; Adger, 2006; Birkmann, 2006; Blaikie et al., 2014).

Physical factors refer to the geographical location of human settlements, in areas at risk, such as settlements near the riverbed, which tend to be more vulnerable to flooding than those located in more distant places, as well as a population seated on the slopes of a volcano, will be more vulnerable of being affected by an eruption than one that is far from the volcano. The economic factor has a direct influence on the risk management process, as the lack of sufficient financial resources would not allow to perform plans or projects, which need to deal with a possible disaster, so infrastructure may not be constructed seismic resistant. All these shortcomings lead to a greater level of vulnerability to the possible occurrence of a destructive event. Finally, the social factors refer to the culture of a population, its ideology and education, the same ones that are conjugated when reacting to a situation of a threat. In the same way, it influences the acceptance and reception of the management plans after a destructive phenomenon has arisen (Gestión Comunitaria de Riesgos - Community Risk Management, 2008).

The vulnerability study is an important factor in determining risk, knowing its variables and indicators, which subsequently allows the understanding of a variety of risk scenarios (in this case of natural origin). Often the exposed elements may present threats of low intensity, therefore, a vulnerability analysis may be a platform for (a) Understanding the usefulness of information generated by different institutional sources and their application to vulnerabilities; (B) Building information based on variables and indicators needed to understand vulnerabilities and easily replicated for local authorities; (C) Interinstitutional and multidisciplinary work of actors responsible for information, land use management and development at national and cantonal level (PNUD, 2011).

The analysis of vulnerability is decisive when preparing the community to support, manage and recover from a destructive event, as this delimits zones according to the value of susceptibility for the considered threat. The types of vulnerability considered are: socioeconomic, physical infrastructure, basic services, community services and organization, communication channels and risk perception. These types are in the current study not understood as knowledge of the environment and adverse events that threaten it, but rather as the greater or lesser capacity of reaction or response of the community to a tsunami, due to the limited time that exists before the arrival of destructing waves to the coast. In order to carry out a correct vulnerability analysis, it has been essential to make field visits, with the objective of obtaining necessary information from the primary source, that is, directly from the inhabitants of the area and also to verify and validate the results.

1. GENERAL DATA

Location

East ☐ Neighborhood ☐
North ☐ Address ☐

2. INFRASTRUCTURE IN YOUR NEIGHBORHOOD

Does the neighborhood have a communal house? Yes ☐ No ☐

Where does the community meet to address important issues? ____________

What is the best time to bring the community or neighborhood together?

Day ________ Time ________ Place ________

Are there local or communal leaders or presidents? Yes ☐ No ☐

Indicate the names, addresses, telephone numbers: ____________

Are there green areas and parks in your neighborhood? Yes ☐ No ☐

Wide ________ Flat ________ Sanitary ________

Which days per week are the most visited by the habitants in these areas?

Monday-Friday ☐ Weekends ☐ Holidays ☐

What number of people approximately visit these areas a week?

0-50 people ☐ 50-100 people ☐ 100-200 people ☐ >200 people ☐

Do people with special abilities / disabilities attend these areas? Yes ☐ No ☐

The house where you and your family live is?

Leased ☐ Own ☐ Borrowed ☐ Antichresis ☐ Other ☐

Do you have basic services in your home?

	Frecuency				Condition		
Service	Yes	No	Occasional	Always	Bad	Regular	Good
Electric power	☐	☐	☐	☐	☐	☐	☐
Street lighting	☐	☐	☐	☐	☐	☐	☐
Landline	☐	☐	☐	☐	☐	☐	☐
Cellular coverage	☐	☐	☐	☐	☐	☐	☐
Drinking water	☐	☐	☐	☐	☐	☐	☐
Other Drinking Water System	☐	☐	☐	☐	Water well ☐ Tank ☐		Piped water ☐ Slope ☐

Wastewater treatment Septic ☐ Latrine ☐ Public sewer ☐

How is garbage eliminated in your neighborhood?

Municipal ☐ Burned ☐ Buried ☐ Recycle ☐

3. ROAD AND TRANSPORTATION IN YOUR NEIGHBORHOOD

Of which material are the main access roads to your neighborhood made of?

Flooring ☐ Cobble ☐ Stone ☐ Ballast ☐ Earth ☐ Other ☐

In what state are the roads in your neighborhood?

Great ☐ Bad ☐ Regular ☐

What type of public transportation do you have in your neighborhood?

Buses ☐ Vans ☐ Metro ☐ Taxis ☐ Other ☐

How many public transport lines serve your neighborhood? ____________

What time until what time is there a shuttle service in your neighborhood? ____________

Figure 7: Fragment of the information capture sheet.

b) Information capture sheet

In order to obtain, homogenize and systematize the field data in a fast way, it has been necessary to design an information capture sheet, with closed questions to facilitate the interaction between interviewers and respondents and the subsequent processing of the data (Fig. 7). Each sheet or card has an identification code and geographic coordinates for its georeferencing, capturing information that has been required for the calculation of partial and total vulnerabilities for each sheet. With the obtained vulnerability values, it has been possible to map the partial and total vulnerabilities in six thematic maps for each city.

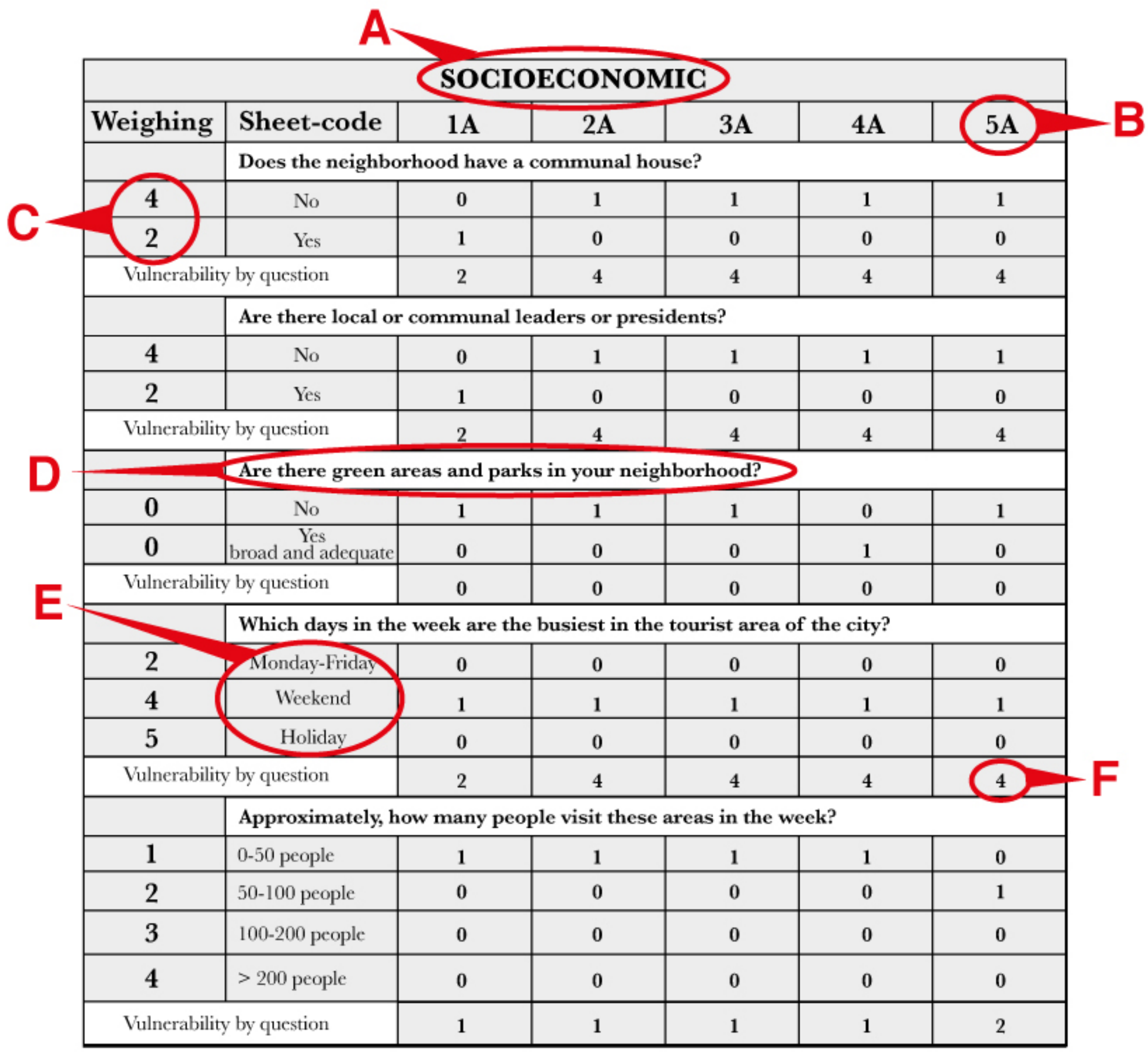

SOCIOECONOMIC						
Weighing	**Sheet-code**	**1A**	**2A**	**3A**	**4A**	**5A**
	Does the neighborhood have a communal house?					
4	No	0	1	1	1	1
2	Yes	1	0	0	0	0
Vulnerability by question		2	4	4	4	4
	Are there local or communal leaders or presidents?					
4	No	0	1	1	1	1
2	Yes	1	0	0	0	0
Vulnerability by question		2	4	4	4	4
	Are there green areas and parks in your neighborhood?					
0	No	1	1	1	0	1
0	Yes broad and adequate	0	0	0	1	0
Vulnerability by question		0	0	0	0	0
	Which days in the week are the busiest in the tourist area of the city?					
2	Monday-Friday	0	0	0	0	0
4	Weekend	1	1	1	1	1
5	Holiday	0	0	0	0	0
Vulnerability by question		2	4	4	4	4
	Approximately, how many people visit these areas in the week?					
1	0-50 people	1	1	1	1	0
2	50-100 people	0	0	0	0	1
3	100-200 people	0	0	0	0	0
4	> 200 people	0	0	0	0	0
Vulnerability by question		1	1	1	1	2

Figure 8: Fragment of the vulnerability matrix. A: Type of vulnerability to the tsunami hazard. B: Identification code of the sheet. C: Weighting assigned to each response. D: Indicators of vulnerability. E: Multiple choice responses. F: Weighted value of vulnerability indicator.

c) Design of the vulnerability matrix

After obtaining the data through the data capture sheets, a vulnerability matrix has been created in a spreadsheet, to tabulate the responses and to assign weights according to the response obtained. We present a fragment of the vulnerability matrix created for the two cities, which includes all the data obtained from the community and the weights assigned to each response. (Fig. 8).

d) Data processing

Each response option has been assigned to a weight according to the degree of influence it may has on the tsunami hazard. Considering the scale of the study, the qualitative vulnerability has been classified into five categories, each of which has its respective percentage quantitative correspondence, as illustrated in Figure 9.

Qualitative vulnerability	Quantitative vulnerability (%)
Very high	100
High	80
Medium	60
Low	40
Very low	20

Figure 9: Assigned categories of qualitative and quantitative vulnerabilities.

Weighted values of each indicator have been obtained from all the tabs obtained in the field, then these values were ordered in a new matrix to obtain a total value for each type of vulnerability. In the vertical sense, the partial vulnerability value has been obtained by applying descriptive statistics, in this case we have used the Mode function, which uses the frequency of weighted values. Below, we present a fragment of the matrix of weighted values of one type of vulnerability (Fig. 10).

Having partial vulnerability values for each type of vulnerability, the mode function has been applied again horizontally to obtain the total vulnerability value by type of vulnerability for the entire study area (Fig. 11).

Finally, in order to obtain total vulnerability values for each sheet, a new matrix has been generated, where the values of partial vulnerability per sheet of all types of vulnerability are recorded. In this case, as there have been scattered values, we applied the statistical function of the arithmetic mean to better adjust to the reality of each city (Fig. 12).

PHYSICAL INFRASTRUCTURE	1A	2A	3A	4A	5A
What is the structural system of your home?	1	1	1	1	1
What is the type of wall-materials of your home?	2	3	2	2	3
What is the type of roof of your home?	4	1	3	3	3
What is the type of the mezzanine system?	1	1	1	1	1
Number of floors of your home?	3	1	4	4	2
Year of construction of your home?	3	2	4	3	2
What is the state of conservation of your home?	2	2	2	3	3
Characteristics of the soil on which your home is located?	5	1	1	1	1
What is the topography of the site?	4	4	4	4	4
What is the type of construction of your home?	1	1	1	1	1
PARTIAL VULNERABILITY BY SHEET	3	1	3	3	3

A B

Figure 10: Fragment of the matrix of weighted values. A: Partial vulnerability per sheet, concerning the physical infrastructure. B: Weighted values of each indicator.

VULNERABILITY SERVICES ORG COMMUNITY	7B	8B	9B	10B	11B	VULNERABILITY SERVICES ORG COMMUNITY
What health unit exists in your neighborhood?	2	2	2	2	2	
What schedule does it accomplish?	1	4	4	4	4	
Who uses frequently health centers in your neighborhood?	3	3	3	3	3	
What types of schools exist in your neighborhood?	6	4	4	6	2	
Does the educational center have large spaces, classrooms in good condition and sanitary batteries?	2	5	5	2	5	
What level of education does the educational institution have?	3	2	2	2	4	
What working days does the educational institution have?	3	3	3	3	3	
In what state is the educational building?	1	1	1	3	1	
Does the neighborhood have cultural or tourist centers?	1	2	2	2	2	
Does the municipality have programs to support ecotourism?	1	1	1	1	1	
Are there libraries in your neighborhood?	2	2	2	1	2	
Is there a community alarm system in your neighborhood?	1	2	2	1	2	
Are there surveillance units or police checkpoints in your neighborhood?	5	5	5	5	5	
Does the neighborhood have a monitoring and surveillance system?	3	3	3	5	5	
Does the neighborhood has hydrants?	1	1	1	1	1	
Does the neighborhood count with a system of shelters in case of emergency?	2	2	2	2	2	
Does the neighborhood have a communal house?	0	0	0	0	0	
Does the neighborhood have leaders or presidents of the neighborhood?	2	5	5	5	5	
PARTIAL VULNERABILITY BY SHEET	2	2	2	2	2	2

A

Figure 11: Fragment of the matrix of partial vulnerability values. A: Total vulnerability by type for the entire study area.

PARTIAL VULNERABILITY VALUES	1A	2A	3A	4A	5A
Socioeconomic	3	3	3	3	3
Infrastructure	3	1	3	3	3
Basic services	4	4	4	4	4
Community services and organization	2	2	2	2	2
Risk perception	5	5	5	5	5
Communication routes	1	1	1	1	1
TOTAL VULNERABILITIES FOR EACH FILE	3	3	3	3	3

A B

Figure 12: Fragment of the total vulnerability matrix per sheet. A: Total vulnerability for each file for the entire study area. B: Values of partial vulnerability for each type of vulnerability.

5. RESULTS AND DISCUSSION

The vulnerability matrix is the instrument that allows the analysis of vulnerability and is the basis for obtaining all further results. The standardized matrix contains six different types of vulnerabilities considered for this study, vulnerability indicators, weights, weighted values, partial vulnerabilities per file, total vulnerabilities by type of vulnerability and total vulnerability values per block in the study. For each city, the respective standardized vulnerability analysis has been performed. Based on the information obtained from the matrix of each city, the following thematic cartography has been generated, which contained six different maps (socioeconomic, physical infrastructure, basic services, community organization, risk perception (reaction capacity) and communication abilities) representing the partial quantitative vulnerabilities. In addition, a total vulnerability map has been obtained for each city (Figs. 14a-f and 21a-f). Subsequently, the star of the total vulnerability has been generated for the study area of each city, which graphically illustrates the percentage values of the six indicated vulnerabilities (Figs. 34 and 35).

5a) Vulnerability in Salinas

The city of Salinas presented vulnerability values in the range of 60% to 80%, corresponding to medium vulnerability (in yellow color) and high (in orange color), respectively (Fig. 13).

Medium Vulnerability Zone of Salinas:

The medium vulnerability zone (Fig. 13, in yellow tonality) occupies an area of 1,047km^2 corresponding to 93% of the urban area. The average total vulnerability value has been assigned for this zone based on a variety of factors, which are described in detail in the following analysis. Along the Salinas boardwalk there are numerous multi-floor, high-rise buildings (usually ten floors), with private apartments of which many of them are luxury, for holiday or rest, being preferably occupied on weekends and holidays. The rest of the year they remain uninhabited. Considering this circumstance, the qualitative vulnerability, from the point of view of movable and immovable property, should be high, due to the degree of affectation that would cause the tsunami in the departments and communal services (Fig. 15).

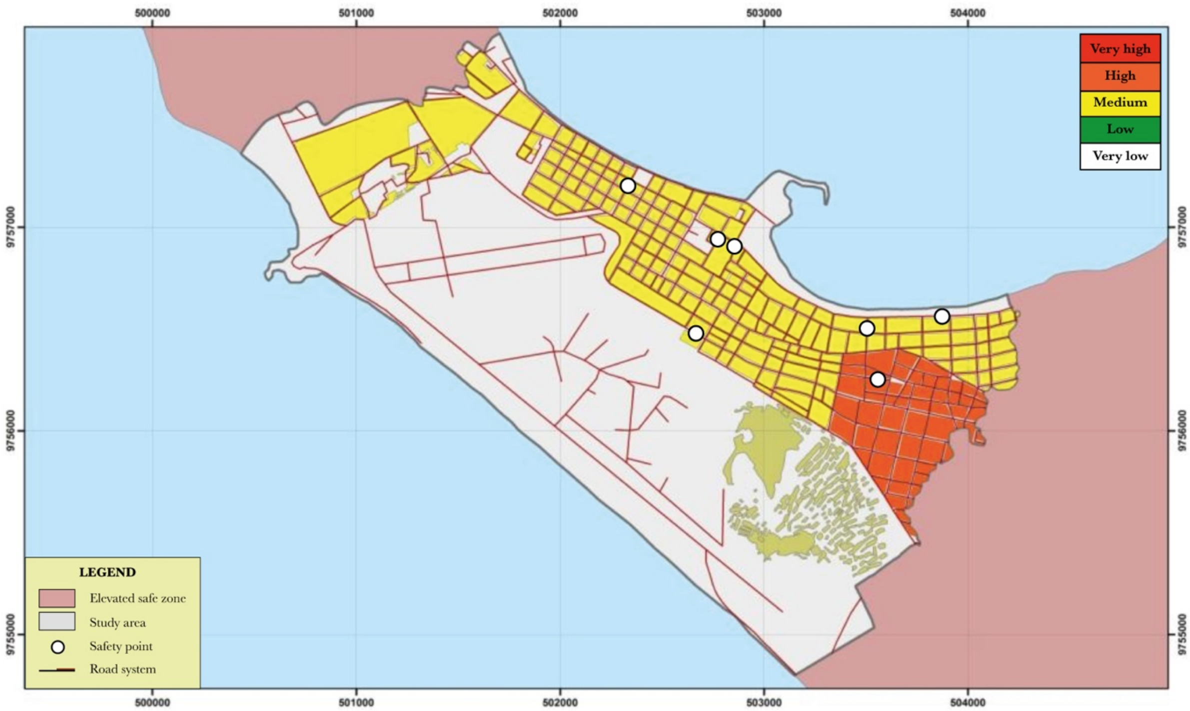

Figure 13: Map of total vulnerability of Salinas.

Figure 15: Communal services of the Riviera del Mar building (Salinas).

However, there are several modifying factors of the such as (a) they are uninhabited most of the year; (b) the impact of the tsunami does not involve 100% of the building, but at worse the first four floors, (c) the economic capacity of their owners is generally high; (d) owners are subject to credit (they are able to obtain timely financing for repairs and replacement of their assets). Therefore, due to these factors, the overall qualitative vulnerability has been assigned to be medium.

The city of Salinas extends itself from the second avenue parallel to the seawall to the salt pits and the runway. Taking into account that the central sector is relatively distant from the beach and the direct impact of the waves, in the event of a tsunami the affect would be caused by permanent secondary flooding due to the morphology of the terrain, with a potential high environmental impact due to contamination and interruption of the basic services. Due to these circumstances, this zone had been initially assigned with a high total vulnerability value. However, after analyzing the responses recorded in the data capture sheets, other vulnerability modifiers have been identified, according to criteria discussed below.

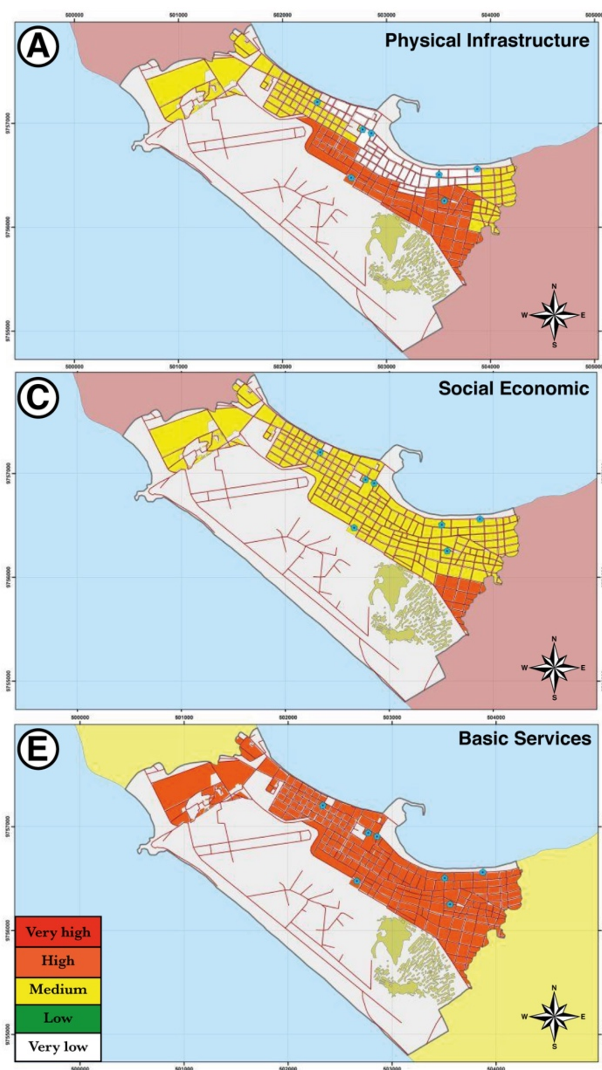

Figure 14 a-f: Specific vulnerability maps of Salinas

Physical infrastructure: In the central area of the city, corresponding to the middle-income class, (Fig. 16), there are constructions that present a maximum of three floors in height with resistant construction materials, in good condition, covered with asbestos cement or reinforced concrete slab. Many are new or in good condition. Therefore, in case of a potential tsunami flood occurrence, they would not suffer major damage to their structural systems. Therefore, they have been assigned to a medium vulnerability value (Fig. 14a).

Figure 16: Type of housing in the central area of Salinas.

Social and economic: The population is markedly stratified according to their economic income, which are directly related to their economic activity. The general public is represented by being public employees, private sector workers, small and micro entrepreneurs, military, among others, whose homes occupy the central area of Salinas (Fig. 13) and constitute the denominated "middle class". Their income ranges from 300 to 600 dollars per month. In terms of the aspects of formal education, most have achieved third-level degrees. This social stratum is moderately vulnerable to any negative events due to their indebtedness capacity, which, although limited, credited as creditors to financial institutions.

On the other hand, informal workers (fishermen, small traders, artisans, domestic workers) constitute the most vulnerable social class because of their low economic resources (low daily income or, at best, the basic monthly wage) and their limited access to health and education services (incomplete basic level). They inhabit the urban - marginal sectors of the city (area near the salt pits, around the cemetery and via Mar Bravo), where, in general, there are no complete basic services because they are settlements, which still seek to be legalized (Fig. 14c).

Basic services: Most of the inhabitants of the central area have complete vital networks, with good functionality and maintenance. In case of tsunami earthquake or tsunami, it is very probable that the service networks are not completely affected, leading to an assignment of these services to be of medium vulnerability (Fig. 14e).

Community services: The presence of the public hospital "Dr. José Garcés Rodríguez" has been evidenced, being located in the area, which is considered to a safe zone (between Quito Avenue and Juan Vargas Street). In the central area of Salinas there are no libraries or cultural development centers, but close to the Salinas market there is an amusement park "Salinas Aqua Club" (Fig. 17), which brings together residents on public holidays. Due to the location, the quality and quantity of such services, a low vulnerability value has been assigned (Fig. 14d).

Figure 17: "Salinas Aqua Club".

Road network: The existing road network in the central area is composed of wide, well-maintained streets and paved avenues (Fig. 18), which would allow a rapid evacuation to the nearby buildings considered to be safety zones. Additionally, due to their characteristics, they would not necessarily be destroyed with a potential flood, leading to a low vulnerability value (Fig. 14f).

Figure 18: State of Salinas roads.

Therefore, by all the factors described above, the total qualitative vulnerability of the analyzed area corresponds to an average value (Fig. 13).

High Vulnerability Zone of Salinas:
The high vulnerability zone (Fig. 13) occupies an area of about 0.299km^2, which corresponds to 7% of the urban area. Although most of the area is far from the beach and consequently free of the direct impact of the waves in the event of a potential tsunami, a high value of vulnerability has been attributed to it, because after the analysis of the responses of the population, we encountered a variety of modifiers of this vulnerability, which will be described detailed below.

Infrastructure: The houses are mostly of one or two floors, of mixed materials (wood and cane), with structural system of roofs of beams of wood or cane and zinc cover and system of mezzanine with timber and cane. The average age of the buildings is of about 30 years. The houses are built at ground level and are in a regular state of conservation. It is therefore clear that at the time of an earthquake that may generates a potential tsunami, these houses have a high probability of being seriously affected, (Fig. 14a), leaving their owners as refugees (Fig. 19).


Figure 19: Mixed constructions in the high vulnerability zone.

Economic and social: The main economic activity of the inhabitants of this area focuses on informal work (small traders, fishermen, artisans, land transport drivers, domestic workers, among others), which make up the low class and the lower middle class. Due to their low economic incomes, they are not considered as creditors by the financial institutions, therefore, they have a reduced capacity of indebtedness and response to face the possible damages caused by tsunami, for which they constitute the most vulnerable population segment in front of a disaster. Socially, high levels of consumption of alcohol, drugs and sale of articles of dubious origin have been evidenced, reason why the zone is considered violent and dangerous, factor that would affect the immediate answer the moment of requiring an evacuation since the individuals may be under the effects of alcohol and hallucinogenic and psychotropic substances, which would alter potentially better behavior.

As the second determining social factor in this area, we identified that the majority of people leave their children in the care of third parties (neighbors and friends), during work hours and therefore in case of an immediate evacuation the first response of these people would not be to evacuate to safety zones, but to return to their place of habitation to reunite with their children and other relatives, a factor that certainly complicate the displacement of the population towards safe areas.

Community services: The sector lacks of a communal house and the neighborhood president could not be identified in the course of this study, so it has been presumed that there is no regular community organization. The nearby educational centers are fiscal and in regular state of maintenance. The existence of relief agencies close to the sector could not be evidenced (Fig. 14d).

Basic services: There are generally no comprehensive basic services because they are de facto settlements, which seek to be legalized (Fig. 14e).

Risk perception: In this context, the scenario is even more critical because according to the obtained answers, there is evidence of a total lack of awareness of the tsunami phenomenon, its effects on the environment and self-protection of the population. In addition to the absence of a contingency plan, there has also been no training at all in risk management (Fig. 14b).
By the factors described above the total qualitative vulnerability of this area has been modified to the category of high vulnerability (Fig. 13)

5b) Vulnerability in Bahía de Caráquez
In the studied area, despite the existence of high quality physical infrastructure, constituting the sector of the highest surplus value as well as having the highest tourist and economic interest, predominates a medium level vulnerability (Fig. 20).

High Vulnerability Zone:
The area of high vulnerability (Figure 20, in orange tonality) occupies an area of 0.132km^2, which corresponds to 92% of the total area of study. An average total vulnerability value has been assigned for this zone based on the analysis detailed further on. Along the pier "Virgilio Ratti", there are buildings of several floors of height (generally nine floors), with predominately particular apartments, many of them of luxury. Among the buildings there are also private houses of one and two floors high (Fig. 22), which would be flooded by a potential tsunami. From the point of view of material goods furniture and estate property, the value of qualitative vulnerability should be high because of the impact degree that a potential tsunami may have on such infrastructure. However, from the analysis of the responses obtained from the data capture sheets, several factors that modify this vulnerability have been identified. Of these are (a) the apartments are for holidays or for rest, therefore, they are preferably used on weekends and holidays; (b) the impact of an expected tsunami would not involve 100% of the building, but the lower floors; (c) the economic capacity and quality of life of their owners is generally high; (d) owners are subject to credit, as they are able to obtain timely financing for repairs and replacement of their assets. Therefore, the vulnerability of the area is modified from high to medium.

Towards the interior of the city, specifically from the second avenue parallel to the pier, is located the central zone of the study area (Fig. 23), in which different indicators have been identified that catalog such as a zone of medium vulnerability. These will be discussed further below.

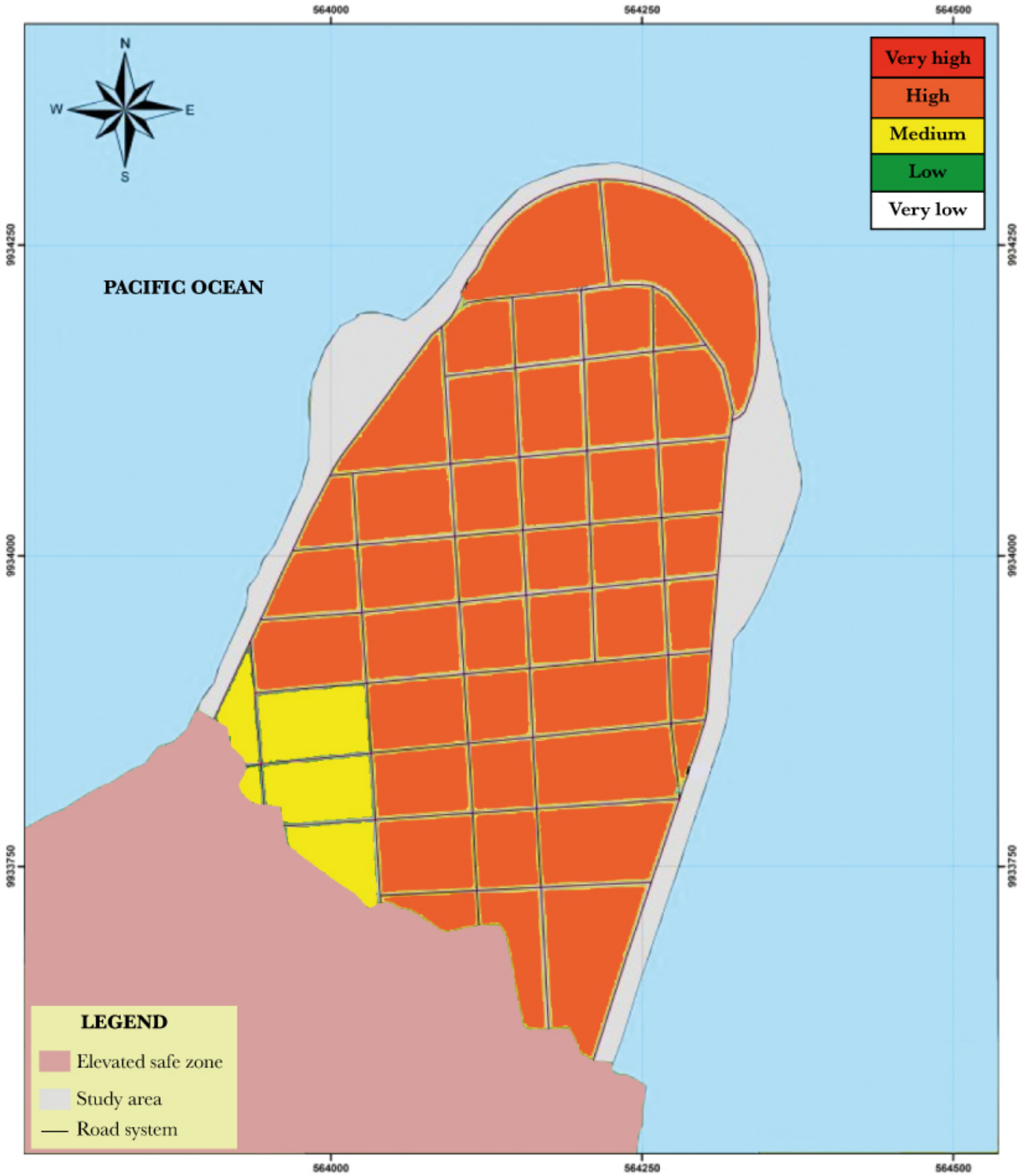

Figure 20: Total vulnerability of Bahía de Caráquez.

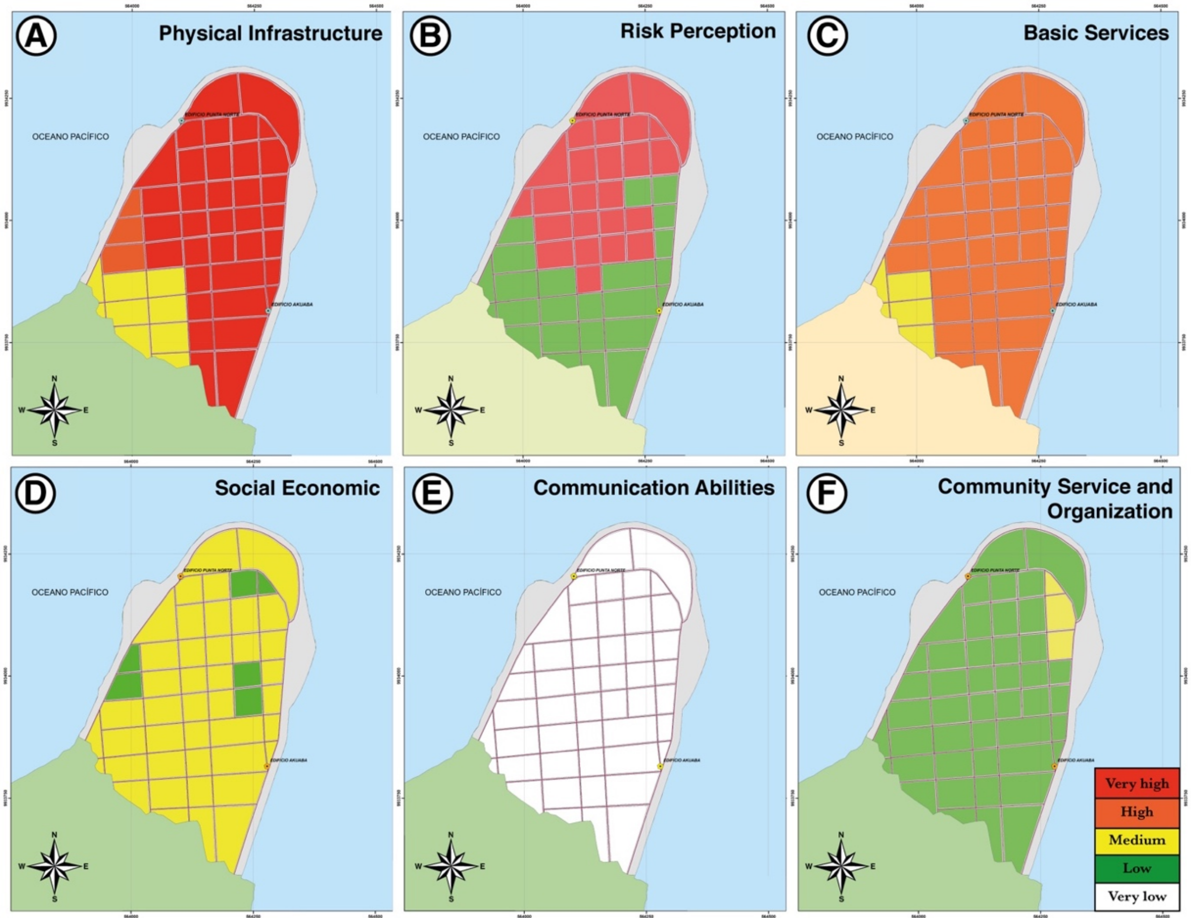

Figure 21 a-f: Specific vulnerability maps of Bahía de Caráquez


Figure 22: Homes located between buildings on the pier "Virgilio Ratti".


Figure 23: Central zone of the study area in Bahía de Caráquez.

Social and economic: The majority of the inhabitants of this area are formal private sector workers who work under a fixed contract and receive a monthly salary ranging from 600 to 900 dollars. With regard to the formal education aspects, most have achieved third level academic degrees and in some fourth level degrees. They own their home and make up the middle and middle - upper social stratum. This stratum is moderately vulnerable to any negative events due to its indebtedness capacity, which accredits them as creditors to financial institutions and could recover in a short time from the damages and losses caused by a potential tsunami.


Figure 24: Types of housing in the central zone of the study area.

Infrastructure: There are buildings with a height ranging from two to five floors, with a main structural system of reinforced concrete, reinforced concrete mezzanines, ceilings with metallic structure and cover of asbestos-cement plates or reinforced concrete slab, in good conserved condition, with a construction age of about 20 years, being upon dry and apparently firm ground (Fig. 24). Therefore, in case of a tsunami flood occurrence, these sites may not suffer major damage to their structural systems. Nonetheless, history has demonstrated otherwise due to the earthquakes of 1998 and 2016 as illustrated in figures 25 to 27 (Trenkamp, 2003; Toulkeridis et al., 2017a; b).

Figure 25: Collapse of the hotel Calypso due to the earthquake with an epicenter close to Bahía de Caráquez on the August, 4 in 1998.


Figure 26 and 27: Strong damage and collapse due to the earthquake of Muisne in April 16, 2016, close to the entrance to the city of Bahía de Caráquez, as well as in the hotel area.

Basic services: Most of the inhabitants of the central area have the complete vital networks, with good functionality and adequate maintenance. In the event of a tsunami earthquake or a tsunami, it is very likely that these networks will not be fully affected and will partially retain their functionality.

Risk Perception: According to the answers obtained in the field research, a high degree of interest is indicated to participate in risk management activities (simulations, training in self-protection of citizens), and, at the same time, a total lack of knowledge of the consequences that may lead with the occurrence of a potential tsunami, and any other adverse events (Fig. 28).

Figure 28: People having fun during a storm. Courtesy by Eduardo Quijije.

Road networks: There are wide, paved roads, in good condition, with little vehicular traffic (Fig. 29), usually open roads for free pedestrian traffic and a very low level of traffic accidents, characteristics that would allow a rapid evacuation to nearby buildings being considered to be safety zones.

Figure 29: Wide and well preserved avenues in the study area.

With these indicators, and based on the assigned weighting and statistical treatment of the vulnerability matrix, a medium-level vulnerability value has been obtained.

Medium Vulnerability Zone:
The area of medium vulnerability (Fig. 20) occupies an area of 0.013km^2 corresponding to 8% of the total study area. This area has very similar characteristics in relation to the area classified as an area of high vulnerability in terms of socioeconomic aspects and physical housing infrastructure. Nonetheless, we encountered a few indicators that modify the degree of vulnerability of this area, as discussed below.

Infrastructure: There are constructions with a height ranging from two to five floors, with a main structural system of reinforced concrete, reinforced concrete mezzanines, ceilings with metallic structure and cover of asbestos-cement plates or reinforced concrete slab, in good condition on dry and firm soil. A reinforced concrete wall has been built on the west side of the pier, where it has been sanded to protect that zone from waves (Fig. 30). In this sector, the wall is up to four meters high and the enclosed area is very close to the pier, which represents an additional protection in case of a tsunami occurrence.

Figure 30: Protective wall in the western sector of the pier.

Basic services: In the central area, most inhabitants have all the basic services available, however, this area in particular, presents problems in terms of cellular telephone coverage, as well as intermittent hydric service of potable water, so that many of the houses are supplied by cisterns (Fig. 31) or water wells.

Figure 31: Cisterns in the medium vulnerability zone.

Community services: The analyzed area has a health center (located between Marañón and Cecilio Intriago streets), which serves eight hours a day (Fig. 32). There are private education institutions with a level of education up to high school and according to information provided by the sector´s residents, have ample spaces and sufficient sanitary services to be used as shelters for people when necessary.

Figure 32: Health center in the low vulnerability area of Bahia de Caráquez.

Risk perception: The inhabitants of the area have a clear notion of the scenario that could occur if a destructive tsunami type event occurs. They feel that the event would affect the whole sector and that the best option is to escape towards elevated places to safeguard their life. They are also interested in participating in simulations and training about risk assessment as well as about self-protection.

Road network: The roads are wide, paved, in good condition, having reduced vehicular traffic, wide sidewalks suitable for pedestrian traffic and a very low rate of traffic accidents, (Fig. 33).

Figure 33: Av. Simón Bolívar (central sector of Bahía de Caráquez).

With these indicators, and based on the assigned weighting and statistical treatment of the vulnerability matrix, a medium vulnerability value has been obtained for this zone.

5c) General results

Vulnerability is defined as the degree of susceptibility of a population to be affected by a negative or adverse event. Such vulnerability is able to be measured according to different criteria such as: socioeconomic, physical infrastructure, basic services, community services, risk perception (knowledge of the environment, negative events and responsiveness) and communication channels. Each of these criteria provides a vulnerability value, which must be analyzed independently and in its entirety, in order to identify weaknesses and strengths in order to incorporate them into a contingency plan or risk management, which allows corrective actions and preventive actions of mitigation as well as preparation and that optimizes the response of the population to a negative event of any nature, in order to safeguard their lives, and as much as possible, their assets.

In the studied cities, which are considered to be strategic and of national importance due to the physical and tourist infrastructure that agglutinate, results have been obtained of the six mentioned vulnerabilities, with their respective maps. These maps allow the spatial location, and a model that predicts the results and incidences of a horizontal or vertical evacuation in function of the variables that intervene in the same, considering the particularities of Salinas and Bahía de Caráquez. Therefore, these results constitute the basic inputs for a risk or contingency management plan, which, with the contribution of this study, should be carried out by the public and private relief and response agencies.

Salinas

In Salinas, we considered and subsequently analyzed six different types of vulnerabilities as the most representative of the reality of this city, and also being adequate to characterize the physical environment as a prerequisite to obtaining any (vertical) evacuation model.

The highest vulnerability demonstrates the basic services, which indicates that most of the inhabitants of the city have complete (in situ) basic services, being functional and in good condition. By having more services, they are also more likely to be totally or partially affected by a tsunami-like event. The most appropriate option to reduce this vulnerability value is to encourage citizens to have alternative systems for the provision of services, such as having cisterns to store potable water, to have generators or other devices for the alternative provision of electric energy and lighting, among others.

Second is the socioeconomic vulnerability and physical infrastructure, both with a value of 60%. It is difficult to change the economic and social condition of a whole population, so it is proposed to promote the culture of saving to face situations of any economic emergency. In terms of physical infrastructure, it is vital that there is a correct and proper municipal ordinance stating that all buildings must have earthquake-resistant designs and materials of good quality, in order to reduce the potential damages caused by the generator earthquake of the potential tsunami.

In terms of risk perception and community organization, vulnerability reaches a value of about 40% because the population knows their environment and perceives damages that may be caused by a potential tsunami. They also have notions of how to react to a phenomenon of this type, although it is necessary to reinforce this knowledge through education campaigns to the population. As for community organization and communal assets, neighborhood committees, with their representatives and community services such as health centers, medical clinics, courts and sports clubs, they have been identified with their respective leaders, which indicates a good community organization that would facilitate any training and coordination, and then subsequently for any needed reaction.

The lowest vulnerability (20%) corresponds to the road network since the roads are wide, paved, in good state of conservation and perfectly functional, which would facilitate any type of evacuation and displacement. Besides that, after the tsunami flood has passed, they would continue to function, albeit in a limited way, to the cleaning of mud and debris.

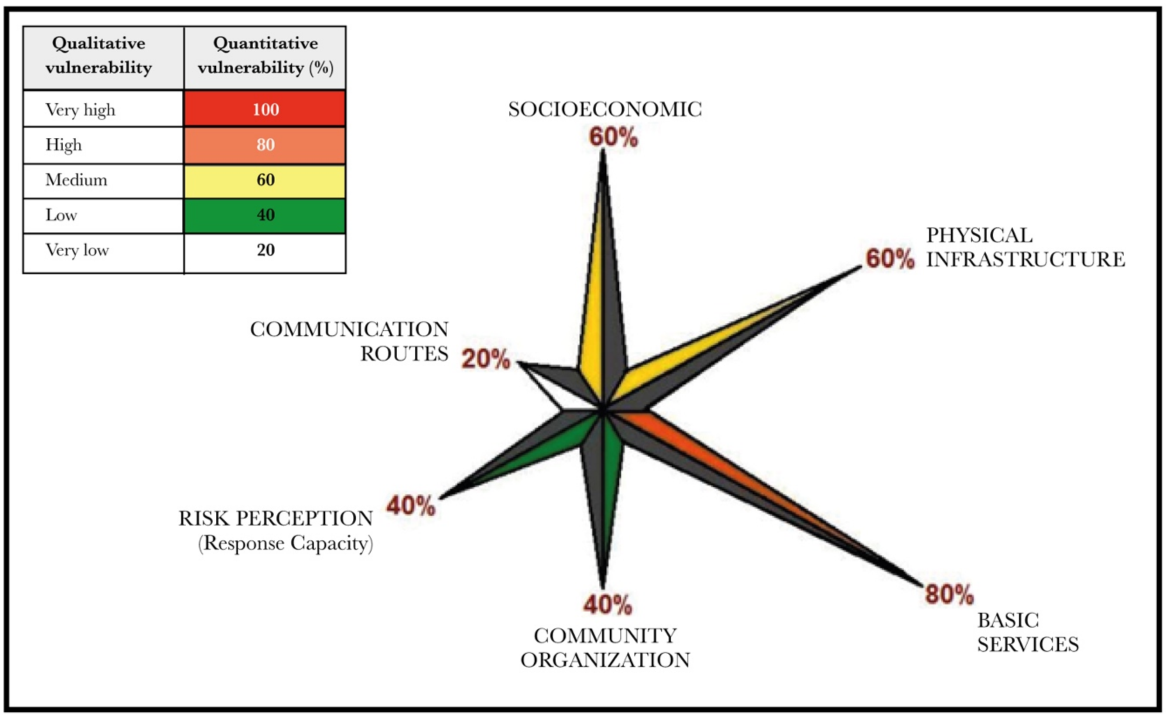

Figure 34: For Salinas, the Vulnerability Star illustrates the different types of vulnerabilities and their level, expressed as a percentage, in respect to a tsunami hazard.

Bahia de Caráquez

Like for Salinas, in Bahía de Caráquez, the same six types of vulnerabilities have been considered and analyzed. The highest vulnerability (100%) is the risk perception, focused from the point of view of ignorance and lack of knowledge about the environment, the capacity of reaction or response of the population and the impact that could cause the potential tsunami phenomenon. This result, apparently, could appear to be a contradiction in a city whose population experienced very insidious negative events in 1998, with the phenomenon El Niño and a severe earthquake (Rodbell et al., 1999; Trenkamp, 2003; Mato and Toulkeridis, 2017), events that certainly have left lessons learned in the population, especially being of scarce resources.

These results may be explained by the analysis and treatment of the information obtained in the field, since it has been evidenced that the population that occupies the study area, in the great majority, is wandering, meaning that they are tourists and people of good economic condition that occupy villas and buildings only during vacation periods and holidays. Consequently, since they do not belong to the environment, they do not know (or have no idea) of what may happen to them if a tsunami event occurs. For this reason, they have not participated (and are not interested) in training workshops, drills and other events to improve their ability to respond. Awareness and training in this high-risk sector should be a priority task of the Relief Organizations and the National Risk Management Secretariat, given that this is the tourist and hotel area of the city, and agglutinates, at the time tourism and a high population density, both of visitors and of those who offers their services to the tourism.

Qualitative vulnerability	Quantitative vulnerability (%)
Very high	100
High	80
Medium	60
Low	40
Very low	20

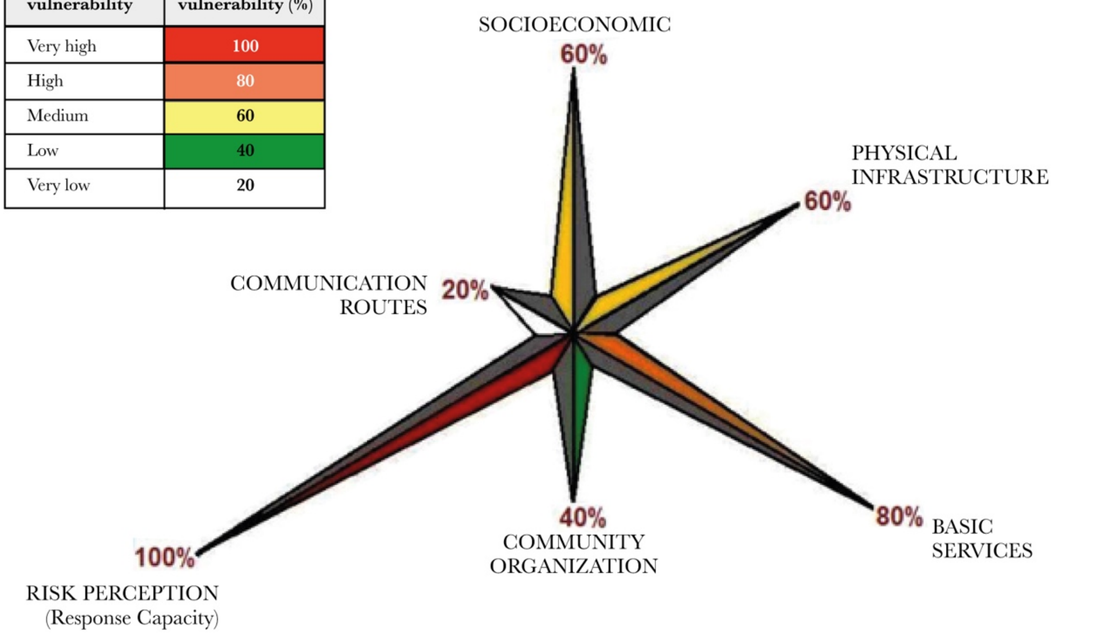

Figure 35: For Bahía de Caráquez, the Vulnerability Star illustrates the different types of vulnerabilities and their level, expressed as a percentage, in respect to a tsunami hazard.

The second highest vulnerability with about 80% is basic services, demonstrating similar benefit-need affection as discussed for the city of Salinas. The third highest vulnerability however, is the socioeconomic vulnerability as well as the physical infrastructure, both with a value of 60%. This value is explained by the fact that the area with the highest surplus value is circumscribed to the seawall. The central zone is occupied by an economically active population made up of public employees and private permanent residents of Bahia, with monthly economic income fluctuating between 400 and 800 dollars. This segment of the population constitutes the middle class of the city and its houses, although comfortable, are modest in their majority, both from the point of view of material goods and as construction materials, indicators that explain the level of obtained vulnerability.

In the community organization and the communal assets, the vulnerability is with 40% low, as there we identified neighborhood committees with their representatives and community services as well as a health center, parks and squares for community recreation, which demonstrates a good community organization that would facilitate any task of training and coordination and, subsequently, reaction.

The lowest vulnerability with 20% refers to the road network since, as previously described, the study area has wide, paved, well-maintained, perfectly functional roads with little vehicular traffic, which would facilitate any type of evacuation and displacement. Besides that, after the flood has passed, this could continue to function, albeit in a limited way until the cleaning of mud and debris.

6. CONCLUSIONS

For the purposes of this investigation, we considered the worst scenario to occur, in order to incorporate variables that include the most unfavorable conditions that may arise, in order to have a greater safety margin to save the highest number of human lives. The information obtained from the data base of the vulnerability matrix allowed the identification of susceptibilities in the study area, through the various values of specific and total vulnerabilities.

The vulnerability analysis towards tsunami hazards carried out in the study areas corresponding to both cities, resulted in a medium to high vulnerability for the population of Salinas and low to medium vulnerability for Bahía de Caráquez, respectively. Both cities have a high vulnerability (80%) for basic services, a medium vulnerability (60%) in social economic issues as well as in physical infrastructure, a low vulnerability (40%) in community organization and the lowest vulnerability (20%) by means of communication.

The great difference between Salinas and Bahía de Caráquez yielded the value of vulnerability due to risk perception. Salinas has a low vulnerability (40%) as its population knows the environment and perceives the damages that could be caused by a potential tsunami. In contrast, Bahía de Caráquez has a high vulnerability (100%), because the population in its great majority that occupies the study area, is wandering and therefore, as they do not belong to the environment, they lack of knowledge or have no notion of potential adverse event with the occurrence of tsunami hazard.

7. REFERENCES

Adger, W. N. (2006). Vulnerability. Global environmental change, 16(3), 268-281.

Alcantara-Ayala, I. (2002). Geomorphology, natural hazards, vulnerability and prevention of natural disasters in developing countries. Geomorphology, 47(2), 107-124.

Alvear Brito, G. J. (2010). Elaboración de una mapa de accesibilidad y modelo de evacuación ante una eventual ocurrencia de Tsunami en las ciudades de Salinas y Bahía de Caraquéz empleando herramientas Geoinformáticas. Unpubl. Bachelor's thesis, Sangolquí, ESPE: 146pp.

Anderson, M. B. (1995). Vulnerability to disaster and sustainable development: A general framework for assessing vulnerability. Disaster Prevention for Sustainable Development: Economic and Policy Issues. Washington, DC: World Bank, 41-59.

Atakan, K. (1995). Mass wasting triggered by the 5 March 1987 Ecuador earthquakes. *Earthquake Engineering*, 29, 21-42.

Barazangi M. and Isacks B.L. (1976): Spatial distribution of earthquakes and subduction of the Nazca Plate beneath South America. *Geology* 4: 686–692.

Beauval, C., Yepes, H., Bakun, W. H., Egred, J., Alvarado, A. and Singaucho, J. C. (2010). Locations and magnitudes of historical earthquakes in the Sierra of Ecuador (1587–1996). *Geophysical Journal International*, 181(3), 1613-1633.

Berz, G. (1988). List of major natural disasters, 1960–1987. *Natural Hazards*, 1(1), 97-99.

Birkmann, J. (2006). Measuring vulnerability to promote disaster-resilient societies: Conceptual frameworks and definitions. Measuring vulnerability to natural hazards: Towards disaster resilient societies, 1, 9-54.

Birkmann, J., & Fernando, N. (2008). Measuring revealed and emergent vulnerabilities of coastal communities to tsunami in Sri Lanka. Disasters, 32(1), 82-105.

Blaikie, P., Cannon, T., Davis, I., & Wisner, B. (2014). At risk: natural hazards, people's vulnerability and disasters. Routledge.

Brizuela, B., Armigliato, A., & Tinti, S. (2014). Assessment of tsunami hazards for the Central American Pacific coast from southern Mexico to northern Peru. *Natural Hazards and Earth System Sciences*, *14*(7), 1889.

Calgaro, E., & Lloyd, K. (2008). Sun, sea, sand and tsunami: examining disaster vulnerability in the tourism community of Khao Lak, Thailand. Singapore Journal of Tropical Geography, 29(3), 288-306.

Cannon, T. (1994). Vulnerability analysis and the explanation of ‘natural’disasters. Disasters, development and environment, 13-30.

Cannon, T. (2000). Vulnerability analysis and disasters. Floods, 1, 45-55.

Chunga, K. and Toulkeridis, T. (2014). First evidence of paleo-tsunami deposits of a major historic event in Ecuador. *Science of Tsunami Hazards*, 33: 55-69.

Cochard, R., Ranamukhaarachchi, S. L., Shivakoti, G. P., Shipin, O. V., Edwards, P. J., & Seeland, K. T. (2008). The 2004 tsunami in Aceh and Southern Thailand: a review on coastal ecosystems, wave hazards and vulnerability. Perspectives in Plant Ecology, Evolution and Systematics, 10(1), 3-40.

Cutter, S. L. (1996). Vulnerability to environmental hazards. Progress in human geography, 20(4), 529-539.

Daly, M.C. (1989). Correlations between Nazca/Farallon plate kinematics and forearc basin evolution in Ecuador. *Tectonics* 8 (4), 769–790.

De Mets, C., Gordon, R.G., Argus, D.F. and Stein, S. (1989). Current plate motions. *Geophys. J.* 101, 425–478.

Dumont, J. F., Santana, E. and Vilema, W. (2005) Morphologic evidence of active motion of the Zambapala Fault, Gulf of Guayaquil (Ecuador). *Geomorphology*, 65(3), 223-239.

Dumont, J. F., Santana, E., Bonnardot, M. A., Pazmiño, N., Pedoja, K. and Scalabrino, B. (2014). Geometry of the coastline and morphology of the convergent continental margin of Ecuador. *Geological Society London Memoirs*, 41(1), 327-338.

Engdahl, E.R. and Villasenor, A. (2002). Global Seismicity: 1900–1999, in International Handbook of Earthquake and Engineering Seismology, Part A, Chapter 41, pp. 665–690, eds Lee, W.H.K., Kanamori, H., Jennings, P.C. and Kisslinger, C., Academic Press.

Freymuller, J.T., Kellogg, J.N., Vega, V. (1993): Plate motions in the north Andean region. *Journal of Geophysical Research*, 98: 21853– 21863.

Fritz, H. M., Petroff, C. M., Catalán, P. A., Cienfuegos, R., Winckler, P., Kalligeris, N., Weiss, R., Barrientos, S.E., Meneses, G., Valderas-Bermejo, C., Ebeling, C., papadopoulos, A., Contreras, M., Almar, R., Dominguez, J.C. and Synolakis, C.E. (2011). Field survey of the 27 February 2010 Chile tsunami. Pure and Applied Geophysics, 168(11), 1989-2010.

Ganse, R. A., and Nelson, J. B. (1982). Catalog of significant earthquakes 2000 BC to 1979, including quantitative casualties and damage. *Bulletin of the Seismological Society of America*, 72(3), 873-877.

Gutscher, M.A., Malavieille, J.S.L. and Collot, J.-Y. (1999). Tectonic segmentation of the North Andean margin: impact of the Carnegie ridge collision. *Earth Planet. Sci. Lett*. 168, 255–270.

Housner, G. (1984). An historical view of earthquake engineering. *Revista de Ingeniería Sísmica*, (31), 1-16.

Hughes, R. A., Pilatasig, L. F. (2002): Cretaceous and Tertiary terrane accretion in the Cordillera Occidental of the Andes of Ecuador. *Tectonophysics*, 345: 29–48.

Jaillard, E., Ordoñez, M., Benitz, S., Jimenez, G., Montengro, N. and Zambrano, G. (1995). Basin development in an accretionary, oceanic-floored fore-arc setting: southern coastal Ecuador during Late Cretaceous–Late Eocene times. In: S.S.R.a.W.H.J., Tankard, A.J. (Eds.), Petroleum Basins of South America. *American Association of Petroleum Geologists*, pp. 615–631.

Kahn, M. E. (2005). The death toll from natural disasters: the role of income, geography, and institutions. *Review of economics and statistics*, 87(2), 271-284.

Kellogg, J.N. and Vega, V. (1995). Tectonic development of Panama, Costa Rica and the Colombian Andes: Constraints from Global Positioning System geodetic studies and gravity. *Geol. Soc. Am. Special Paper,* 295, 75–90.

Kellogg, J.N. and Vega, V. (1995). Tectonic development of Panama, Costa Rica and the Colombian Andes: Constraints from Global Positioning System geodetic studies and gravity. *Geol. Soc. Am. Special Paper,* 295, 75–90.

Khasalamwa, S. (2009). Is 'build back better' a response to vulnerability? Analysis of the post

tsunami humanitarian interventions in Sri Lanka. Norsk Geografisk Tidsskrift-Norwegian Journal of Geography, vol. 63, no 1, p. 73-88.
Leone, F., Lavigne, F., Paris, R., Denain, J. C., & Vinet, F. (2011). A spatial analysis of the December 26th, 2004 tsunami-induced damages: Lessons learned for a better risk assessment integrating buildings vulnerability. Applied Geography, 31(1), 363-375.
Levine, C. (2004). The concept of vulnerability in disaster research. Journal of Traumatic Stress, 17(5), 395-402.
Lonsdale, P. (1978). Ecuadorian Subduction System. *Bulletin of the American Association of Petroleum Geologists*, 62: 2454– 2477.
Madani, S., Khaleghi, S., & Jannat, M. R. A. (2017). Assessing building vulnerability to tsunami using the PTVA-3 model: A case study of Chabahar Bay, Iran. Natural Hazards, 85(1), 349-359.
Mato, F. and Toulkeridis, T., 2017: The missing Link in El Niño's phenomenon generation. Science of Tsunami Hazards, 36: 128-144.
Mendoza C. and Dewey J.W. (1984): Seismicity associated with the Great Colombia – Ecuador Earthquakes of 1942, 1958, and 1979: Implications for barriers models of earthquake rupture. *Bull. Seism. Soc. Am*. 74 (2): 577–593.
Mori, N., Takahashi, T., Yasuda, T., & Yanagisawa, H. (2011). Survey of 2011 Tohoku earthquake tsunami inundation and run-up. Geophysical research letters, 38(7).
Morrow, B. H. (1999). Identifying and mapping community vulnerability. Disasters, 23(1), 1-18.
Muhari, A., Imamura, F., Koshimura, S., & Post, J. (2011). Examination of three practical run-up models for assessing tsunami impact on highly populated areas. Natural Hazards and Earth System Sciences, 11, 3107-3123.
Navas, L., Caiza, P. and Toulkeridis, T., 2018: An evaluated comparison between the molecule and steel framing construction systems – implications for the seismic vulnerable Ecuador. Malaysia Construction Research Journal (MCRJ), 24 (1): in press
Omira, R., Baptista, M. A., Miranda, J. M., Toto, E., Catita, C., & Catalao, J. (2010). Tsunami vulnerability assessment of Casablanca-Morocco using numerical modelling and GIS tools. Natural hazards, 54(1), 75-95.
Papathoma, M., & Dominey-Howes, D. (2003). Tsunami vulnerability assessment and its implications for coastal hazard analysis and disaster management planning, Gulf of Corinth, Greece. Natural Hazards and Earth System Science, 3(6), 733-747.
Papathoma, M., Dominey-Howes, D., Zong, Y., & Smith, D. (2003). Assessing tsunami vulnerability, an example from Herakleio, Crete. Natural Hazards and Earth System Science, 3(5), 377-389.
Pararas-Carayannis, G. (2012): Potential of tsunami generation along the Colombia/Ecuador subduction margin and the Dolores-Guayaquil Mega-Thrust. *Science of Tsunami Hazards*, 31, 3: 209-230.
Pararas-Carayannis, G., 2018: Brief history of early pioneering tsunami research - Part A. Science of Tsunami Hazards, 37(1), 49-129.
Parra, H., Benito, M. B. and Gaspar-Escribano, J. M. (2016). Seismic hazard assessment in continental Ecuador. *Bulletin of Earthquake Engineering*, 14(8), 2129-2159.
Paton, D., & Johnston, D. (2001). Disasters and communities: vulnerability, resilience and preparedness. Disaster Prevention and Management: An International Journal, 10(4),

270-277.
PNUD (Programa de las Naciones Unidas para el Desarrollo Oficina Ecuador), 2011: Propuesta Metodológica de Análisis de Vulnerabilidades, Quito, Ecuador. 109pp
Rodbell, D. T., Seltzer, G. O., Anderson, D. M., Abbott, M. B., Enfield, D. B., & Newman, J. H. (1999). An~ 15,000-year record of El Niño-driven alluviation in southwestern Ecuador. *Science*, *283*(5401), 516-520.
Rodriguez, F., D'Howitt, M.C., Toulkeridis, T., Salazar, R., Romero, G.R., Moya, V.R. and Padilla, O., 2016: Economic evaluation and significance of early relocation vs. complete destruction by a potential tsunami of a coastal city in Ecuador, Science of Tsunami Hazards., 35 (1): 18-33.
Schuster, R. L., Nieto Thomas, A. S., O'Rourke, T. D., Crespo, E. and Plaza-Nieto, G. (1996). Mass wasting triggered by the 5 March 1987 Ecuador earthquakes. *Engineering geology*, 42(1), 1-23.
Shimozono, T., & Sato, S. (2016). Coastal vulnerability analysis during tsunami-induced levee overflow and breaching by a high-resolution flood model. Coastal Engineering, 107, 116-126.
Shumway, G. (1954). Carnegie ridge and cocos ridge in the East Equatorial Pacific. *The Journal of Geology,* 62(6), 573-586.
Thomalla, F., Downing, T., Spanger-Siegfried, E., Han, G., & Rockström, J. (2006). Reducing hazard vulnerability: towards a common approach between disaster risk reduction and climate adaptation. Disasters, 30(1), 39-48.
Tibaldi, A., Ferrari, L. and Pasquarè, G. (1995). Landslides triggered by earthquakes and their relations with faults and mountain slope geometry: an example from Ecuador. *Geomorphology*, 11(3), 215-226.
Toulkeridis, T. (2011): Volcanic Galápagos Volcánico. Ediecuatorial, Quito, Ecuador: 364pp.
Toulkeridis, T. (2013): Volcanes Activos Ecuador. Santa Rita, Quito, Ecuador: 152 pp
Toulkeridis, T., & Zach, I. (2017). Wind directions of volcanic ash-charged clouds in Ecuador–implications for the public and flight safety. Geomatics, Natural Hazards and Risk, 8(2), 242-256.
Toulkeridis, T., Chunga, K., Rentería, W., Rodriguez, F., Mato, F., Nikolaou, S., D'Howitt, M.C., Besenzon, D., Ruiz, H., Parra, H. and Vera-Grunauer, X., 2017b. The 7.8 M w Earthquake and tsunami of 16th April 2016 in Ecuador: Seismic Evaluation, Geological Field Survey and Economic Implications. Science of Tsunami Hazards, 36(4): 197-242.
Toulkeridis, T., Parra, H., Mato, F., Cruz D´Howitt, M., Sandoval, W., Padilla Almeida, O., Rentería, W., Rodríguez Espinosa, F., Salazar Martinez, R., Cueva Girón, J., Taipe Quispe, A. and Bernaza Quiñonez, L., 2017a: Contrasting results of potential tsunami hazards in Muisne, central coast of Ecuador. Science of Tsunami Hazards, 36: 13-40.
Toulkeridis, T., Mato, F., Toulkeridis-Estrella, K., Perez Salinas, J.C., Tapia, S. and Fuertes, W., 2018: Real-Time Radioactive Precursor of the April 16, 2016 Mw 7.8 Earthquake and Tsunami in Ecuador. Science of Tsunami Hazards, 37: 34-48
Trenkamp, R. A. (2003). Interplate strain, wide plate margin deformation, intraplate strain: The GPS analysis spectrum. ProQuest Dissertations and Theses; Thesis (Ph.D.), University of South Carolina, 2003; Volume: 64-03, Section: B, page: 1144: 122 p.
Trenkamp, R., Kellogg, J.N., Freymueller, J.T., Hector Mora, P. (2002). Wide plate margin

deformation, southern Central America and northwestern South America, CASA GPS observations. *J. South Am. Earth Sci*. 15, 157–171.
Turner, B. L., Kasperson, R. E., Matson, P. A., McCarthy, J. J., Corell, R. W., Christensen, L., Eckley, N., Kasperson, J.X., Luers, a., Martello, M.L., Polsky, C., Pulsipher, A. and Schiller, A. (2003). A framework for vulnerability analysis in sustainability science. Proceedings of the national academy of sciences, 100(14), 8074-8079.
USGS/NEIC (United States Geological Survey/National Earthquake Information Center) (2017). Search Earthquake catalogue, http://earthquake.usgs.gov/earthquakes/search/
Vargas, G., Farías, M., Carretier, S., Tassara, A., Baize, S., & Melnick, D. (2011). Coastal uplift and tsunami effects associated to the 2010 Mw8. 8 Maule earthquake in Central Chile. Andean Geology, 38(1), 219-238.
Varley, A. (1994). Disasters, development and environment. J. Wiley: 1-116
Wilchez-Chaux, G. (1993). La vulnerabilidad global. In Maskrey, Andrew, comp. Los desastres no son naturales. s.l, Red de Estudios Sociales en Prevención de Desastres en América Latina. 9-50
Wood, N. J., Burton, C. G., & Cutter, S. L. (2010). Community variations in social vulnerability to Cascadia-related tsunamis in the US Pacific Northwest. Natural Hazards, 52(2), 369-389.
Ye, L., Kanamori, H., Avouac, J. P., Li, L., Cheung, K. F., and Lay, T. (2016). The 16 April 2016, M W 7.8 (M S 7.5) Ecuador earthquake: A quasi-repeat of the 1942 M S 7.5 earthquake and partial re-rupture of the 1906 M S 8.6 Colombia–Ecuador earthquake. *Earth and Planetary Science Letters*, 454, 248-258.

ISSN 8755-6839

SCIENCE OF TSUNAMI HAZARDS

Journal of Tsunami Society International

Volume 37 Number 3 2018

EVALUATION OF TSUNAMI DANGER FOR THE WESTERN COAST OF THE BLACK SEA BY POSSIBLE CATASTROPHIC UNDERWATER EARTHQUAKES

R.Kh.Mazova[1], Kolchina E.A.[2],

[1]*R.E. Alekseev Nizhny Novgorod State Technical University, Nizhny Novgorod, Russia, e-mail: raissamazova@yandex.ru*

[2]*LCC SPE Prima, Nizhny Novgorod, Russia, kolchinaelena@yandex.ru*

ABSTRACT

The present study deals with the numerical simulation of generation and propagation of tsunami waves from hypothetical earthquake sources along the western coast of the Black Sea. Potential strong earthquakes with a magnitude M = 7.3 with sources localized both in the regions of historical earthquakes and regions determined by the basic geostructures of the Caucasian and Crimean coasts are considered. The mechanism of earthquake realization is considered in the framework of the keyboard block model of the earthquake source. The source is assumed to be three-block, with different character of the motion of the keyboard blocks for each of the considered scenarios of the earthquake. For each scenario, numerical simulation of tsunami source generation and further tsunami wave propagation to the west coast were carried out. Histograms of the wave height distribution along the entire coastline were obtained, and the results obtained were compared to determine the most dangerous parts of the coast from strong earthquakes. The wavelet analysis of the wave characteristics obtained for each scenario was carried out. Wave fields near the cities of Varna and Odessa are analyzed from far-fleld and mid-field seismic sources and the intensity of wave processes is estimated.

Key words: *earthquake source, tsunami waves, numerical simulation, histograms of the wave height distribution, spectral characteristics of the wave field .*

INTRODUCTION

It is well known that the western part of the Black Sea is blocked off the eastern part by an underwater ridge, and, as noted in [1]: "Tsunami sources in the eastern part of the sea almost do not transmit wave energy to its western part (Fig. 1) . And conversely, the waves excited in the western part of the sea are relatively weak in its eastern part. This depression is separated from the similar West-Black- Sea depression by the subcontinental block of the earth's crust - the Andrusov ridge, extending in the meridional direction from the southern coast of Crimea almost to the coast of Turkey.

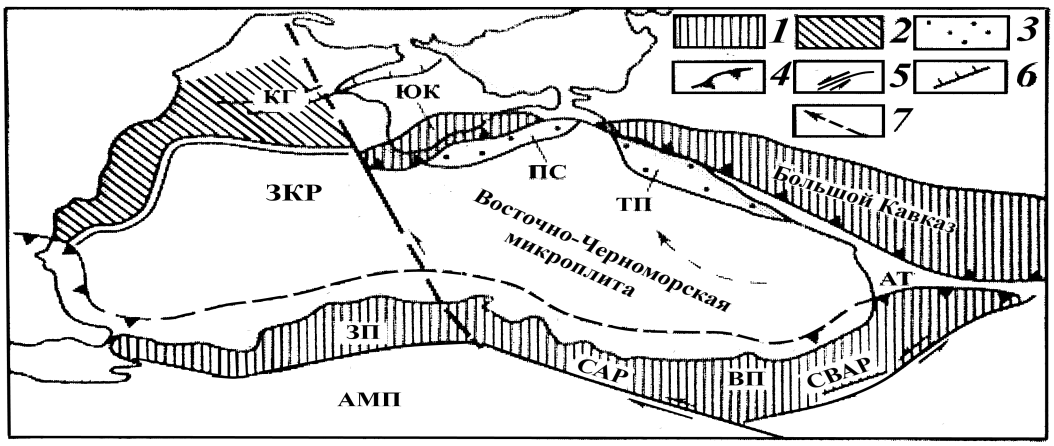

Fig. 1. The Eastern-Black-Sea microplate [2].

The figure above shows the schemes of active faults in the Crimean-Caucasian region, which depict different types of faults on the earth's crust [2]. As follows from these works, seismically active regions in this region are located in the north-east, south and south-west of the Black Sea depression, and in the northwestern region, in fact, earthquakes are rare. However, events like tsunami on the north-west coast were observed, both in the past centuries, and in the present one. So, on January 23, 1838 in the Odessa harbor, the intense excitement of the sea destroyed the ships. Apparently, this was due to an earthquake with a magnitude of M = 6.9 [3,4]. Already in our century on July 5, 2007, an event like a tsunami occurred on the Bulgarian Black Sea coast: "The excitement of the sea like a tsunami lasted several hours, small fishing boats were thrown on the beach of Balchik and Kavarna [5]. Figure 1 clearly shows that the Black Sea basin is divided into two parts: the West Crimean fault, which can be traced on the Odessa shelf and acts as a transfer zone. It is assumed that the West Crimean fault connects to the North Anatolian fault in the region to the south of Sinop (Fig.1) [2]. Thus, this fault plays the most important role of the largest transformational structure in the Black Sea basin [2]. The principal feature of the research carried out in this work is associated with the generation of tsunami waves by a kinematic source, considered in the keyboard model of the earthquake [6,7]. In contrast to the traditional formulation of tsunami studies in the Black Sea (piston source [8-13]), and from sources whose shape is a function of time [1; 14-17], seismic source consisting of several keyboard blocks are considered taking into account the kinematic and dynamic processes occurring in them during the earthquake [18-20]. Those, the movement of blocks with different directions of velocities up or down relative to the initial position of the sea bottom before the seismic shock is considered. The direction of movement in the source is consistent with the typical directions of ups and downs in historical sources, with the closest localization to the considered region of earthquakes [18-20]. To analyze the nature of tsunami source generation by a seismic source and the character of wave processes in a given water area, three types of model sources localized both in the regions of historical earthquakes and in "seismic gaps", determined by the basic geo-structures of the Caucasus and Crimean coasts [2; 21; 22] are considered.

1. Numerical simulation of generation and propagation of tsunami waves

. A nonlinear system of shallow water equations in a two-dimensional formulation (see, for example, [18, 19]) was used to describe the process of generation and propagation of a wave caused by movements of keyboard blocks in a seismic source, taking into account dissipative effects and bottom friction.

$$\begin{cases} \frac{\partial u}{\partial t} + u\frac{\partial u}{\partial x} + v\frac{\partial u}{\partial y} + g\frac{\partial \eta}{\partial x} = f_1 \\ \frac{\partial v}{\partial t} + u\frac{\partial v}{\partial x} + v\frac{\partial v}{\partial y} + g\frac{\partial \eta}{\partial y} = f_2 \\ \frac{\partial \eta}{\partial t} + \frac{\partial}{\partial x}[(\eta + H - B)u] + \frac{\partial}{\partial y}[(\eta + H - B)v] = \frac{\partial B}{\partial t} \end{cases} \qquad (1)$$

x, y are the spatial coordinates along the axes Ox and Oy, respectively, *t* is the time; $u(x, y, t)$, $v(x, y, t)$ are the velocity components along the Ox and Oy axes; $\eta(x, y, t)$ is the perturbation of the free surface with respect to its quiet level; *H* is the maximum depth of the basin, $B(x,y,t)$ is the change in the bottom of the basin (accounting characteristics of the dynamic seismic focus); *g* is the acceleration of gravity, where $f_1 = \frac{-C_h}{H+\eta}u\sqrt{u^2+v^2}$, $f_2 = \frac{-C_h}{H+\eta}v\sqrt{u^2+v^2}$ are the bottom friction coefficients, C_h –is the bottom friction coefficient. In the numerical solution, we used a scheme constructed by analogy with the scheme [23]. For modeling, the Black Sea bathymetry was used with a resolution of 500 m. The simulation was performed with a time step of

1 s. In the last seaward point, at a depth of 4 m, the condition of total reflection is set, allowing to fix at this depth the maximum and minimum values of the shift of the wave level. Using this data, it is easy to determine the maximum value of the runup on the coast (see, for example, [24, 25]).

The effect of the transform structure of the Black Sea basin on the formation of wave fields near the cities of Varna, Odessa, Yevpatoriya, Yalta and Feodosiya is analyzed from seismic sources located on both sides of the fault, using a complex keyboard block source of the earthquake. Both near-field and far-field seismic sources were considered. The nature of the movement of the blocks is shown in Table 1. Four scenarios for generation of tsunami waves by seismic sources A, B, F, G (see Fig.2) are considered, consisting of three blocks located on both sides of the fault.

Table 1. Block motion characteristics.

Number of block	1	2	3
Initial time of block motion , T_0 (c)	0	20	10
Final time of block motion, T (c)	10	50	20
Block uplift time, B (м)	1.75	1.75	1.75

It is important that, one of the source (source G) is located directly in the zone of the ridge. In all scenarios, a strong earthquake with a magnitude of M = 7.3 is considered.

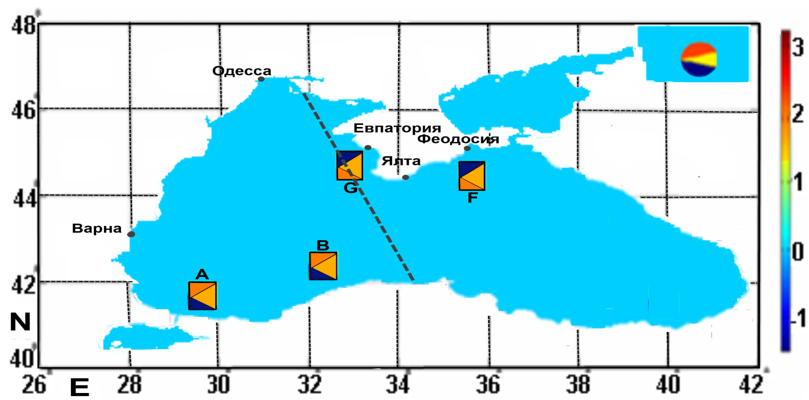

Fig. 2. The East-Black-Sea microplate with hypothetical seismic source [19,20].

The figure shows a schematic representation of the Black Sea basin, divided into two parts by the West Crimean fault with hypothetical seismic source [19,20].

Scenario 1. The generation of a tsunami wave by a seismic source A, located in the south-west of the water area is considered. It is clearly seen from Fig. 3 that at the 400th second we have a uniform circular wave front, 1 m high, towards the west coast and a wave front with a height of more than 3 m to the nearest south-west coast.

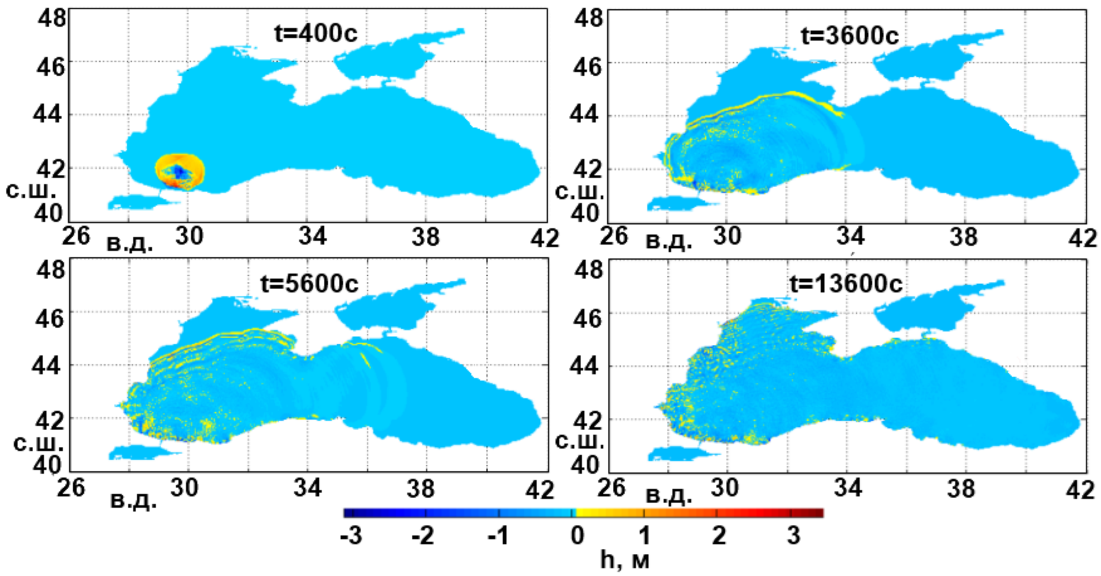

Fig. 3. The characteristic position of the wave fronts for 4 time moments: t = 400 s, t = 3600 s, t = 5600s, t = 13600 s for the seismic source A.

After about an hour the wave front with a wave height of up to 0.8 m, reaches the city of Varna and a 10cm front approaches Yalta; in an hour and a half the wave of 40 cm will approach the city of Yevpatoriya. To Odessa, a wave of 40cm will fit in 3.5 hours. In all the points considered in this scenario, the first wave will approach the beach with the crest (Fig. 3).

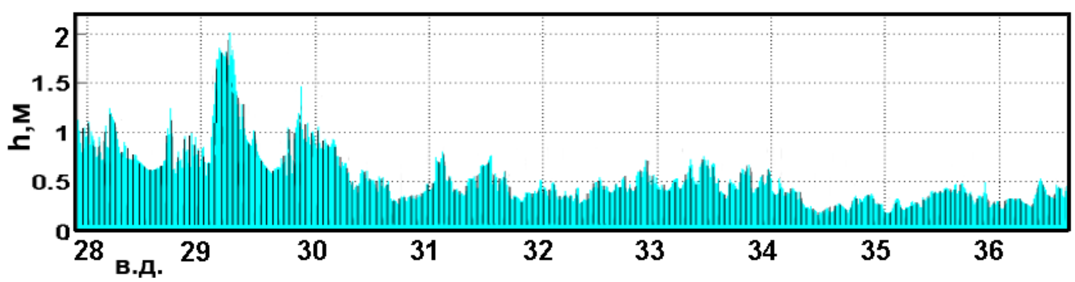

Fig. 4. A histogram of the maximum wave height distribution for the source A.

Figure 4 clearly shows that the maximum of the wave heights in the western part of the Black Sea coastline considered is, on average, about 1 m, and in some areas even of 1.8 m-2 m. At the same time, in the eastern part of this region, the maximum wave height in average is about 0.5 m and there are only a few local maxima not exceeding 0.7 m.

Scenario 2. In this scenario, the generation of a tsunami wave by a seismic source B located also to the west of the underwater ridge. At the 400th second, we have an almost circular wave front with a height of up to 1.5 m. Two distinct fronts reaching the western and north-western coasts are clearly visible. Unlike the previous computation, the wave heights approaching the selected points on the coast will be significantly lower. Figure 5 shows the positions of the wave fronts for 4 time moments.

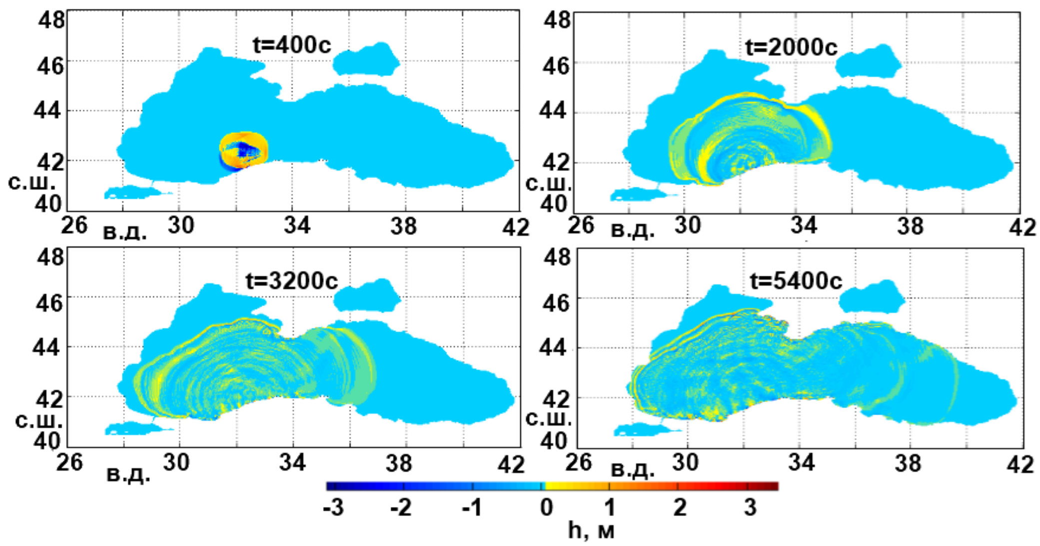

Fig. 5. Characteristic position of the wave fronts for 4 time moments: t = 400 s, t = 2000 s, t = 3200 s, t = 5400 s for the seismic source B.

In contrast to the previous scenario, where a local peak up to 2 m high is located in a direction perpendicular to the location of the source [26], in this case there is no (Fig. 6). The distribution of the maximums of the wave heights is uniform throughout the considered coastline and averages about 0.8 m.

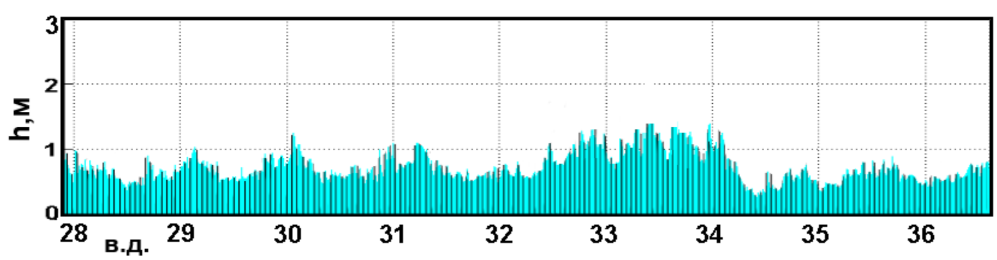

Fig.6. The histogram of the maximum wave height distribution of the (source B).

Scenario 3. The generation of a tsunami wave by a seismic source F located east of the ridge is considered. The source is set in such a way that the movement of one of the blocks downward is oriented towards the shore. In Feodosiya, the first wave will be a wave of rundown (the mareograms are shown in Fig. 7).

The next positive crest will reach 1.7 m. To the cities of Yevpatoriya and Yalta, a wave with a maximum height of 20-30 cm is suitable. In points near the cities of Odessa and Varna, the wave is practically not observed.

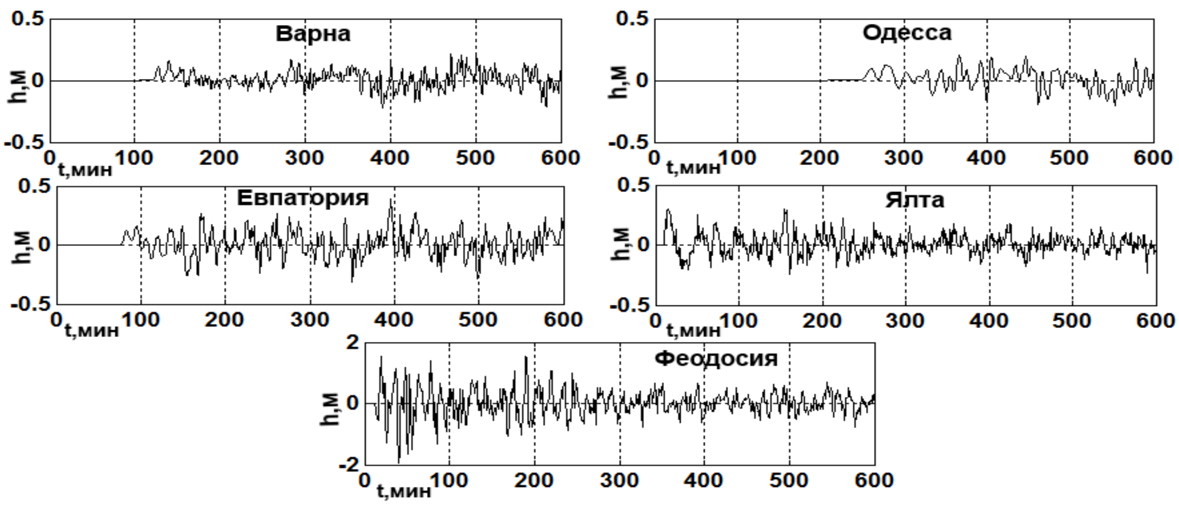

Fig. 7. Tide-gauge records for 5 points of Ukrainian and Bulgarian coasts for the source F.

In the western part of the Black Sea, the maximum wave height is 20-30 cm (Fig.8.). In the eastern part, the maximums of wave heights increase and range from 1 m to 3 m in the region of the local peak.

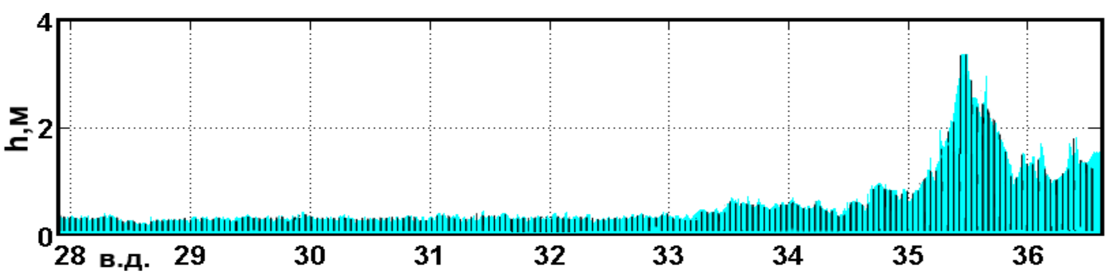

Fig. 8. The histogram of the maximum wave heights distribution for the source F.

Scenario 4. In this scenario, the source G is localized in the zone of the underwater ridge, i.e. one of the source blocks is located to the left of the ridge, and the location of the rest corresponds to Fig. 9, which shows the location of the main geostructures in the Crimean and Caucasian coasts of the Black Sea. To the coast of Yevpatoriya, the first wave comes back, after it 2 m wave is going: to the cities Yalta and Feodosia a 10-15 cm wave is coming.

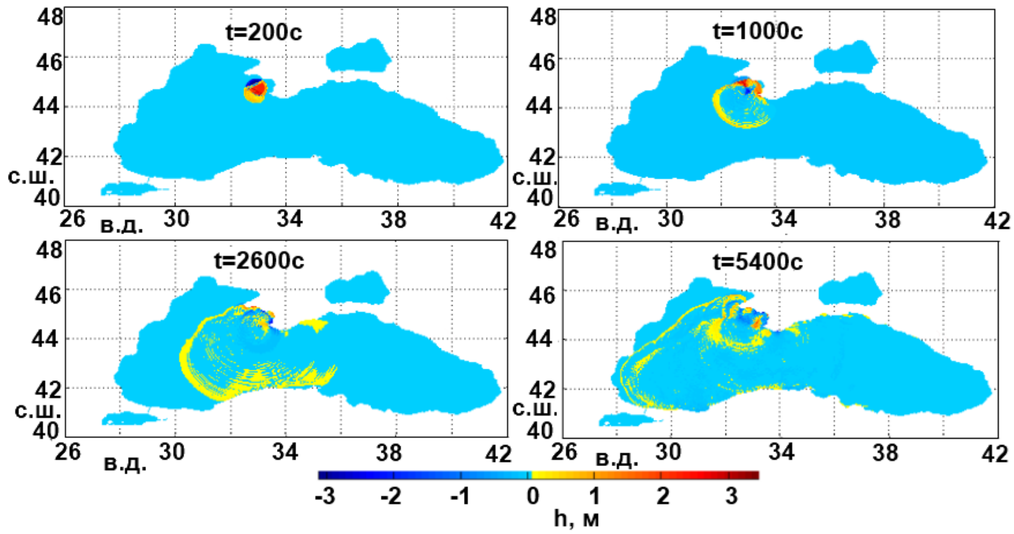

Fig. 9. The characteristic position of the wave fronts for 4 time moments: t = 200 s, t = 1000 s, t = 2600 s, t = 5400 s for the seismic source G.

To Odessa, the wave approaches a positive crest, and the maximum wave, about 1 m, was not the first wave (Fig. 9). Positive wave crest with 10-30 cm high approaches the city of Varna. At a time of about 40 minutes, a well-formed front is visible, moving to the west coast of the water area. After an hour and a half two well-defined fronts are formed, the first of which reaches the coast near the city of Varna.

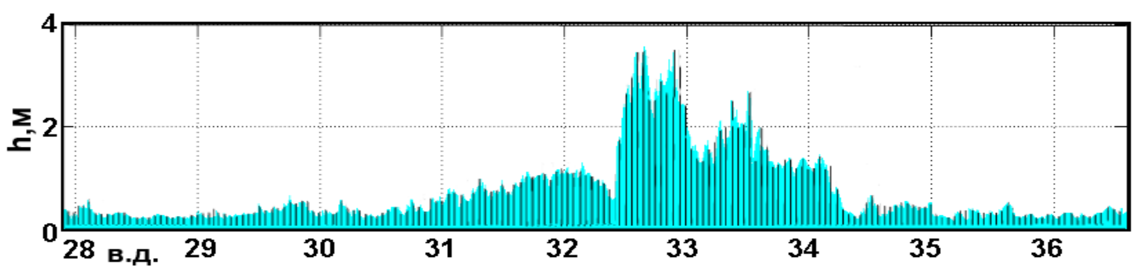

Fig.10. The histogram of the maximum wave heights distribution of the (source G).

Fig. 10 clearly shows that in the vicinity of 32.30 E. a dip is observed and at the west the maximum wave heights do not exceed 1 m, however, from 32.30 E. up to 33.50 E wave heights reach 2.5 m and 3.5 m.

Table 2. Maximum wave heights for 4 scenarios in five cities: Varna, Odessa, Evpatopiya, Yalta, Feodosiya

City	Maximum wave (m) at 4m isobate			
	source A	source B	source F	source G
1. Varna	0.8	0.5	0.1	0.3
2. Odessa	0.3	1	0.1	1
3. Evpatoriya	0.4	1	0.3	2
4. Yalta	0.1	0.2	0.25	0.15
5. Feodosiya	0.2	0.6	1.7	0.1

From Fig. 11 and Table 2. it is clear that the maximum wave heights on the north-west and west coasts do not exceed 2.1 m from the far-field A and B sources. At the same time, the distribution of the maximum wave heights from B is uniform and equals 0.8- 0.9 m.

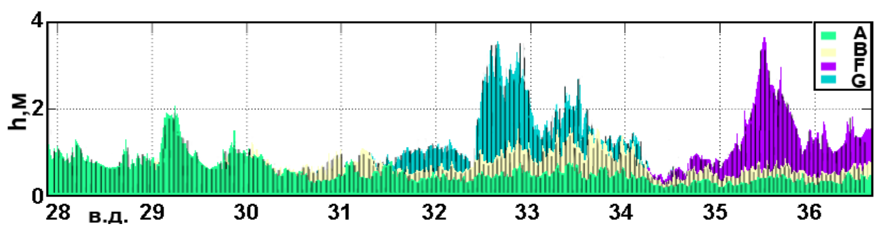

Fig. 11. A histogram of the maximum wave height distribution along the Black Sea coast for A, B, F, G sources.

When calculating tsunami from near-field F and G sources (considering that the keyboard source of the elliptical shape was considered, which does not give an additional refraction contribution from the corners), the maximum wave heights reach 3.5 m.

2. Spectral analysis of possible catastrophic tsunamis for western Black Sea coast.

Using the results of above computations for the generation and propagation of tsunami waves in the water area, a one-dimensional and two-dimensional (wavelet) spectral analysis was performed and the spectral characteristics of tsunami waves were obtained in a given area of the water basin [27, 28]. To analyze the propagation of energy in the water area from the far-field and mid-field seismic sources G, F and B (see Fig. 2), the wave fields near the cities of Varna and Odessa are analyzed. Fig. 12 shows the calculated tide gauges from a virtual tide gauge located in the seaside point near Varna, on a 4 m isobath. The wavelet spectrograms constructed for it from far-field and mid-field seismic sources are shown in Fig. 12 (a, b, c).

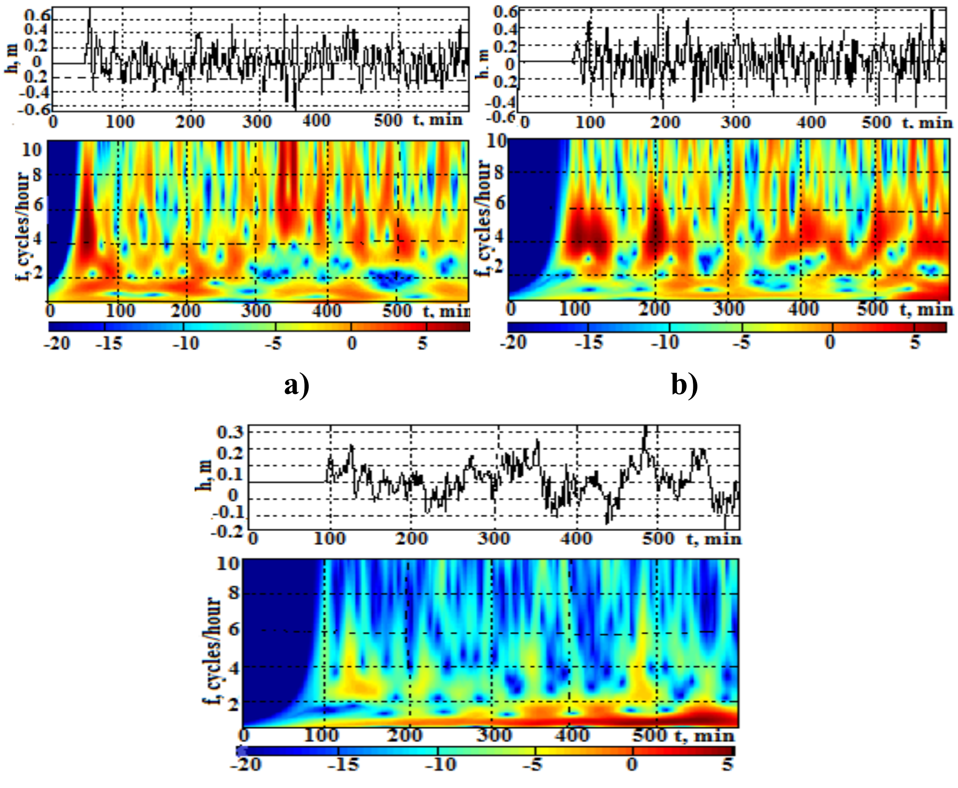

Fig. 12. Tide-gauge records and wavelet-spectrograms for the city of Varna from seismic sources: a) for the mid-field source B; b) for the far-field source G; c) for the far-field source F.

For the source B: The largest amplitude of waves on the 4th isobath is 70 cm. The wave reaches the tide gauge in 40 minutes. It follows from the calculations of the spectra that there are two powerful outbursts at intervals of 30 to 70 min in the range 3.5 to 8 cycles/hour (cph) (waves with duration 17-8 min) to 10 dB and at the interval 340-360 min from 4 to 10 cph, i.e. for 15-6-minute waves, with an energy of up to 8 dB. Those, the most intense are waves with a duration in the range of 6-17 min, which is in good agreement with the tsunami process. Also, in the calculated spectrum, three regions of low-frequency components of a weaker intensity are obtained up to 5 dB with frequencies from 1 to 2 cph at intervals from 20 to 100 min, from 170 to 240 min and from 400 to 480 min, a large fraction of the energy is concentrated in the high-frequency region from 6 to 10 dB.

For the source G: The largest amplitude of the waves on the 4th isobath is 55 cm, however, the amplitude of the first wave is not more than 20 cm. Due to the location of the source, the wave comes to the point 40 minutes later than from the source B. Calculation of the spectrogram shows that in this case the main energy is localized in two regions - in the interval from 80 to 140 min and 180 - 220 min. In the first case, the energy is concentrated, basically, from 2.2 to 6 cph, i.e. The greatest energy up to 7 dB is carried by 25-10 min of the wave. There are also several areas of lower intensity up to 3 dB for the 3-6 cph range, i.e. for 20-10 min of waves. The picture for high-frequency components is similar to the calculation for the source B, which may indicate significant reflections of waves in the shelf zone.

For the source F: For this point, the source VI is a far-field source. The wave approaches the point in 1 hour 40min. The largest wave amplitudes on the 4th isobath are 35 cm, however, the first wave does not have the maximum amplitude. The greatest energy of waves is concentrated in the range up to 1 to 2 cph from 300 to 600 min, i.e. for 30-60 minute waves. The greatest energy is up to 5 dB from 450 to 580 min. High-frequency components in this case are practically absent.

From this analysis it is clear that even for a strong earthquake the Black Sea coast of Bulgaria will not be exposed to significant danger, long-wave wave components do not concentrate significant energy, which is possibly associated with strong wave refraction. This conclusion agrees well with the conclusions of [24, 25]. For analysis of the northwestern part of the Black Sea coast, a seashore point was chosen, located near Odessa. Tide-gauge records of the computed wave fields from three virtual seismic sources G, F and B, and the wavelet spectrograms corresponding to them, are shown in Fig. 13.

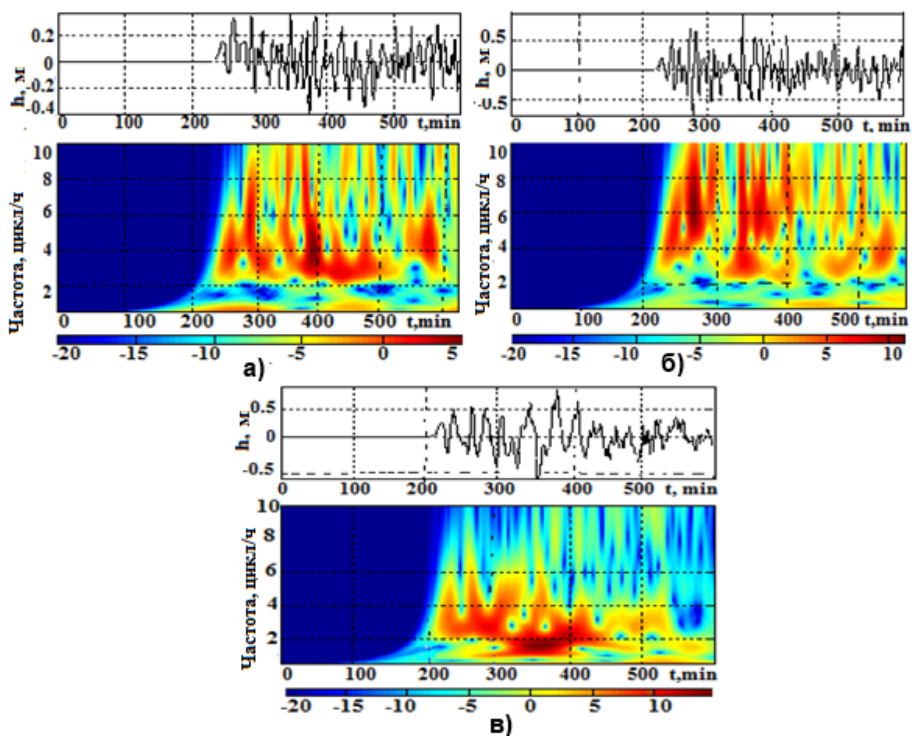

Fig. 13. Tide-gauge records and wavelet spectrograms for Odessa from far-field source: a) for the source B; b) for the source G; c) for the source F.

For the source B: the source of the far-field field, maximum wave amplitudes up to 40 cm. All energy up to 5 dB is concentrated in the region of 370-400 min in the elongated region from 2.5 to 5.7 cph, which corresponds to waves of duration from 10 to 24 min. Areas of lower intensity are almost evenly distributed over the interval 220-500 min. At 280 min, 350 and 370 min in the range of 2-10 cph, the wave intensity is of the order of 3 dB.

For the source of G: the greatest energy is concentrated in the interval 280-300 min, to 14 dB from 5 to 8 dB, i.e. for waves with a duration of 5 to 7.5 min. A smaller intensity of up to 8 dB is observed in the interval from 230 to 320 min, and from 350 to 430 min. The energy is evenly distributed over all frequencies from 2 to 10 cph.

For the source of F: the greatest energy is concentrated in the interval 340-400 min to 20 dB for frequencies from 1 to 2 cph, which corresponds to durations of 30-60 min.. Intervals with lower intensity are also observed in the regions from 220 to 320 min and from 370 to 450 in the 2-4 cph, including some localized regions of zero intensity.

CONCLUSIONS

Thus, even for a strong earthquake with a magnitude of M = 7.3, the points located on the western coast of the Black Sea will not be seriously endangered, the long-wave components will not have significant energy for large damages on the shore. The obtained values of the maximum wave heights are directly related to the choice of the scenario for the realization of an earthquake in hypothetical seismic sources, in those cases when the first vertical downward movement in the source is oriented toward the coast. Such an implementation of the earthquake leads to the appearance of a negative wave front (a depression wave) directed toward the coast. As shown in [29, 30], in this case a substantial increase in the wave extending to the shelf is possible. In addition, the recalculation from the isobath to the dry shore leads to a significant increase in the height of the wave. In this connection, the values of the calculated wave heights from the model seismic sources on the 4-meter and 10-meter isobath given in the work can be considered as the lower estimate for determining the wave heights on the shore. The spectral analysis showed that the largest wave energy will be mainly concentrated in the low-frequency component of the spectrum, which corresponds to wave periods of the order of 12-30 min. The most dangerous in this case are near-field seismic sources, in which the greatest intensity of wave energy can reach 50 dB. However, spectral analysis showed that the energy of the approaching wave and the localization of the epicenter of the earthquake are not correlated.

ACKNOWLEDGEMENT

This work was supported by a grant from the Russian Science Foundation (project No. 14-50-00095).

REFERENCES

1. Dotsenko S.F., Solovyov S.L. On the role of residual displacements of the ocean floor in the generation of tsunamis by underwater earthquakes // Oceanology v.35, No. 1, P.25-31, 1995.
2. Kazmin V.G., Lobkovsky L.I., Pustovitenko B.G., Modern kinematics of microplates in the Black Sea-South Caspian region, Okeanologiya v.44 No. 5. pp. 600-610. 2004.
3. Solovyeva O.N., Dotsenko S.F., Kuzin I.P., Levin B.V., Tsunami in the Black Sea: historical events, seismic sources and patterns of distribution // Oceanology v. 44. No. 3. p.679-685. 2004.
4. Pelinovsky E.N., Preliminary estimates of tsunami for the northern Black Sea, Phys. Chem.Earth v. 24A. P. 175-178. 1999.
5. [http://bg-faq.astrela.com/nature/tsunami_tidal_wave.htm].
6. Lobkovsky L.I., Baranov BV Keyboard model of strong earthquakes in island arcs and active continental margins // Doklady of the Academy of Sciences of the USSR. V. 275. № 4. P. 843-847. 1984.
7. Lobkovsky L.I., Kerchman V.I., Baranov B. V., Pristavkina E.I. Analysis of seismotectonic processes in subduction zones from the standpoint of a keyboardmodel of great eartgquakes // Tectonophysics V.199, P.211-236, 1991.
8. Basov B.I., Kajstrenko V.M., Levin B.V., Poplavsky A.A., Simonov K.V., Kharlamov A.A. Some results of physical modeling of the processes of excitation and propagation of tsunami // in: Tsunami Generation and Wave Emission on the Shore, M .: Radio and Communication, 1984, P.68-72.
9. Gusyakov V.K., Chubarov LB. Numerical simulation of tsunami excitation and propagation in the coastal zone. Izv. AN SSSR. Physics of the Earth v.21, No. 11, P. 53-64, 1987.
10. Dotsenko SF, Sergeevsky B.Yu., Cherkesov L.V. Generation of spatial tsunami waves by bottom motions of finite duration // Tsunami Studies No. 2, Moscow: Nauka, 1987, p. 27-34 (in Russian).
11. Zaitsev A.I., Kozelkov A.S., Kurkin A.A., Pelinovsky E.N., Talipova T.G., Yalchiner A.S., Tsunami modeling in the Black Sea // Izvestiya AIIN RF, PMM T. 3. P. 27-34. 2002.
12. Levin B.V. A review of the work on the experimental modeling of tsunami excitation // in the book: Methods for calculating the origin and distribution of tsunamis. Moscow: Nauka, 1978, p.125-139 (in Russian).

13. Levin B.V., Nosov M.A. Physics of tsunami // M .: Janus-K, 2005.- 360 p.
14. Dotsenko S.F. Excitation of tsunami waves in continuously stratified motions of the bottom section // Tsunami Studies No. 3, Moscow: MGFK under the Presidium of the USSR Academy of Sciences, 1988, p.7-17.
15. Nosov M.A. Comparative analysis of excitation of tsunami by piston and running shifts of the bottom // Volcanology and seismology № 6, C.70-75, 1995.
16. Okada Y. Surface deformation due to shear and tensile faults in a half space // Bull.Seismol.Soc.Am., V.75, P.1135-1154, 1985.
17. Rangielov B., Possible tsunami deposits discovered on the Bulgarian Black Sea coast and some implications. // in: Submarine Landslides and Tsunamis (Kluwer Acad.Publ., 2003), P. 237-242.
18. Mazova R.E., Tresvyatskaya E.A. Numerical Simulation of Long Water Wave Generation by Dynamic Seismic Source and Their Propagation for Black Sea Basin. Russ. J. Earth Sci. V.8, ES5001, doi: 10.2205 / 2006ES000208 http: //dx.doi. org / 10.2205 / 2006ES000214 (2006).
19. Mazova R.Kh., Kiselman B.A., Kolchina E.A. Numerical simulation of tsunami wave height distribution for the Turkish Black Sea coast in the nonlinear dynamic keyboard of the underwater seismic source // J.of Comp.and Appl. Math., V.259, P. 887-896 (2013), http: //dx.doi .org / 10.1016 / j.cam.2013.08.034
20. Mazova R.KH., Kiselman BA, Osipenko NN, Kolchina E.A. Analysis of spectral characteristics of the Black Sea tsunami / / Proceedings of Nizhny Novgorod State Technical University. R.E. Alekseeva, 2013, No. 2 (99), P.52-66.
21. Chebanenko, I.I. Scheme of deep faults on the Crimean and Caucasian coasts of the Black Sea / II. Chebanenko, et al., Geol. journal. 2003. № 1. P. 54-58.
22. Soloveva, ON Seismicity and tsunami of the north-eastern part of the Black Sea / O.N. Solovyov, I.P. Kuzin // Oceanology. 2005. №45. Pp. 826-833.
23. Sielecki A., Wurtele M. The numerical integration of the non-linear shallow-water equations with sloping boundaries // J. Comp. Phys. V.6, P.219-236, 1970.
24. Golubtsova T.S., Mazova R.Kh. The roll of a wave of variable shape // in the book. "Oscillations and waves in the mechanics of a continuous medium", Gorky: ed. GPI, 1989, P.52-63 (in Russian).
25. Pelonovsky E.N., Mazova R.Kh. Exact analytical solutions of nonlinear problems of tsunami wave runup on slopes with different profiles // Natural Hazards V.6, P. 227-241, 1992
26. Nikonov A.A. Tsunami on the shores of the Black and Azov Seas // Izvestiya RAN. Physics of the Earth. T.33. № 1. P. 86 - 96. 1997

27. Vetterli M., Kovacevic J., Goyal V. - Foundation of Signal Processing, Cambridge University Press (ISBN 110703860X), 2013, 707p.
28. Mallat Stephane «A wavelet tour of signal processing» // Academic Press, 1999.
29. Dotsenko SF, Konovalov A.V. Numerical simulation of tsunami wave propagation in the open part of the Black Sea // Marine hydrophysical journal. No. 1. P. 67-80. 1995.
30. Kulikov E.A., Poole S.L., Rabinovich A.B. Spectrum of long waves in the open ocean and radiation tides // in: Wave processes in the northwestern part of the Pacific Ocean, Vladivostok: Fae-East NTS USSR Acad.of Sci., 1980, P.28-38 (in Russian).

ISSN 8755-6839

SCIENCE OF **TSUNAMI HAZARDS**

Journal of Tsunami Society International

Volume 37 **Number 3** **2018**

VULNERABILITY ANALYSIS BASED ON TSUNAMI HAZARDS IN CRUCITA, CENTRAL COASTAL OF ECUADOR

Julio Cesar Celorio-Saltos[1], Jhonny Marcelo García-Arias[1], Alfredo Bienvenido Guerra-Luque[1] Grey Barragan-Aroca[1] and Theofilos Toulkeridis[2]*

[1]Escuela de Gestión de Riesgo, Facultad de Ciencias de la Salud y del Ser Humano, Universidad Estatal de Bolívar, Guaranda, Ecuador
[2]Universidad de las Fuerzas Armadas ESPE, Sangolquí, Ecuador

*Corresponding author: ttoulkeridis@espe.edu.ec

ABSTRACT

In the coastal center of Ecuador is situated the touristic village of Crucita, which has 13 km large, very flat beach extension, being potentially extremely vulnerable by a future tsunami impact. Therefore, an extensive study has been performed about the vulnerability of the population, of the response authorities and of the infrastructure for tsunami hazards. Once the different variables were analyzed, the different levels of vulnerability in the population of the Crucita parish have been evidenced. In this framework, among the main findings have been the general low knowledge of the population about tsunamis and their hazards, the absence of evacuation plans, the high level of exposure of the physical infrastructure (housing, basic services and telecommunications), and the absence of institutional capacities to respond to a situation of emergencies and / or disasters in general, and of tsunamis in particular.

Keywords: population vulnerability, economic vulnerability, physical structural vulnerability, institutional capacity, degree of exposure

1. INTRODUCTION

Ecuador is one of the few countries on the planet, where all types of plate boundaries are present, represented by the East Pacific Rise, the Galápagos Spreading Center, the Hess Rift, the Ecuadorian trench and the Guayaquil-Caracas Mega Fault (Fig. 1; Gutscher et al., 1999; 2000; Dumont et al., 2005; Toulkeridis, 2011; 2013; Dumont et al., 2014). Based on these plate tectonic movements and being located in a tropical area, which has been frequently exposed to a variety of climatic processes, this small Andean country has been targeted to a high amount of natural disasters such as landslides, flooding, drought, volcanism, earthquakes and tsunamis (Schuster et al., 1996; Harden, 2001; Massonne and Toulkeridis, 2012; Toulkeridis, 2013; Chunga and Toulkeridis, 2014; Toulkeridis et al., 2015; Toulkeridis et al., 2017; Mato and Toulkeridis, 2017; Toulkeridis and Zach, 2017; Pararas-Carayannis and Zoll, 2017; Jaramillo Castelo et al., 2018; Zafrir Vallejo et al., 2018). Therefore, Ecuador has been considered to be a mega vulnerable country, due to exposure to various hazards throughout the national territory, many of which have caused material losses and unfortunately also disproportionally many human lives (Toulkeridis, 2016; Rodriguez et al., 2017; Navas et al., 2018).

Among the natural disasters are various origins of tsunamis, such as severe local tsunamis which hit Ecuador on several occasions, of which the last occurred more than three decades ago, in 1979 (Pararas-Carayannis, 1980; Herd et al., 1981; Mendoza and Dewey, 1984; Beck and Ruff, 1984; Pararas-Carayannis, 2018). Many citizens in Ecuador didn't realize that with the most current strong earthquake in 2016 in the coastal region, also a local tsunami has been generated, with minor damages (Ye et al., 2016; Toulkeridis et al., 2017). Nonetheless, as regional and far-reaching tsunamis have impacted in different, but less severe forms the coasts of Ecuador a great concern has been generated in the population that is settled in such vulnerable sites. The shocking images in the news media of the tsunamis generated in Chile in 2010, Japan in 2011 or in Mexico in 2017 (Delouis et al., 2010; Pararas-Carayannis, G., 2010; Simons et al., 2011; Pararas-Carayannis, G., 2014; Okuwaki and Yagi, 2017), have created a general fear in the Ecuadorian population, which is expecting sooner or later a similar disaster on their own settlements. Thus, it has been considered fundamental to carry out an investigation to determine the level of vulnerability towards tsunami hazards for the population, authorities and their infrastructure (Pararas-Carayannis, 1983; 1988).

Based on the aforementioned, the main objective of this research work has been to identify the vulnerability level of tsunami hazards in the Crucita parish, a typical touristic site in central coastal Ecuador. In this sense, the main objective has been to contribute to the generation of knowledge about the factors that contribute to the increase or decrease of vulnerability towards tsunamis, while some of these may have been directly intervened.

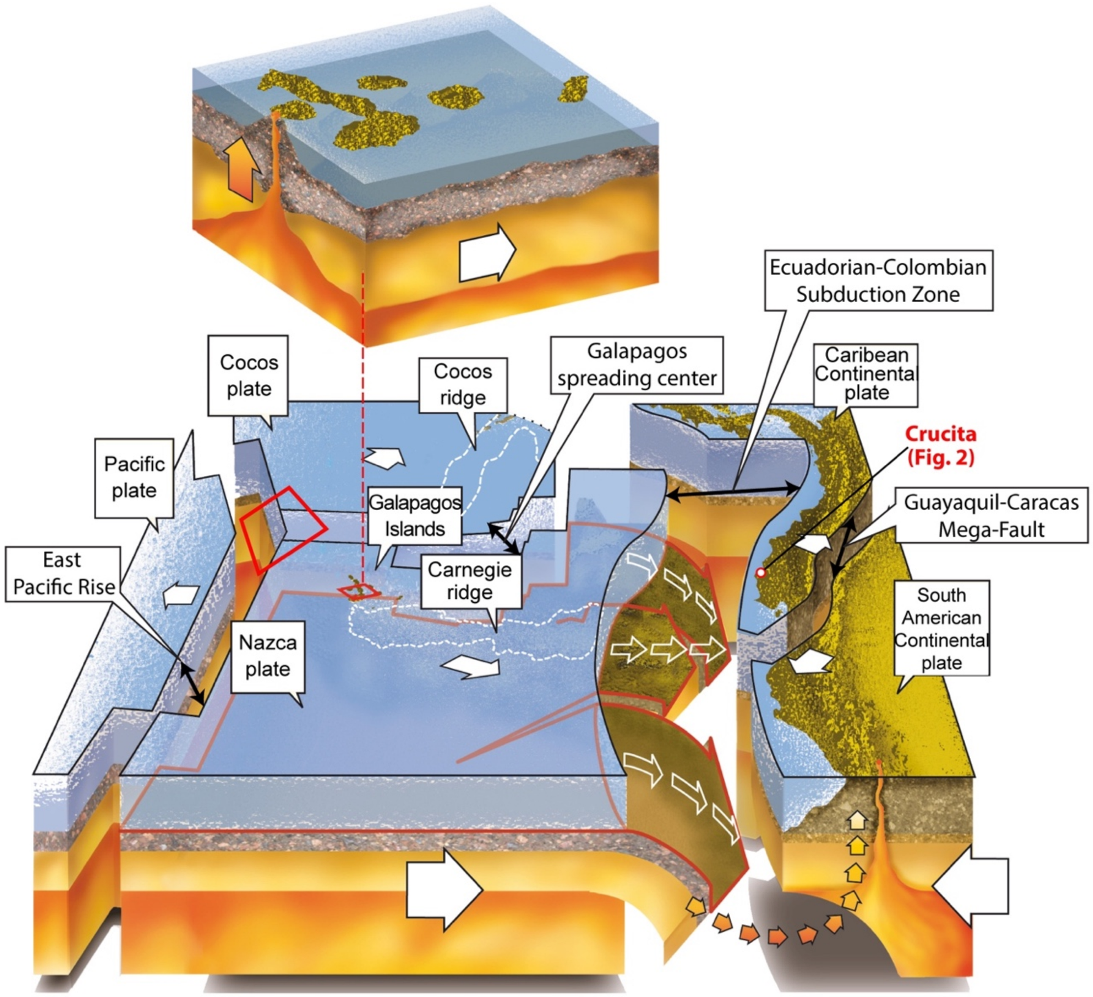

Fig. 1: Geodynamic setting of Ecuador with associated oceanic and continental plates and a variety of plate boundaries, such as the divergent plate boundaries named East Pacific Rise and Galapagos Spreading Center, the convergent plate boundary represented by the Ecuadorian-Colombian Subduction zone, as well as the transcurrent plate boundary represented by the Guayaquil-Caracas Maga-Fault. Also shown the Galapagos Islands and the Carnegie Ridge. Adapted from Toulkeridis, 2013, modified of Toulkeridis et al., 2017a.

2. STUDY AREA AND POTENTIAL TSUANAMI HAZARDS

Crucita is one of the seven rural parishes of the Portoviejo canton with urban characteristics for being a tourist attraction, having 13 km of beach extension (Fig. 2). Although the village is located at an altitude of up to 200 meters above sea level, its average height for the area with the highest people concentration and urban settings is of about 2.5 m.a.s.l. (Fig. 3). The relief of the parish is composed of a fairly regular flat area that is part of the Portoviejo River valley and a high area covered by a dry forest. Crucita is located on a alluvial plain composed of silty sediments with loose conglomerates that give shape to a flat, undulating surface, which rises towards the southeast in a high-pitched sector, composed of white to reddish shales and thin sandstone layers. Crucita extends from the so-called Punta de Charapotó to the North to the Punta de Jaramijó to the South, in an open bay where the beach is composed of thin sandy bars near the shore. In this section of the coastal profile the bottom is sandy and the depths are regular, with shafts (slope of the oceanic shelf) of 10 and 20 m, that cross at a distance of 0.50 and 1.50 miles from the coast. Furthermore, the contours in this area are very pronounced, being up to 10 m, with an average slope of 2% from which it gradually softens until it reaches 0.8% in the 20 m depths. Due to the bathymetric profile and the shape of the bay, the height of the waves are able to increase slightly, and then burst forcefully up to 1 km onshore, destroying weak constructions (wood, cane, block) in the flat area.

Fig. 2: Overview of Crucita from the southern hillside of the parrish.

Due to its geographical location, the Crucita parish is potentially exposed to tsunami hazards, as it has been documented several times after the occurrence of local earthquakes, such as January 31, 1906 (8.8 Mw), October 2, 1933 (6.9 Mw), of December 12, 1953 (7.3 Mw) of January 19, 1958 (7.8 Mw), December 12, 1979 (8.2 Mw) and April 16, 2016 (7.8 Mw) (Berninghausen, 1962; Kanamori and McNally, 1982; Pararas-Carayannis, 2012; Toulkeridis et al., 2017a; 2017b; 2018). However, the earthquake with a distant origin tsunami, which occurred on March 11, 2011 in Japan with a magnitude of 8.9 on the Richter scale (Simons et al., 2011; Norio et al., 2011), have generated a considerable run-up that reached an altitude of 3.24 m during the high tide, causing effects on greater and lesser degree in populations that are located on the coastline, including the village itself (Rentería et al., 2012; Lynett et al., 2013). Due to this facts, it has been evidenced, that the population of Crucita does not have tools for organization and preparation towards tsunami hazards being of local, regional or distant origin, which causes its inhabitants to present conditions of vulnerability in their response capabilities.

Of the twelve documented earthquakes that have occurred nearby during the last 130 years, with intensities greater than 6.0 degrees on the Richter scale, five have been related to local geological faults and the remaining seven with the subduction zone (Fig. 1; Table 1). Crucita is situated just 75 east of the suture zone, between the Nazca plate with the Caribbean and South American continental plates, lying in a strong and active seismic zone, as evidenced also by the map for Seismic Design of the Ecuadorian Construction Standard (NEC, 2014), where the soil may receive accelerations equal to or greater than 0.50 g. Furthermore, the deformations generated by subduction trigger the formation of active fault systems that have been the source of earthquakes on the continental shelf. In the case of Manabí, the surface is affected by the Jama, Bahia de Caráquez, Calceta, Jipijapa and Julcuy geological faults among several minor ones (Egüez et al., 2003).

Table 1: Earthquakes occurred during the last 130 years in Manabí. Data from Lopez (2013) and USGS (2016).

Year	Lat.	Long.	Depth	Magnitude	Intensity	Distance Epicenter to Crucita in km
1896	-0.51	-80.45		7.0	IX	33 Km
1937	-0.50	-80.00		6.5	VIII	68 Km
1942	-0.01	-80.12	50 Km	7.8	IX	110 Km
1956	-0.50	-80.50		6.9		34 Km
1958	-0.50	-81.00		6.2		65 Km
1959	-1.00	-80.50		6.4		16 Km
1961	-0.40	-80.40	56 Km	6.3	VIII	52 Km
1962	-1.30	-80.40	75 Km	6.3	VIII	50 Km
1964	-0.84	-80.29	34 Km	6.0	VIII	25 Km
1990	-0.13	-80.28	53 Km	6.1	VIII	84 Km
1998	-0.55	-80.53	39 Km	7.1	VIII	33 Km
2016	-0.35	-79.92	21 Km	7.8	IX	110 Km

Based on the aforementioned recurrence of earthquake hazards, the following effects are able to coccur in the area of Crucita: (a) partial and complete destruction of houses and buildings; (b) Affectation of the population due to the loss of homes, livelihoods and relatives as well as injuries and alteration of the emotional state; (c) Affectation and destruction of the basic service networks and with it the suspension of the corresponding services; (d) Destruction of the roads by subsidence and liquefaction; (e) Fire, tsunami flooding, when magnitude overcomes 7.5 on the Richter scale.

3. METHODOLOGY

The study of vulnerability about tsunami hazards in Crucita, has been developed on a simple random sample of ten public institutions and 389 inhabitants being located in the center, north and northeast side of the Crucita parish. The study area extends along 13 km of beach on an area of around 63.26 km^2, of which only 8.77 km^2 (13.86%) is currently destined for housing occupation, tourism services such as accommodation and food, development of commercial activities, operation of the public administration, networks of basic services, education and health facilities.

For the development of the research the type of descriptive, qualitative and quantitative study has been used, as such is based on an analysis of the physical characteristics of the structures and networks of services, the social, economic, educational, cultural, institutional policies as well as the institutional and community capacities. This allows an alphanumeric evaluation of the obtained results in order to estimate the vulnerability level from the specific to the general, depending on the independent and dependent variables. This may explains in a descriptive way the results of the current research for a subsequent adequate decision making process.

Based on the analysis of methodologies used for the analysis and evaluation of vulnerability factors such as the Methodology for Vulnerability Analysis at the Municipal Level proposed by the United Nations Development Programme and the National Secretary of Risk assessment (UNDP-SNGR, 2011), Methodology for Vulnerability Assessment proposed by the Disaster Prevention in the Andean Community (PREDECAN, 2009) and the Basic Manual for the Estimation of Risk developed by the National Institute of Civil Defense, the National Directorate of Prevention and the Unit for Studies and Risk Assessment (INDECI- DINAPRE- UEER, 2006). An alpha numerical methodology has been defined for estimating vulnerability to the threat of tsunamis, which includes indicators and evaluation parameters related to four aspects of analysis, namely structural, social, institutional and community. Therefore, the present methodology contemplates the following criteria for its application: a) selection of indicators and evaluation parameters; b) qualitative and quantitative analysis of indicators. c) weighting of indicators; d) estimation of the level of vulnerability; e) survey by sampling.

a) Selection of indicators and evaluation parameters

The selection of the type and number of indicators and evaluation parameters have been dependent on the independent and dependent variables of the present study. The same ones that have been organized for their application in ten matrix fields that allowed the verification of elements in the field. The first matrix field allows for an appreciation of the level of structural physical vulnerability of the household, according to the resistance they may have to the occurrence of tsunamis, in relation to the distance of the houses from the shore of the high tide (Table 2).

The second matrix field determines the level of vulnerability of service networks in relation to the access and functionality of systems for the provision of basic services, by checking co-verage, redundancy of systems and dependence on other levels (cantonal, provincial, national) for its respective operation (Table 3).

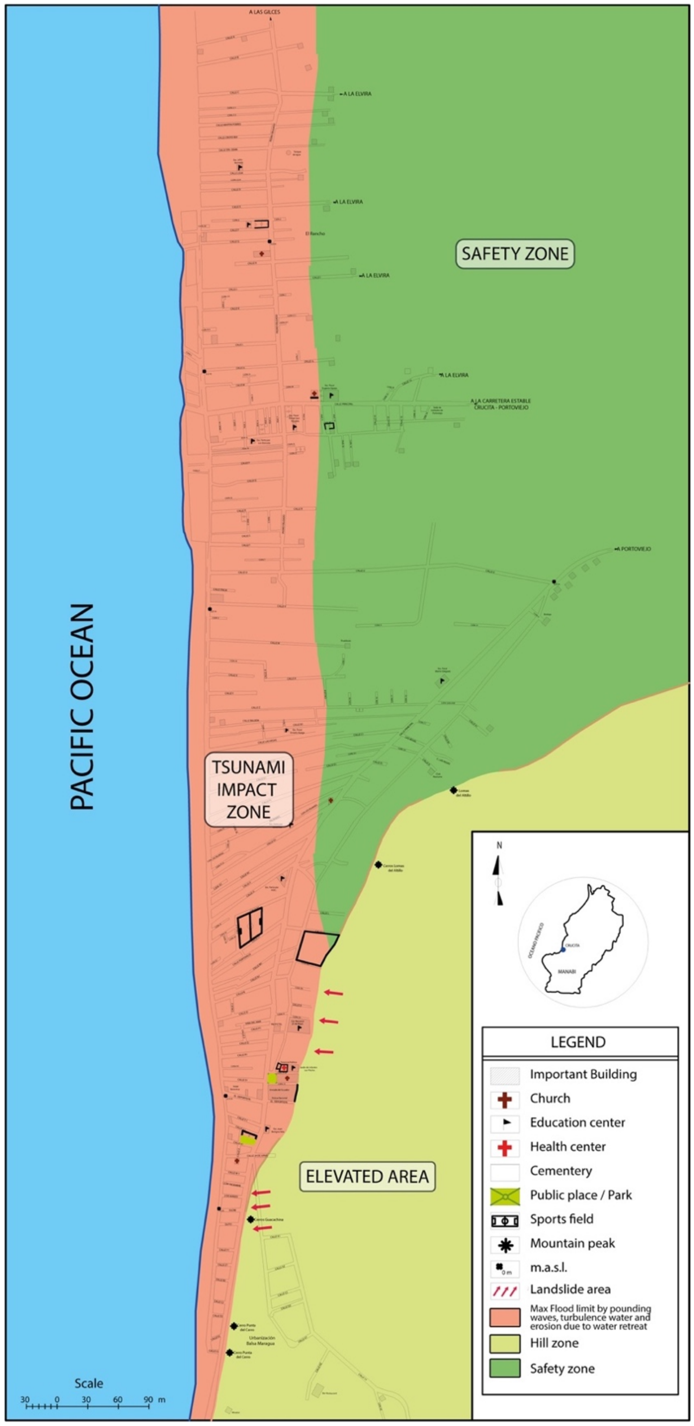

Fig. 2: Tsunami impact area and safety zone of Crucita. Based on Cruz and Vasquez (2010).

Fig. 4: a) Indication to avoid parking in order to be able to evacuate in one of the main roads perpendicular to the ocean´s shore line; b) Typical warning sign and indication of evacuation direction for incoming tsunamis; c) Coastal barrier, more likely for high tides; d) sign for tsunamis above barrier, being less visible from the beach; e) Sign of safety zone from tsunamis; f) Abandoned outlook point for rescue stuff, at priod of storming sea (red flagg) and evacuation sign of tsunamis. All photos taken in Crucita.

The third matrix field, defines the level of social vulnerability in relation to the existing social organization for the sustainability of processes, citizen participation in activities of coexistence and development, as well as the access of families to basic services and social order (Table 4).

The fourth matrix field determines the level of economic vulnerability of the family core according to the total income per family, the type of housing and the number of people that make up the family nucleus (Table 5).

The fifth matrix field, allows to define the level of educational vulnerability, in relation to the level of formal education reached by family members, as well as training on tsunami preparedness that they may have received (Table 6).

The sixth matrix field, allows to define the level of cultural vulnerability of the population towards tsunami hazards, through the verification of prescriptive elements such as the knowledge and occurrence of the aforementioned hazards, as well as the attitude of the people facing a possible occurrence of tsunamis in the Ecuadorian coasts (Table 7).

The seventh matrix field is aimed to identify the political and institutional elements that guarantee the reduction of disaster risk in the parish, and allows determining the level of institutional political vulnerability through state and local policies, budgetary availability to promote processes of disaster risk reduction, the existence of control and planning mechanisms, as well as the development of actions to reduce disaster risk and staff training (Table 8).

The eighth matrix field allows to determine the level of vulnerability of the essential elements existing in the parish, by verifying the location of the same in relation to the high tide and its functional condition (Table 9).

The ninth matrix field is related to the identification of the capacity level of the parish institutions for the management of the response to emergency and or disaster situations (Table 10).

1. Variable about physical structure

1) With which type of material has been constructed your living place?

a) Reinforced concrete ☐	b) Metallic structure ☐	c) Wooden structure ☐
d) Structure of cane (light) ☐	e) Supporting wall structure ☐	f) Supporting wall structure ☐
	g) Mixed wood / concrete ☐	

2) What type of housing cover has been used?

a) Metal cover ☐	b) Reinforced concret slab ☐	c) Wood and zinc beams ☐
d) Cane and zinc ☐		e) Wood and tile beams ☐

Fig. 5: Example of a field record (matrix) format.

Finally, the tenth matrix field is related to the identification of the level of community capacity to reduce risks and act in case of emergency and or disaster, through the verification of existence or not of Risk Management Committees, Emergency Community Brigades, knowledge about the location of meeting points and marked evacuation routes, a tsunami warning system, temporary accommodation and emergency plan, the availability of emergency family plans, as well as the participation in simulation drills or exercises (Fig. 4a-f; Table 11). The final result has been a set of 55 indicators with their respective evaluation parameters, which for their verification have been organized in field matrices (Fig. 5).

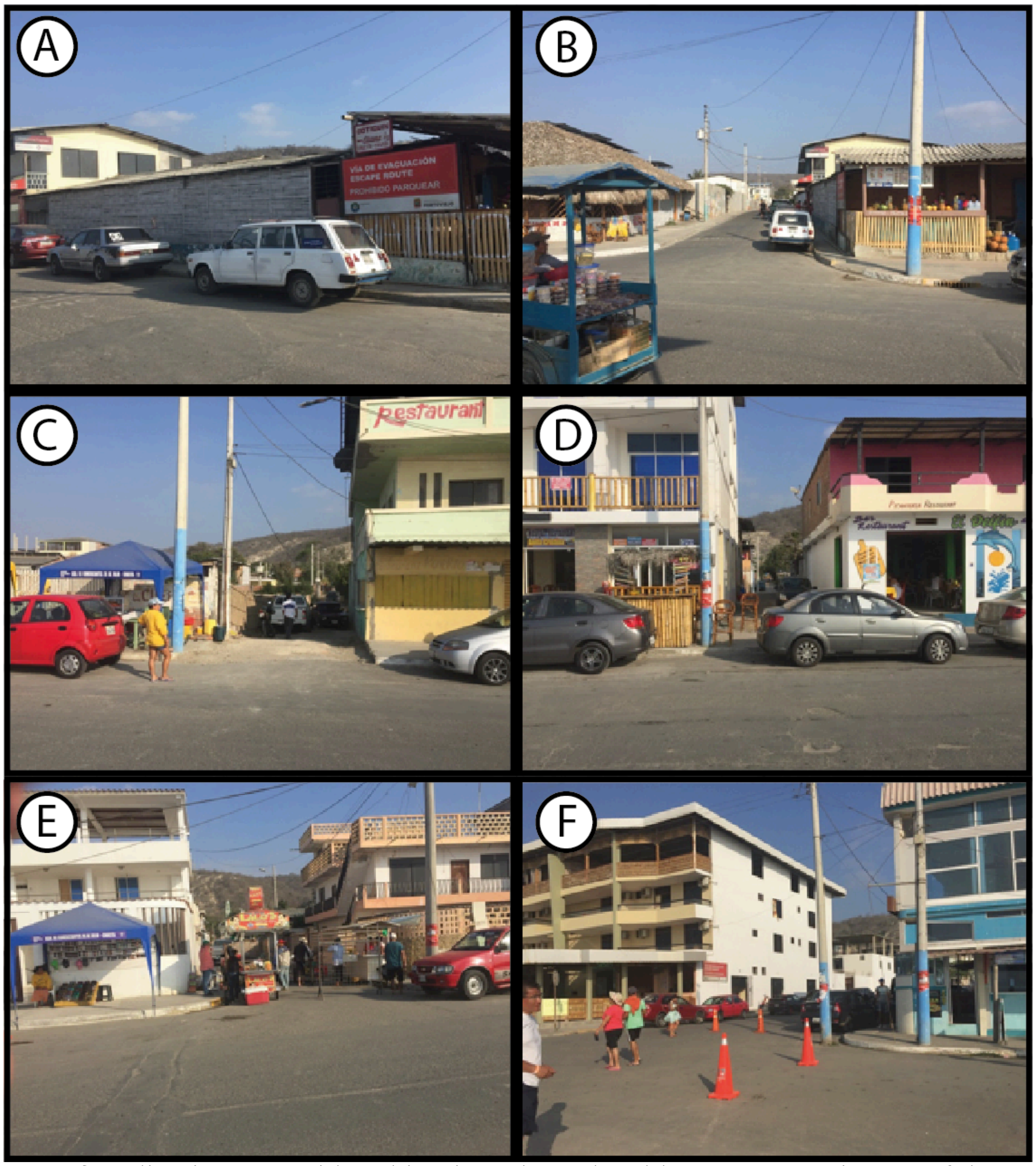

Fig. 5: a-f) Indication to avoid parking in order to be able to evacuate in one of the main roads perpendicular to the ocean´s shore line and the lack of doing so. All photos taken in Crucita.

b) Qualitative and quantitative analysis of indicators

The qualitative and quantitative analysis of the variables has been carried out based on the rating of the indicators, based on a numerical scale of 0.50 to 2, which assigns a level of importance to each of the indicators. Where for the case of independent variables: 2.00 is very important, 1.50 is important, 1.00 is moderately important, 0.50 is unimportant. The result has been the distribution of numerical values for the qualification of each of the indicators, according to their classification as indicated in Tables 2-11.

Table 2: Parameters for the qualification of indicators of the vulnerability of the physical structure. Based on PNUD-SNGR (2011).

Indicators	**Evaluation parameters**	**Qualification**
Structural system	Reinforced concrete	0,5
	Metallic structure	1
	Wooden structure	2
	Structure of cane (light)	2
	Mixed (wood, concrete, metallic)	1,5
Type of housing	Reinforced concrete slab	0,5
	Metal cover	1
	Beams made of wood and zinc	1,5
	Beams of cane and zinc	2
	Wood and tile beams	1,5
Number of floors	1 floor	2
	2 floors	1,5
	3 floors	1
	4 floors	0,5
	More than 4 floors	0,5
Construction age	Between 1950 and 1980	2
	Between 1980 and 2000	1
	After 2000	0,5
Closeness to the sea	Less than 500 meters from the beach	2
	Between 501 to 1000 meters from the beach	1,5
	Between 1001 and 1500 meters from the beach	1
	More than 1500 meters from the beach	0,5
Site topography	Flat	2
	Below the level of the road	1,5
	On the level of the road	1
	On the escarpment	0,5
Relative state	Good	0,5
	Acceptable	1
	Regular	1,5
	Bad	2

Table 3: Parameters for the qualification of indicators of the vulnerability of basic service networks. Based on PREDECAN (2009).

Indicators	Evaluation parameters	Qualification
Access to drinking water	Yes	0,5
	No	2
Reliance of the potable water system	More than one	0,5
	One	1
	None	2
Drinking water system dependence	With reliance	2
	Without reliance	0,5
Access to sewage	Yes	0,5
	No	2
Reliance to the sewer system	More than one	0,5
	One	1
	None	2
Reliance to the sewage system	With reliance	2
	Without reliance	0,5
Access to electric energy	Yes	0,5
	No	2
Redundancy of the electric power system	More than one	0,5
	One	1
	None	2
Reliance to the electric power system	With reliance	2
	Without reliance	0,5
Access to communication	Yes	0,5
	No	2
Redundancy of the communication system	More than one	0,5
	One	1
Reliance to the communication system	With reliance	2
	Without reliance	0,5

Table 4: Parameters for the rating of social vulnerability indicators. Based on PREDECAN (2009).

Indicators	Evaluation parameters	Qualification
Organization level	Acceptable	0,5
	Insufficient	1,5
	Any	2
Participation	Frequent	0,5
	Infrequent	1,5
	Any	2
Age and dependency condition	Less than 15 years	2
	More than 65 years	2
	Equal to one and more than two people with disabilities	2
Access to health services, education, employment, potable water, sewerage, electric power, communication	Yes	0,5
	No	2
Access to education	Yes	0,5
	No	2
Access to employement	Yes	0,5
	No	2
Access to potable water	Yes	0,5
	No	2
Access a sewerage	Yes	0,5
	No	2
Access to electric power	Yes	0,5
	No	2
Access to communication	Yes	0,5
	No	2

Table 5: Parameters for the rating of indicators of economic vulnerability. Based on PREDECAN (2009).

Indicators	Evaluation parameters	Qualification
Unsatisfied basic needs	Less than a minimum wage	2
	Between 1 and 3 minimum wages	1
	More than 3 minimum wages	0,5
Type of housing	Department	0,5
	House or villa	1
	Hut	1,5
	Farm, hoval o shack	2
Overcrowding	Less than 5 people	0,5
	Between 6 and 7 people	1,5
	More than 8 people	2

Table 6: Parameters for the qualification of indicators of educational vulnerability. Based on INDECI- DINAPRE- UEER (2006).

Indicators	Evaluation parameters	Qualification
Education level	None	2
	Primary	1,5
	High school	1
	Higher education	0,5
Tsunami education programs	Permanent	0,5
	Intermittent	1,5
	Sporadic	1
	Does not exist	2
Training programs on tsunamis	Permanent	0,5
	Intermittent	1,5
	Sporadic	1
	Does not exist	2
Broadcast campaigns	Permanent	0,5
	Intermittent	1,5
	Sporadic	1
	Does not exist	2

Table 7: Parameters for the qualification of indicators of cultural vulnerability.

Indicators	Evaluation parameters	Qualification
Knowledge about tsunami hazards	Enough	2
	Insufficient	1,5
	None	0,5
Knowledge about the occurrence of tsunamis	Knows	0,5
	Does not know	2
Behavior towards the occurrence of tsunamis	Acceptance	0,5
	Indifferent	1,5
	Denial	2

Table 8: Parameters for the qualification of indicators of the vulnerability of institutional policy. Based on PNUD-SNGR (2011).

Indicators	Evaluation parameters	Qualification
Local risk management policies	Yes	0,5
	No	2
	Does not apply	2
Institutional risk management plan	Yes	0,5
	No	2
	Does not apply	2
Governamental risk management policy	Yes	0,5
	No	2
Budget established for risk management	Yes	0,5
	No	2
Mechanisms for the application of policies	Yes	0,5
	No	2
Disaster risk reduction activities	Yes	0,5
	No	2
Staff training	Yes	0,5
	No	2

Table 9: Parameters for the qualification of indicators of the vulnerability of essential elements. Based on PNUD-SNGR (2011)

Indicators	Evaluation parameters	Qualification
Exposure level	Less than 500 meters from the beach	2
	Between 501 to 1000 meters from the beach	1,5
	Between 1001 and 1500 meters from the beach	1
	More than 1500 meters from the beach	0,5
Structural vulnerability	high	2
	Medium	1,5
	Low	0,5
Accessibility	Accessible	0,5
	Less accessible	1,5
	Inaccessible	2
Redundancy systems	More than one	0,5
	One	1
	None	2
Reliance	With reliance	2
	Without reliance	0,5

Table 10: Parameters for the qualification of indicators of the institutional capacity of response.

Indicators	**Evaluation parameters**	**Qualification**
Committee of Emerging Operations (CEO) of the parrish	Yes	0,5
	No	2
	It does not work	2
Response institutions	Yes	0,5
	No	2
	Doesn´t know	2
Signposted meeting points	Yes	0,5
	No	2
	Doesn´t know	2
Signposted evacuation routes	Yes	0,5
	No	2
	Doesn´t know	2
Alarm system for tsunamis	Yes	0,5
	No	2
	Doesn´t know	2
Temporary shelters	Yes	0,5
	No	2
	Doesn´t know	2
Risk maps	Yes	0,5
	No	2
	Doesn´t know	2
Emergency plan	Yes	0,5
	No	2
	Does not apply	2
Drills	Once	1
	Twice	0,5
	Never	2

Table 11. Parameters for the qualification of community capacity indicators.

Indicators	Evaluation parameters	Qualification
Risk management committees	They do Exist	0,5
	Do not exist	2
	Exist, but they do not work	2
Emergency brigades	They do Exist	0,5
	Do not exist	2
	Exist, but they do not work	2
Meeting points	They do Exist	0,5
	Do not exist	2
	Unknown	2
Evacuation routes	Known	0,5
	Unknown	2
Alarm for tsunamis	Known	0,5
	Unknown	2
Temporary shelters	Known	0,5
	Unknown	2
Tsunami contingency plan	Known	0,5
	Unknown	2
Family emergency plan	Known	0,5
	Unknown	2
Participation in drills	Known	0,5
	Unknown	2

c) Weighting of indicators

Once each of the indicators has been qualified, the results of each of the indicators have been weighted by assigning comparative importance by pairs of indicators, for which the Analytical Hierarchical Process (AHP) has been used as a method. For example, the exposure level of the Crucita Health Center (C1) is as important as the level of structural vulnerability of the Center (C2), but both are three times more important than access to the Health Center (C3). In terms of percentage distribution it means that C1 reaches 34.08%, C2 some 16.06% and C3 some 19.02% of the real value, as demonstrated in tables 12 and 13.

Table 12: Assignment of comparative importance between criteria

Indicators:		**C1**	**C2**	**C3**	**C4**	**C5**
Exposure level	**C1**	1	1	3	2	2
Vulnerability	**C2**	1	1	1/3	1/2	1/2
Accessibility	**C3**	1/3	1/3	1	2	2
Redundancy system	**C4**	1/2	1/2	2/3	1	2
Reliance	**C5**	1/2	1/2	2/3	1	1
	Total	**3,33**	**3,33**	**5,67**	**6,50**	**7,50**

Table 13: Normalization of results by comparative criteria

	C1	C2	C3	C4	C5	Weight	Weight (%)
C1	0,30	0,30	0,53	0,31	0,27	0,34	34,08
C2	0,30	0,30	0,06	0,08	0,07	0,16	16,06
C3	0,10	0,10	0,18	0,31	0,27	0,19	19,02
C4	0,15	0,15	0,12	0,15	0,27	0,17	16,77
C5	0,15	0,15	0,12	0,15	0,13	0,14	14,10
Total	**1,00**	**1,00**	**1,00**	**1,00**	**1,00**	**1,00**	**100**

The results of the peer-to-peer comparison exercise allowed to assign the weights according to the level of importance to each of the indicators by type of vulnerability, as documented in the tables 14 to 23.

Table 14: Indicators of the structural physical vulnerability

Indicator	Values of the indicator	Weighing
Structural system	0.50, 1, 1.50, 2	26
Type of housing	0.50, 1, 1.50, 2	10
Number of floors	0.50, 1, 1.50, 2	6
Construction age	0.50, 1, 1.50, 2	3
Closeness to the sea	0.50, 1, 1.50, 2	26
Site topography	0.50, 1, 1.50, 2	26
Relative state	0.50, 1, 1.50, 2	3
Total		**100**

Table 15: Vulnerability indicators of basic service networks

Indicator	Values of the indicator	Weighing
Access to drinking water	0.50, 2	20
Reliance of the potable water system	0.50, 1, 2	12
Drinking water system dependence	0.50, 2	12
Access to sewage	0.50, 2	15
Reliance to the sewer system	0.50, 1, 2	7,5
Reliance to the sewage system	0.50, 2	7,5
Access to electric energy	0.50, 2	7
Redundancy of the electric power system	0.50, 1, 2	3
Reliance to the electric power system	0.50, 2	3
Access to communication	0.50, 2	7
Redundancy of the communication system	0.50, 1, 2	3
Reliance to the communication system	0.50, 2	3
Total		**100**

Table 16: Indicators of social vulnerability

Indicator	Values of the indicator	Weighing
Organization level	0.50, 1.50, 2	24,7
Participation	0.50, 1.50, 2	24,7
Age and dependency condition	2	24,7
Access to health services	0.50, 2	4,9
Access to education services	0.50, 2	4,9
Access to employment	0.50, 2	4,9
Access to potable water	0.50, 2	2,7
Access a sewerage	0.50, 2	2,7
Access to electric power	0.50, 2	2,7
Access to communication	0.50, 2	2,7
Total		**100**

Table 17: Economic vulnerability indicators

Indicator	Values of the indicator	Weighing
Unsatisfied basic needs	0.50, 1, 2	48,6
Type of housing	0.50, 1, 1.50, 2	35,2
Overcrowding	0.50, 1, 2	16,2
Total		**100**

Table 18: Educational vulnerability indicators

Indicator	Values of the indicator	Weighing
Education level	0.50, 1, 1.50, 2	42,9
Tsunami education programs	0.50, 1, 1.50, 2	21,4
Training programs on tsunamis	0.50, 1, 1.50, 2	21,4
Broadcast campaigns	0.50, 1, 1.50, 2	14,3
Total		**100**

Table 19: Indicators of cultural vulnerability

Indicator	Values of the indicator	Weighing
Knowledge about tsunami hazards	0.50, 1.50, 2	30
Knowledge about the occurrence of tsunamis	0.50, 2	30
Behavior towards the occurrence of tsunamis	0.50, 1.50, 2	40
Total		**100**

Table 20: Indicators of the institutional policy vulnerability

Indicator	Values of the indicator	Weighing
Local risk management policies	0.50, 2	29,9
Institutional risk management plan	0.50, 2	15,3
Governamental risk management policy	0.50, 2	27
Budget established for risk management	0.50, 2	10
Mechanisms for the application of policies	0.50, 2	6
Disaster risk reduction activities	0.50, 2	6
Staff training	0.50, 2	6
Total		**100**

Table 21: Vulnerability indicators of essential elements

Indicator	Values of the indicator	Weighing
Exposure level	0.50, 1, 1.50, 2	30
Structural vulnerability	0.50, 1.50, 2	26
Accessibility	0.50, 1.50, 2	12
Redundancy systems	0.50, 1.50, 2	16
Reliance	0.50, 2	16
Total		**100**

Table 22: Institutional capacity indicators

Indicator	Values of the indicator	Weighing
CEO of the parrish	0.50, 2	19,1
Response institutions	0.50, 2	17
Signposted meeting points	0.50, 2	5,3
Signposted evacuation routes	0.50, 2	3,8
Alarm system for tsunamis	0.50, 2	6,4
Temporary shelters	0.50, 2	3,8
Risk maps	0.50, 2	19,1
Emergency plan	0.50, 2	6,4
Drills	0.50, 1, 2	19,1
Total		**100**

Table 23: Community capacity indicators

Indicator	Values of the indicator	Weighing
Risk management committees	0.50, 2	19,1
Emergency brigades	0.50, 2	17
Meeting points	0.50, 2	5,3
Evacuation routes	0.50, 2	3,8
Alarm for tsunamis	0.50, 2	6,4
Temporary shelters	0.50, 2	3,8
Tsunami contingency plan	0.50, 2	6,4
Family emergency plan	0.50, 2	19,1
Participation in drills	0.50, 2	19,1
Total		**100**

d) Estimation of vulnerability level

We have used as a qualification method to determine the level of vulnerability, the three-thirds criterion (3/3), which consists of assigning ranges to the traditional qualitative scale of high, medium and low by numeric values from 0.01 to 2, where the intermediate values have been taken into account, for example 0.33, 1.35, 189, etc. The qualification method allowed decisions to be made, when it hs been not easy to qualify the variable between high and medium, or between medium and low. Herevy, we avoided any bias of the information when estimating the level of vulnerability of the parish.

For the purposes of the present analysis, the following ranges have been established:

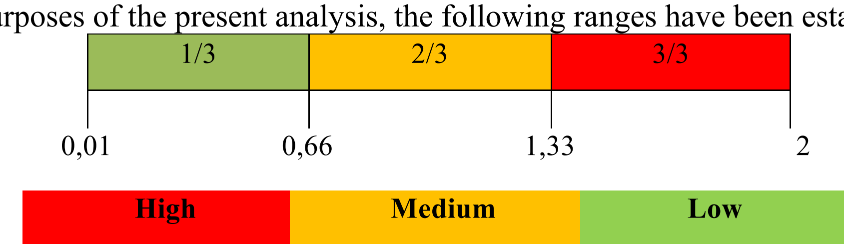

Based on the established ranges and once the field data have been obtained, the assessment parameters and the weighting of each of the indicators using a database have been carried out as the last step in the automated evaluation process. Thus, after crossing the qualifications and indicator weights, the final result of the estimation of the level of vulnerability of the parish have been obtained, as demonstrated in table 24.

e) Survey by sampling

Such survey consisted in applying a series of 55 questions in a random way to 389 people and 10 institutions of the Crucita parish. Therefore, interviews have been conducted for the population and authorities and / or technicians of the different public institutions of

Table 24: Matrix example of the evaluation of cultural vulnerability

LOCATION DATA					Knowledge about tsubami hazards	30%	Knowledge about occurrence of tsunamis	30%	Behavior towards the ocurrence of tsunamis	40%	CRITERION 3/3	
Code	Sector	Closeness to the sea	Longitude	Latitude		Qualification		Qualification		Qualification	Vulnerability assessment	Cultural Vulnerability
AR 01	Arenales	300	551965	9905534	Natural event	0,5	No	2	Denial	2	1,55	High
AR 02	Arenales	30	551744	9905538	Natural event	0,5	No	2	Denial	2	1,55	High
AR 03	Arenales	80	551818	9905534	Natural event	0,5	No	2	Denial	2	1,55	High
AR 04	Arenales	80	551825	9905541	Natural event	0,5	No	2	Denial	2	1,55	High
AR 05	Arenales	20	551722	9905504	Natural event	0,5	No	2	Denial	2	1,55	High

the parish, in order to obtain primary data. The application of the surveys has been based on the use of questionnaires and field registration formats, established from the definition of a set of criteria and evaluation parameters for each type of vulnerability and capacity. The same ones that have been organized for their application in ten matrix fields that allowed the verification of the elements in the field. For the development of the present analysis, a sample of 389 people with a margin of error of 5% has been obtained.

The communities where the surveys have been applied are Crucita Parochial Headquarters (272 surveys), Los Arenales (8), Los Ranchos (49), Las Gilses (26), La Sequita (12), San Silvestre (20), La Boca (2). The distribution of the sample has been performed randomly, taking as reference the level of consolidation of the different communities and the principle of parochial coverage in relation to the location of the communities in the South Center, North Center, Northeast and North Crucita.

4. RESULTS AND DISCUSSION

Vulnerability of physical structures

Seven different questions have been used to encounter the vulnerabilities of the physical structures as listed in table 2 using the indicator values of table 14. Thus, the result has been that the vulnerability level is high with 91% and median with 9%, with an intermediate quantitative value between the lower and upper limit of the high level (1.56).

High 91%	Medium 9%	Low 0%

This result has been obtained by weighing the quantitative values by the weight corresponding to each one of the factors of the physical structure vulnerability, which allowed obtaining partial values, which when added together determined the level of vulnerability, as detailed in the given example from Table 25.

Table 25: Example of the estimation of the physical structure vulnerability

LOCATION DATA		VERIFICATION VARIABLES							CRITERION 3/3	
CODE	SECTOR	STRUCTURAL SYSTE	TYPE OF HOUSIN	NUMBER OF FLOO	CONSTRUCTION AGE	CLOSENESS TO THE SEA	SITE TOPOGRAPHY	RELATIVE STATE	LEVEL OF VULNERABILITY	
		0,26%	0,10%	0,06%	0,03%	0,26%	0,26%	0,03%		
AR 001	ARENALES	1,5	2	2	1	1,5	2	0,5	1,665	High
AR 002	ARENALES	1,5	1,5	2	1	2	2	1,5	1,775	High
AR 003	ARENALES	1,5	1,5	2	0,5	2	2	1,5	1,76	High
AR 004	ARENALES	1,5	1,5	2	1	2	2	1,5	1,775	High
AR 005	ARENALES	1,5	2	2	2	2	2	1,5	1,855	High
AR 006	ARENALES	1,5	1,5	2	1	2	2	1,5	1,775	High
AR 007	ARENALES	1,5	1,5	2	1	2	2	0,5	1,745	High
AR 008	ARENALES	1,5	1,5	2	0,5	1,5	2	2	1,645	High
CR 009	CRUCITA	1,5	2	2	1	2	2	1,5	1,825	High
CR 010	CRUCITA	0,5	1	1,5	2	2	2	0,5	1,435	High

CRITERIA AND RANGES TO DETERMINE VULNERABILITY LEVEL					
Valuation criteria		Vulnerability level ranges			
2	Very high	High	1,33 - 2	1,7255	High
1,5	High	Medium	0,67 - 1,32	VULNERABILITY LEVEL OF PHYSICAL STRUCTURE	
1	Medium	Low	0 -0,66		
0,5	Low				

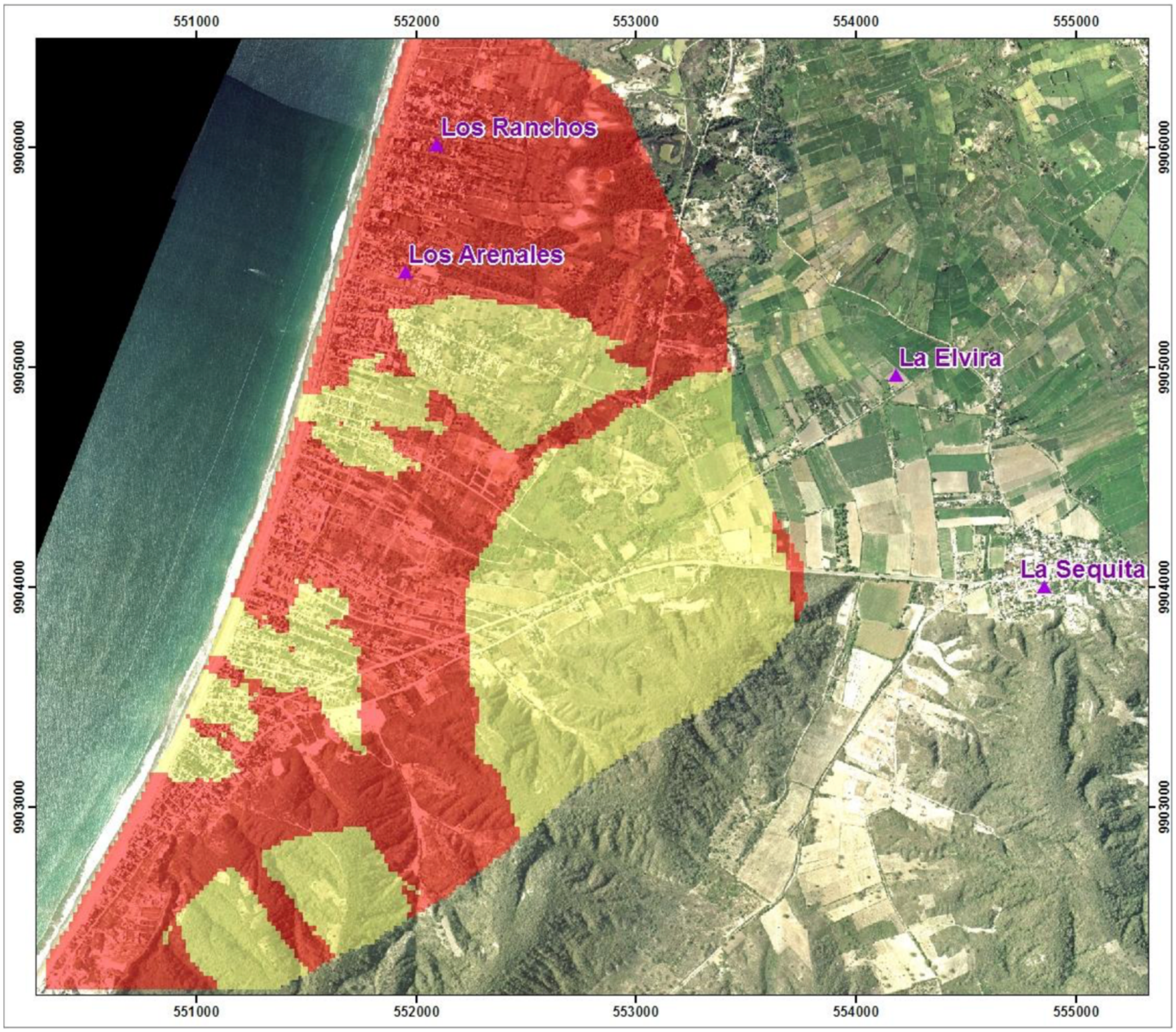

Fig. 6: Map of Crucita indicating the vulnerability of physical structures, based on the present survey.

Fig. 7: Typical vulnerable buildings in the beach area of Crucita.

Vulnerability of Basic Services Networks

Three different questions have been used to encounter the vulnerabilities of the basic service networks, as listed in table 3 using the indicator values in table 15. Thus, the result has been that the level of vulnerability is high (100%), with a quantitative value close to the upper limit of the high level (1.72%).

High 100%	**Medium 0%**	**Low 0%**

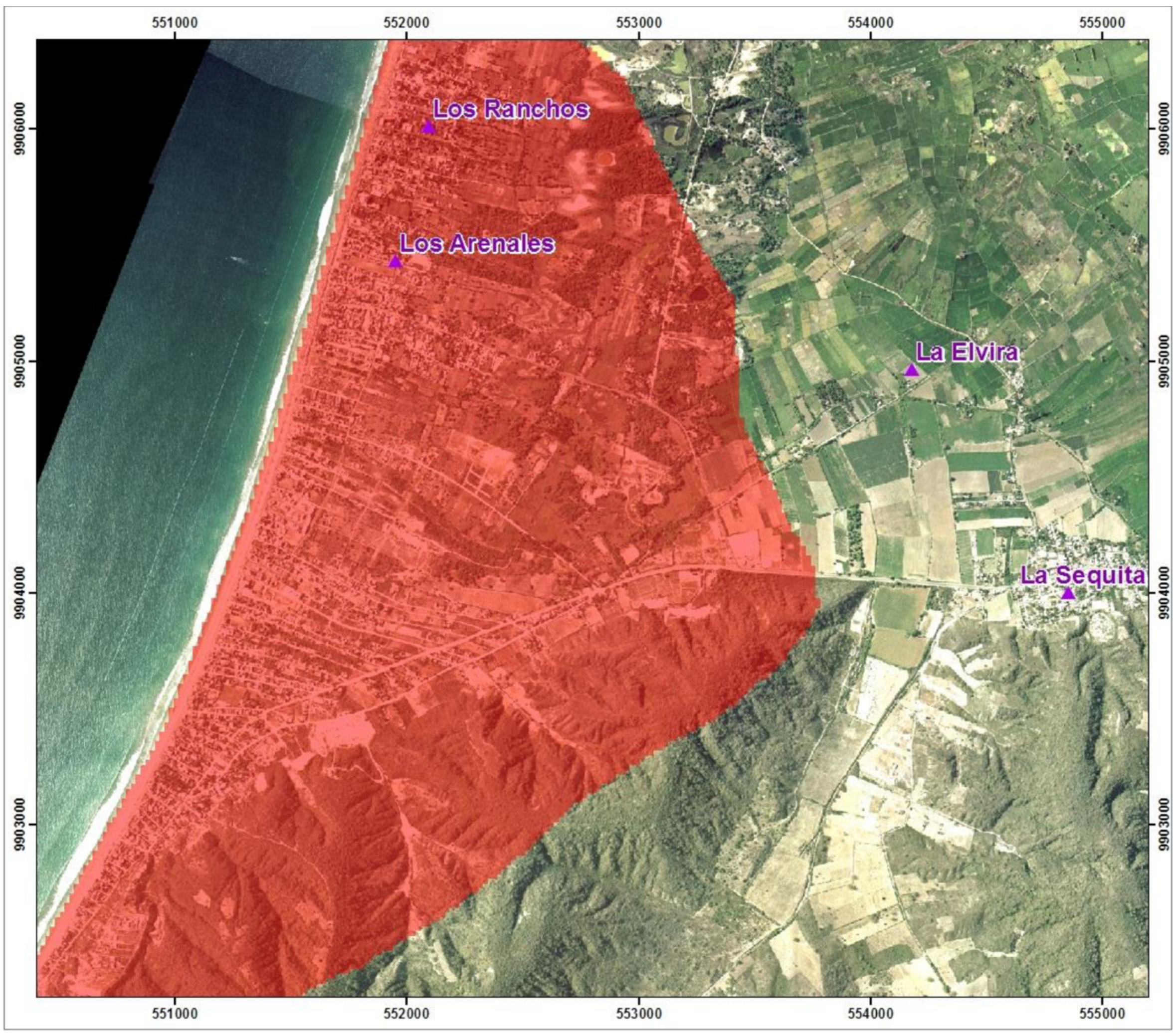

Fig. 8: Map of Crucita indicating the vulnerability of basic services networks, based on the present survey.

Social Vulnerability

Four different questions have been used to encounter social vulnerabilities, as listed in Table 4 using the indicator values in Table 16. Thus, the result has been that the level of vulnerability is mostly average (82.26%), with a quantitative value of 1.20 being near the lower limit of the high level.

High 17,48%	**Medium 82,26%**	**Low 0,26%**

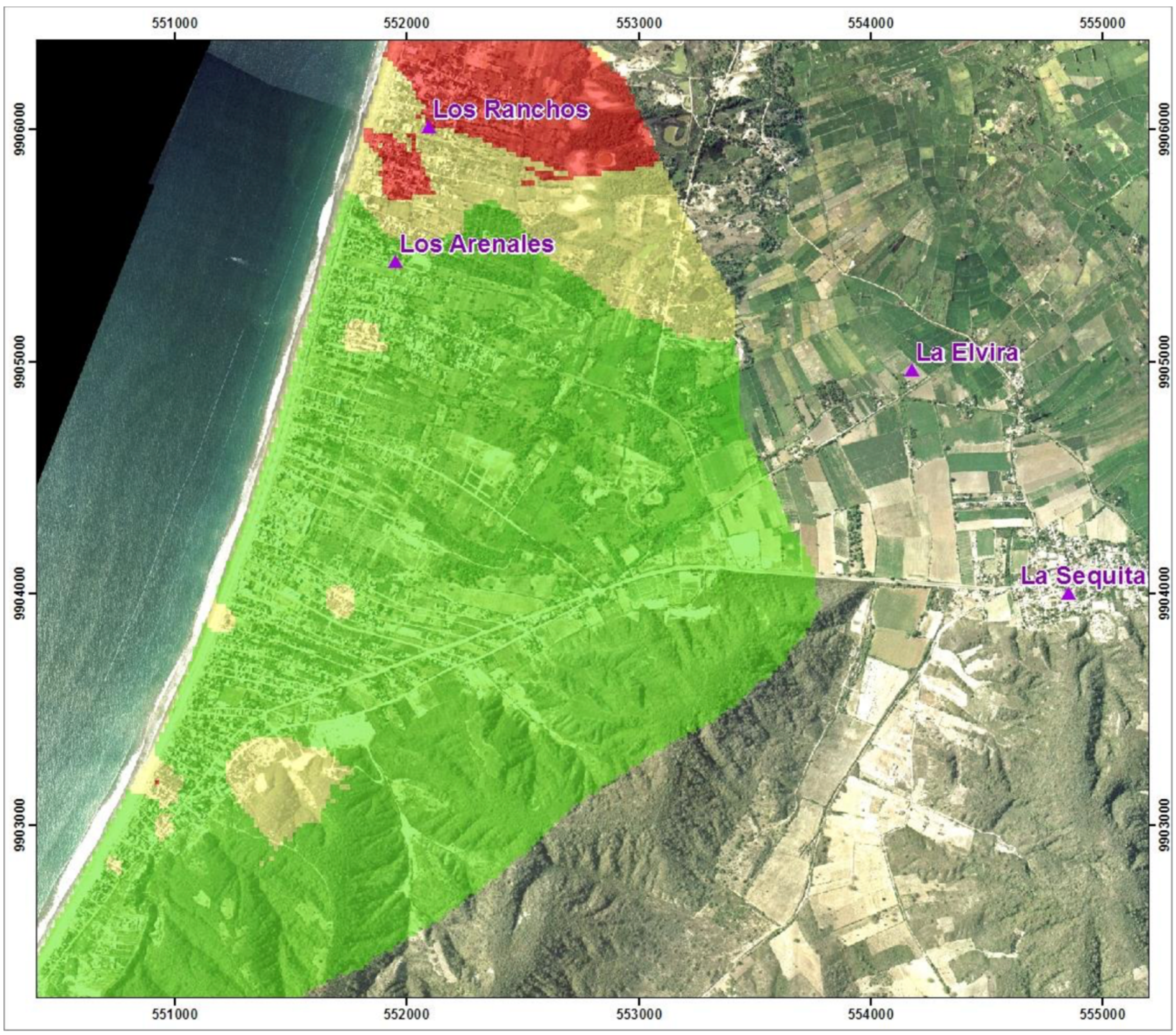

Fig. 9: Map of Crucita indicating the social vulnerability, based on the present survey.

Economic Vulnerability

Three different questions have been used to encounter the economic vulnerabilities, as listed in table 5 using the indicator values in table 17. Thus, the result has been that the level of vulnerability is mainly high (76%), with a quantitative value close to the lower limit of the level high (1.34).

High 76%	Medium 24%	Low 0%

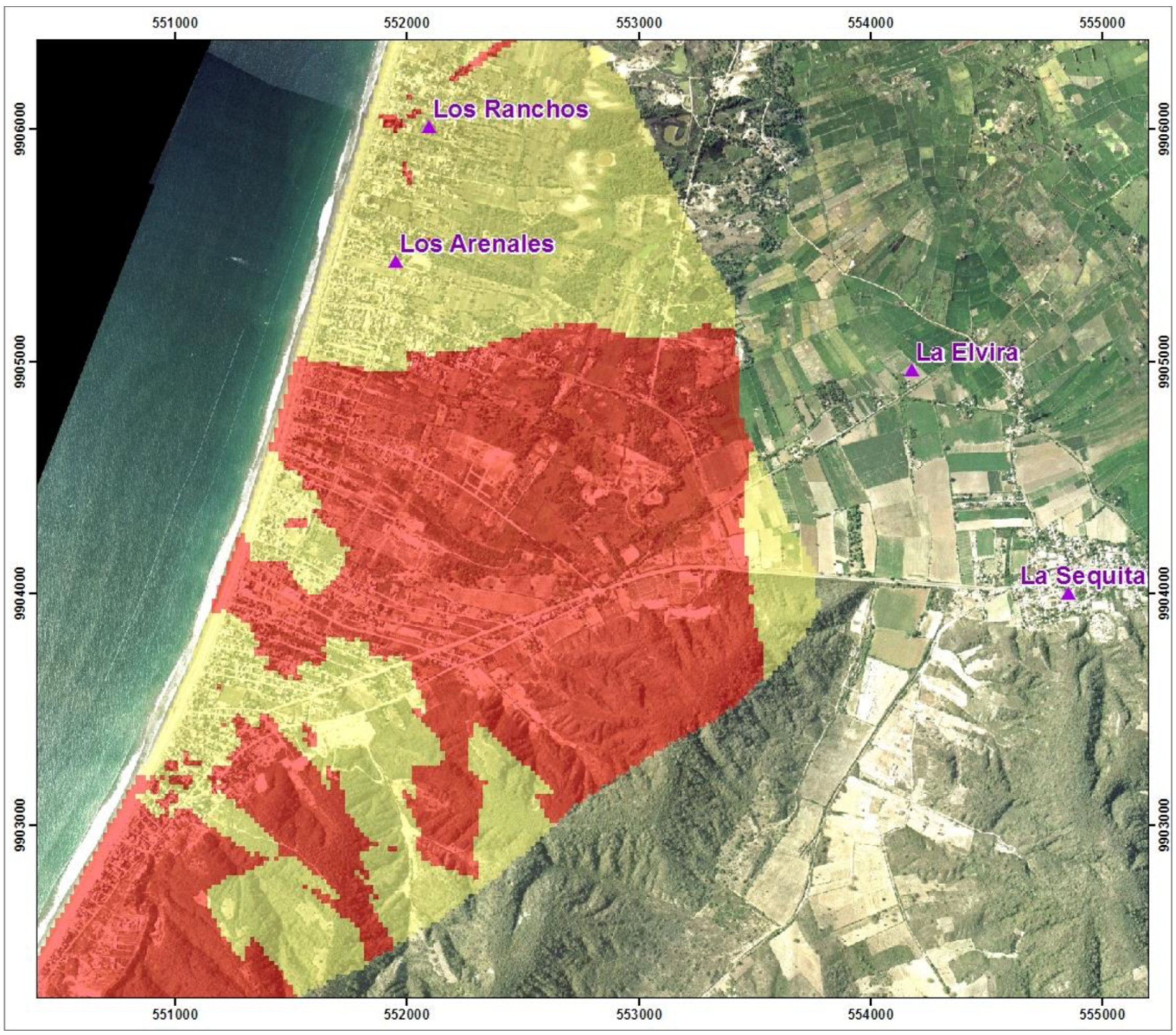

Fig. 10: Map of Crucita indicating the economic vulnerability, based on the present survey.

Vulnerability in Education

Two different questions have been used to find social vulnerabilities, as listed in table 6 using the indicator values in table 18. Thus, the result has been that the vulnerability level is mostly high (85%), with a near quantitative value at the lower limit of the high level (1.41).

High 85%	Medium 15%	Low 0%

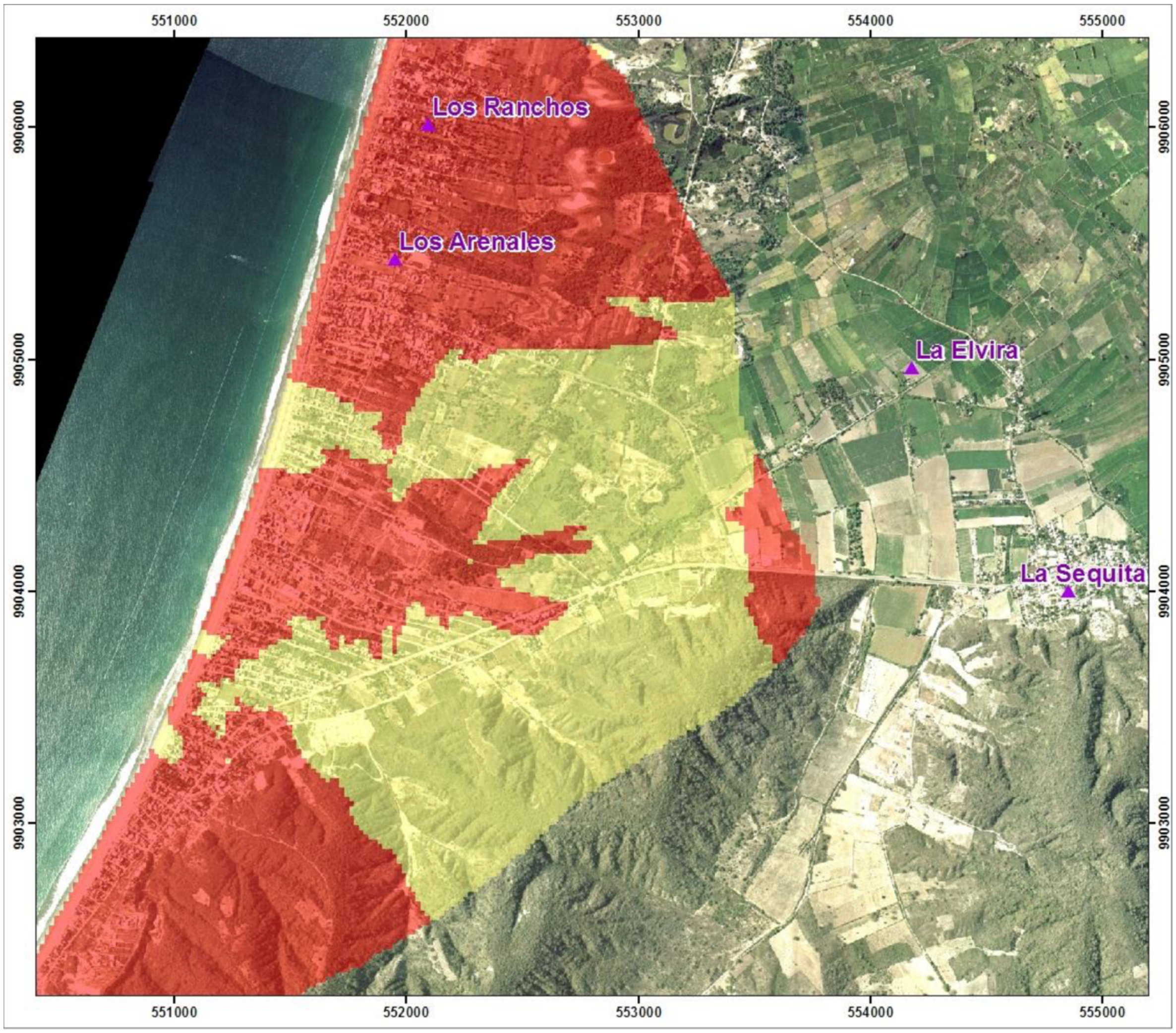

Fig. 11: Map of Crucita indicating the educational vulnerability, based on the present survey.

Cultural Vulnerability

Two different questions have been used to encounter cultural vulnerabilities, as listed in Table 7 using the indicator values of Table 19. Thus, the result has been that the level of vulnerability is high (99%), with a quantitative value close to lower limit of the high level (1.47).

High 99%	Medium 1%	Low 0%

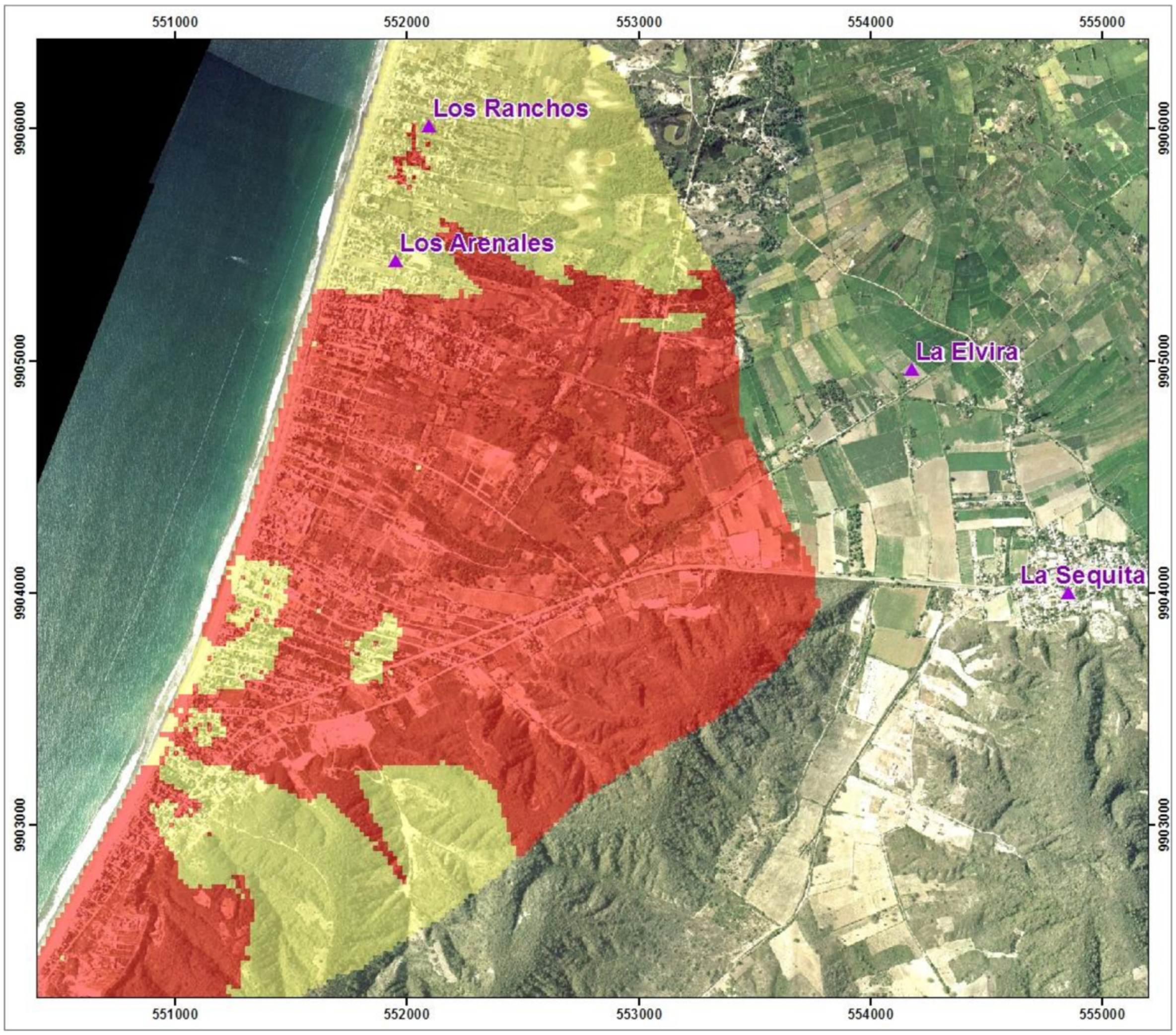

Fig. 12: Map of Crucita indicating the cultural vulnerability, based on the present survey.

Community capacity

Three different questions have been used to encounter cultural vulnerabilities, as listed in table 8 using the indicator values in table 20. Thus, the result has been that the capacity level is low (100%), with a quantitative value close to upper limit of the high level (1.94).

Low 100%	Medium 0%	High 0%

Fig. 14: Map of Crucita indicating the vulnerability of the community capacity, based on the present survey.

For the development of the present analysis on the results of the institutional level, a sample of ten institutions have been selected. For the purposes of interviews and surveys, it corresponded to the level of institutional policy vulnerability, vulnerability of essential elements and institutional capacity. The identified institutions are: Crucita Parish Council, Political Tenure, Crucita Fire Department, 25 de Mayo School, Juan Benigno Vela School, Ecuador Navy-Harbor Captaincy, National Police, National Telecommunications Corporation, Crucita Health Center, Municipal Tourism Company.

Institutional Policy Vulnerability

Below are the results obtained for each type of vulnerability (institutional policy and essential elements) and institutional capacity through the introduction of the following five queries, as listed in table 9 using the indicator values in table 21. Thus, it has been obtained as a result that the level of vulnerability is mostly high (80%), with a quantitative value close to the upper limit of the high level (1.70).

High 80%	**Medium 20%**	**Low 0%**

Vulnerability of Essential Elements

Five different questions have been used to encounter the vulnerabilities of the essential elements, as listed in table 10 using the indicator values in table 22. Thus, the result has been that the vulnerability level is high (96%), with a value quantitative close to the upper limit of the high level (1.52).

High 96%	**Medium 4%**	**Low 0%**

Institutional capacity

Three different questions have been used to find out the level of institutional capacity, as listed in table 11 using the indicator values in Table 23. In terms of institutional capacity, the result has been that the capacity level is low, with a value quantitative close to the upper limit of the high level (1.50).

Low 100%	**Medium 0%**	**High 0%**

After having performed the individual estimation of each type of vulnerability (physical, services, social, economic, educational, cultural, institutional and essential elements) and capacity (community and institutional), it has been determined that a level of a general vulnerability, which for effect of the present study has been called "total or population vulnerability". Such vulnerability defines in general terms the condition of the vulnerability of the population in relation to tsunami hazards, where there are factors that influence the rest, which allows us to establish a road map for reducing vulnerability. Based on the above, it has been possible to identify that the types of vulnerability that influence the increase in vulnerability are those related to the knowledge and culture of the population, because there are physical conditions determined by elements that are difficult to modify territorially, like the location of homes, institutions and essential elements in the studied territory.

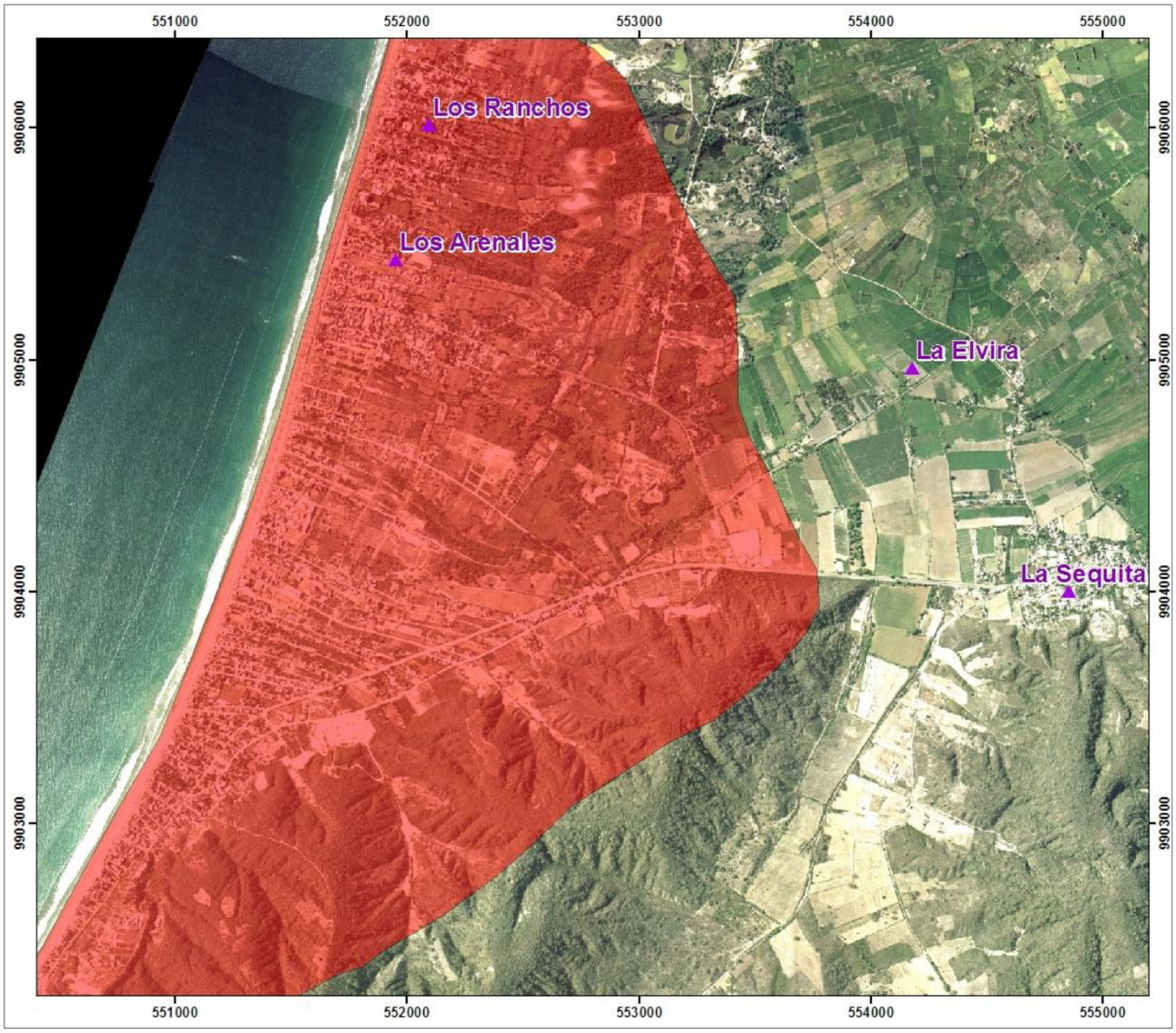

Fig. 15: Map of Crucita indicating the overall vulnerability, based on the present survey.

Public Vulnerability

When performing comparative exercises with real cases and cases where the existing conditions are modified after a vulnerability reduction process, an average reduction of vulnerability of up to 52% has been obtained. Therefore, the factors that influence the increase in vulnerability are social, educational, cultural, institutional and community and institutional capacities. Being these, factors that have been subject to the organization and participation of community and institutional performer. In conclusion after having realized the analysis of each of the types of vulnerability and crossing with the results of institutional and community capacity, the result has been that the level of population vulnerability has been high (93%, 1.63).

Low 92,5%	**Medium 7,5%**	**High 0%**

5. SUMMARY AND CONCLUSIONS

The conclusions have been defined based on eight axes of interest, prioritized from the obtained results, from which the following points may be deduced:

1. *The location of Crucita in relation to the subduction zone determines the level of exposure of the Parish towards tsunami hazards.*

Crucita is located approximately 75 km east from the edge of the subduction zone, within the cenral area of the Manabi province, where historically the highest number of seismic events have been concentrated, respectively. This places Crucita in a condition of high exposure for the population, their homes, buildings, livelihoods and basic services. In the same way, the location of buildings and houses in relation to the edge of the high tide, determine that the population's exposure to the tsunami hazards is high, as a consequence that approximately 97% of buildings and homes are less 1000 m from the edge of the high tide.

2. *The variation of people according to the time of year and day of the week increases the number of inhabitants susceptible to be affected by the tsunami occurrence.*

Until 2001, Crucita have had a total population of 11,068 inhabitants, while in 2010 it increased to 14,050 inhabitants with an annual growth rate of 2.65%, indicating that the Parish has a tendency of population growth. On the other hand, being a local, national and international tourist destination, the population increases between 20 and 80%, according to the time of year and day of the week, and therefore the number of people susceptible to be affected by the occurrence of tsunamis.

3. *The inadequate land use and occupation increases the level of Parochial vulnerability towards tsunami hazards.*

The commercial, tourist and residential growth of Crucita has been developed along 13 km of beach area, in two consolidated areas being less than 1 km from the edge of the high tide, such as Parrish Cabecera and the north central sector of the main Parrish. Areas where narrow roads without a direct connection to a safe meeting point, as well as the construction of condominiums at the height of high traffic roads, do not allow a fast evacuation in the event of a tsunami warning or the occurrence of it. On the other hand, there are extensive areas that are not well established and have as their current land use, urbanization and development of tourism activities, which, in the absence of adequate urban and road planning, contributes to the increase of Parochial vulnerability in relation to road variables, infrastructure and evacuation routes.

4. *The high recurrence of tsunamis determines that the Parish could be affected by the occurrence of tsunamis.*

In the period between the years 1800 and 2017, there has been one tsunami of tectonic origin in the coasts of Manabi and six that affected the Ecuadorian coast. This indicates that the recurrence of local tsunamis is medium high, while the recurrence of distant tsunamis is very high, despite the fact that their wave propagation through the Pacific Ocean did not reach Ecuadorian coasts, with the exception of the tsunami generated by the Japanese earthquake in 2011.

5. *Tsunami hazards in relation to the probability of flooding due to the displacement of salt water to the coast, is high for the population being located less than 1000 m from the edge of the high tide*

6.

The topographic and bathymetric characteristics of Crucita and its beaches are favorable for flooding due to tsunami, since there is an average slope of 2% in the case of the bathymetry and average levels of 12 m above sea level in the case of the flat surface of the parish. Considering also that the northern limit of the Parish is delimited by the basin of the river Portoviejo, where communities settled in the vicinity of the banks of the existing river. The tsunami hazard map indicates that there is a high probability of flooding by tsunami with up to the maximum height of 12 masl, affecting by direct impact more than 95% of the flat surface of the parish

7. *The Parochial vulnerability level, resulted to be of a high vulnerability with 100% of the cases, being defined from the analysis of the physical variables of housing and service, social, educational, economic, cultural and institutional policies*

The current analysis yielded several results, such as that 91% of the homes have a high level of vulnerability in physical structure, due to the fact that most of the structural condition of the houses have been constructed of wood and concrete, with roofs is made of wood and zinc beams, havin in average one floor, being constructed between 1980 and 2000 and being located at a distance of less than 500 m from the edge of the high tide on a flat surface.

100% of service networks have a high level of vulnerability, because basic services do not have any redundancy and are dependent on the cantonal level for their functionality, despite the fact that service coverage is greater than 70%, with the exception of the sewer that does not exist. Some 82.26% of the inquired families have a medium level of social vulnerability, although in most cases the participation level has been infrequent. Additionally, the members of the family are in an age of dependency.

Some 76% of the families have a high level of economic vulnerability with a tendency to average, because most of the average family income is less than a minimum wage. The type of housing is light house or villa, but the level of overcrowding is in the usual range of average people per family.

Approximately 85% of families have a high level of educational vulnerability, because there are no educational and training programs aimed to prepare the population to act and reduce their vulnerability to tsunami hazards, as well as awareness campaigns, although the population in its majority has access to education.

Almost all (99%) of the families have a high level of cultural vulnerability, due to the fact that the majority of the population does not have the experience of having experienced a tsunami impact, which has been evidenced by the tsunami warning due to the 8.9

earthquake that occurred in Japan in 2011. A large number of families have a skeptical of the tsunamis and the signals prior to their occurrence.aptitude about the occurrence of tsunamis in Ecuadorian coasts. However, they have knowledge about the origin. Eight out of ten institutions in the Parish, have a high level of vulnerability, as there is no complete compliance with national and local policies for risk management. These institutions do not count with a budget for the development of DRR actions, management institutions plans of risks and training for staff on the subject of risk management. Some 96% of the essential elements have a high level of vulnerability, despite having a high level of importance for citizens in normal situations and with greater emphasis on emergency situations to ensure the continuity of humanitarian rights such as access to education and health in emergency situations.

7. *The level of Parochial capacity, defined from the analysis of institutional and community capacity variables, yielded as a result that vulnerability for 100% of cases is high*

All of the institutions (100%) have a low capacity to respond to a tsunamigenic event, because there is no Parochial CEO or it does not work, as well as an alarm system for tsunamis, emergency or contingency plans and risk maps. Evacuation routes and meeting points are not marked, although there are response organizations in the parish, temporary shelters and participation of once every year in simulation exercises with educational establishments. 100% of the families have a low capacity for risk reduction and response, due to the fact that there are no Risk Management Committees, Community Emergency Brigades and Parochial Contingency Plans. There is a lack of knowledge of meeting points, evacuation routes and temporary shelters. The participation in simulation exercises or drills is low and there is a lack of emergency family plans.

8. *The total vulnerability of the Parish in relation to the types of vulnerability analyzed in this study, as well as the capacities identified, determined that the level of the Parochial vulnerability is high.*

This is due to the fact that the study elements with the highest incidence for the determination of final results are institutional and community capacity, followed by physical structure vulnerability and service networks, institutional, cultural and educational policy. Therefore, vulnerability reduction actions should be aimed at improving institutional and community capacities, which in terms of incidence are 48% important. Also, reducing to the minimum the institutional, cultural and educational political vulnerability, which in incidence methods have a 16% importance.

With respect to physical structure vulnerabilities, service networks and essential elements, prospective actions should be taken to avoid the increase of vulnerability linked to development. In the same way, the reduction of social and economic vulnerability will depend on the application of policies that resolve unsatisfied basic needs. By modifying the indicated values of vulnerability and capacity, the result is the reduction of the Parochial vulnerability by 46%. Varying from 1.65 points typified as high, to 0.89 points typified as average.

6. REFERENCES

Beck, S. L., & Ruff, L. J. (1984). The rupture process of the great 1979 Colombia earthquake: Evidence for the asperity model. Journal of Geophysical Research: Solid Earth, 89(B11), 9281-9291.

Berninghausen, W.H., 1962. Tsunamis reported from the west coast of South America 1562-1960. Bull. of the Seismological Soc. of America, 52 (4): 915-921.

Cruz D´Howitt, M. and Vásquez, N., 2010: Elaboración de 33 cartas - croquis de amenazas por tsunami y análisis de riesgos en la costa ecuatoriana utilizando indicadores geomorfológicos y socio-ambientales. Revista Geoespacial, 7: 1-20

Chunga, K., & Toulkeridis, T. (2014). First evidence of paleo-tsunami deposits of a major historic event in Ecuador. Science of Tsunami Hazards, 33(1): 55-69.

Delouis, B., Nocquet, J. M., & Vallée, M. (2010). Slip distribution of the February 27, 2010 Mw= 8.8 Maule earthquake, central Chile, from static and high-rate GPS, InSAR, and broadband teleseismic data. Geophysical Research Letters, 37(17).

Dumont, J. F., Santana, E., & Vilema, W. (2005). Morphologic evidence of active motion of the Zambapala Fault, Gulf of Guayaquil (Ecuador). Geomorphology, 65(3), 223-239.

Dumont, J. F., Santana, E., Bonnardot, M. A., Pazmiño, N., Pedoja, K., & Scalabrino, B. (2014). Geometry of the coastline and morphology of the convergent continental margin of Ecuador. Geological Society, London, Memoirs, 41(1), 327-338.

Gutscher, M.A., Malavieille, J.S.L., Collot, J.-Y., 1999. Tectonic segmentation of the North Andean margin: impact of the Carnegie Ridge collision. Earth and Planetary Science Letters 168, 255–270. Gutscher, M.-A., Spakman, W., Bijward, H., Engdahl, E.R., 2000. Geodynamics of flat subduction: Seismicity and tomographic constraints from the Andean margin. Tectonics 19 (5), 814–833.

Harden, C. (2001). Sediment movement and catastrophic events: The 1993 rockslide at La Josefina, Ecuador. Physical Geography, 22(4), 305-320.

Herd, D. G., Youd, T. L., Meyer, H., Arango, J. L., Person, W. J., & Mendoza, C. (1981). The great tumaco, colombia earthquake of 12 december 1979. Science, 211(4481), 441-445.

INDECI- DINAPRE- UEER (Instituto Nacional de Defensa Civil - Dirección Nacional de Prevención - Unidad de Estudios y Evaluación de Riesgos), 2006: Manual Básico para la Estimación del Riesgo. Lima, Perú: 73pp

Jaramillo Castelo, C.A., Padilla Almeida, O., Cruz D´Howitt, M. and Toulkeridis, T. (2018). Comparative determination of the probability of landslide occurrences and susceptibility in central Quito, Ecuador”. 5th International Conference on eDemocracy and eGovernment, ICEDEG 2018, 136-143.

Kanamori, H. and McNally, K.C., 1982. Variable rupture mode of the subduction zone along the Ecuador-Colombia coast. Bulletin of the Seismological Society of America, 72(4): 1241-1253.

López, M. C. (2013). Cronología de tsunamis en ecuador desde 1586 a 2012. La Técnica, (11): 50-59.

Lynett, P., Weiss, R., Renteria, W., Morales, G. D. L. T., Son, S., Arcos, M. E. M., & MacInnes, B. T. (2013). Coastal impacts of the March 11th Tohoku, Japan tsunami in the Galapagos Islands. Pure and Applied Geophysics, 170(6-8), 1189-1206.

Massonne, H. J., & Toulkeridis, T. (2012). Widespread relics of high-pressure metamorphism confirm major terrane accretion in Ecuador: a new example from the Northern Andes. International Geology Review, 54(1), 67-80.

Mato, F., & Toulkeridis, T. (2017). The missing Link in El Niño's phenomenon generation. Science of Tsunami Hazards, 36(3), 128-144.

Mendoza, C., & Dewey, J. W. (1984). Seismicity associated with the great Colombia-Ecuador earthquakes of 1942, 1958, and 1979: Implications for barrier models of earthquake rupture. Bulletin of the seismological society of America, 74(2), 577-593.

Navas, L., Caiza, P. and Toulkeridis. T., 2018: An evaluated comparison between the molecule and steel framing construction systems – implications for the seismic vulnerable Ecuador. Malaysian Construction Research Journal, 23: in press

NEC (Norma Ecuatoriana de la Construcción), 2014: Geotecnia y diseño de cimentaciones en el Ecuador, Acuerdo ministerial 0028. 19 de agosto de 2014:18-19.

Norio, O., Ye, T., Kajitani, Y., Shi, P., & Tatano, H. (2011). The 2011 eastern Japan great earthquake disaster: Overview and comments. International Journal of Disaster Risk Science, 2(1), 34-42.

Okuwaki, R., & Yagi, Y. (2017). Rupture Process During the Mw 8.1 2017 Chiapas Mexico Earthquake: Shallow Intraplate Normal Faulting by Slab Bending. Geophysical Research Letters, 44(23).

Pararas-Carayannis, G. (1980). Earthquake and tsunami of 12 December 1979 in Colombia. Tsunami Newsletter, 13(1), 1-9.

Pararas-Carayannis, G. 1980: The Earthquake and Tsunami of December 12, 1979, in Colombia. Intern. Tsunami Information Center Report, Abstracted article in Tsunami Newsletter, Vol. XIII, No. 1.

Pararas-Carayannis G., 1983. The Tsunami Impact on Society. Tsunamis - Their Science and Engineering.: Terra Scientific Publishing Company, Tokyo, pp. 3-8 ,1983.

Pararas-Carayannis, G. 1988. Risk Assessment of the Tsunami Hazard in Natural and Man-Made Hazards, In Natural and Man-Made Hazards, D. Reidal, Netherlands, pp.171-181, 1988 (LL).

Pararas-Carayannis, G., 2010: The earthquake and tsunami of 27 February 2010 in Chile– Evaluation of source mechanism and of near and far-field tsunami effects. Science of Tsunami Hazards, 29, 2: 96-126.

Pararas-Carayannis, G., 2012: Potential of tsunami generation along the Colombia/Ecuador subduction margin and the Dolores-Guayaquil Mega-Thrust. Science of Tsunami Hazards, 31, 3: 209-230.

Pararas-Carayannis, G., 2014. The Great Tohoku-Oki earthquake and tsunami of March 11, 2011 in Japan: A critical review and evaluation of the tsunami source mechanism. Pure and applied geophysics, 171(12): 3257-3278.

Pararas-Carayannis, G. and Zoll, P., 2017: Incipient evaluation of temporal el nino and other climatic anomalies in triggering earthquakes and tsunamis – case study: The earthquake and tsunami of 16thapril 2016 in Ecuador. Science of Tsunami Hazards, 36(4), 262-291.

Pararas-Carayannis, G., 2018: Brief history of early pioneering tsunami research – Part A. Science of Tsunami Hazards, 37(1), 49-129.

PNUD-SNGR (Programa de Naciones Unidas para el Desarrollo - Secretaría Nacional de Gestión de Riesgos) de Ecuador, 2011: Sistematización de la Metodología de Análisis de Vulnerabilidades a nivel Municipal. Quito, Ecuador: 15pp

PREDECAN (Prevención de Desastres en la Comunidad Andina), 2009: Serie: Experiencias significativas de desarrollo local frente a los riesgos de desastres: Proyecto piloto participativo en gestión local del riesgo de desastres en el cantón Portoviejo. Lima, Peru: 40pp

Rentería, W., Lynett, P., Weiss, R. & De La Torre, G. (2012). Informe de la investigación de campo de los efectos del tsunami de Japón Marzo 2011, en las islas Galápagos. Acta Oceanográ ca del Pací co. Vol. 17(1): 177 - 203.

Rodriguez, F., Toulkeridis, T., Sandoval, W., Padilla, O., & Mato, F. (2017). Economic risk assessment of Cotopaxi volcano, Ecuador, in case of a future lahar emplacement. Natural Hazards, 85(1), 605-618.

Schuster, R. L., NietoThomas, A. S., O'Rourke, T. D., Crespo, E., & Plaza-Nieto, G. (1996). Mass wasting triggered by the 5 March 1987 Ecuador earthquakes. Engineering geology, 42(1), 1-23.

Simons, M., Minson, S.E., Sladen, A., Ortega, F., Jiang, J., Owen, S.E., Meng, L., Ampuero, J.P., Wei, S., Chu, R. and Helmberger, D.V., 2011. The 2011 magnitude 9.0 Tohoku-Oki earthquake: Mosaicking the megathrust from seconds to centuries. science, 332(6036), pp.1421-1425.

Toulkeridis, T., 2011: Volcanic Galápagos Volcánico. Ediecuatorial, Quito, Ecuador: 364 pp

Toulkeridis, T., 2013: Volcanes activos Ecuador. Santa Rita, Quito, Ecuador: 152pp

Toulkeridis, T., & Zach, I. (2017). Wind directions of volcanic ash-charged clouds in Ecuador–implications for the public and flight safety. Geomatics, Natural Hazards and Risk, 8(2), 242-256.

Toulkeridis, T., 2016: The Evaluation of unexpected results of a seismic hazard applied to a modern Hydroelectric center in central Ecuador. Journal of Structural Engineering (India), 43, 4: 373-380.

Toulkeridis, T., Arroyo, C.R., Cruz D'Howitt, M., Debut, A., Vaca, A.V., Cumbal, L., Mato, F. and Aguilera, E., 2015. Evaluation of the initial stage of the reactivated Cotopaxi volcano-analysis of the first ejected fine-grained material. Natural Hazards and Earth System Sciences Discussions, 3: 6947-6976.

Toulkeridis, T., Chunga, K., Rentería, W., Rodriguez, F., Mato, F., Nikolaou, S., D'Howitt, M.C., Besenzon, D., Ruiz, H., Parra, H. and Vera-Grunauer, X., 2017b. The 7.8 M w Earthquake and tsunami of 16th April 2016 in Ecuador: Seismic Evaluation, Geological Field Survey and Economic Implications. Science of Tsunami Hazards, 36(4): 197-242.

Toulkeridis, T., Parra, H., Mato, F., Cruz D´Howitt, M., Sandoval, W., Padilla Almeida, O., Rentería, W., Rodríguez Espinosa, F., Salazar Martinez, R., Cueva Girón, J., Taipe Quispe, A. and Bernaza Quiñonez, L., 2017a: Contrasting results of potential tsunami hazards in Muisne, central coast of Ecuador. Science of Tsunami Hazards, 36: 13-40.

Toulkeridis, T., Mato, F., Toulkeridis-Estrella, K., Perez Salinas, J.C., Tapia, S. and Fuertes, W., 2018: Real-Time Radioactive Precursor of the April 16, 2016 Mw 7.8 Earthquake and Tsunami in Ecuador. Science of Tsunami Hazards, 37: 34-48

USGS (United States Geological Service), 2016: M7.8 - 29km SSE of Muisne, Ecuador.http://earthquake.usgs.gov/earthquakes/eventpage/us20005j32#general

Ye, L., Kanamori, H., Avouac, J. P., Li, L., Cheung, K. F., & Lay, T. (2016). The 16 April 2016, M W 7.8 (M S 7.5) Ecuador earthquake: A quasi-repeat of the 1942 M S 7.5 earthquake and partial re-rupture of the 1906 M S 8.6 Colombia–Ecuador earthquake. Earth and Planetary Science Letters, 454, 248-258.

Zafrir Vallejo, R., Padilla Almeida, O., Cruz D´Howitt, M., Toulkeridis, T., Rodriguez Espinosa, F., Mato, F. and Morales Muñoz, B. (2018). Numerical probability modeling of past, present and future landslide occurrences in nothern Quito, Ecuador – Economic implications and risk assessment”. 5th International Conference on eDemocracy and eGovernment, ICEDEG 2018, 117-125.

ISSN 8755-6839

SCIENCE OF **TSUNAMI HAZARDS**

Journal of Tsunami Society International

Volume 37 Number 3 2018

TSUNAMI SOCIETY INTERNATIONAL, 1741 Ala Moana Blvd. #70, Honolulu, HI 96815, USA.

WWW.TSUNAMISOCIETY.ORG